



Università degli Studi di Napoli “Federico II”

Dipartimento di Ingegneria dei Materiali e delle Strutture

Centro di Ricerca Interdipartimentale sui Biomateriali (C.R.I.B)

Tesi di Dottorato di Ricerca in Ingegneria dei Biomateriali

*XXVII Ciclo*

*Biopolymeric Scaffold obtained By Electrospinning for  
Intima Vessel Regeneration*

Coordinatore

Prof Giuseppe Mensitieri

Tutor

Prof. Paolo A. Netti

Prof. Filippo Causa

Dottorando

Dr. Marta Putzu

*Perplexity is the beginning of knowledge.*

K. Gibran

*A Davide*

## Sommario

<b>1</b>	<b>CHAPTER: CARDIOVASCULAR DISEASES AND ATHEROSCLEROSIS</b>	<b>9</b>
1.1	STRUCTURE OF ARTERIES	10
1.2	VASCULAR TISSUE AND PLAQUE FORMATION	11
1.3	SURGICAL TREATMENT IN ATHEROSCLEROSIS	14
1.4	<b>BIBLIOGRAPHY</b>	18
<b>2</b>	<b>CHAPTER: TISSUE ENGINEERING</b>	<b>20</b>
2.1	INTRODUCTION	21
2.2	TISSUE REGENERATION:SCAFFOLDS AND BIOMATERIALS	22
2.3	SCAFFOLD DEVELOPMENT FOR CARDIOVASCULAR DISEASES	27
2.4	<b>BIBLIOGRAPHY</b>	30
<b>3</b>	<b>CHAPTER: ELECTROSPINNING</b>	<b>33</b>
3.1	INTRODUCTION	34
3.2	TECHNIQUE PRINCIPLES	36
3.3	ELECTROSPINNING SCAFFOLD PRODUCTION: TISSUE ENGINEERING VASCULAR GRAFTS (TEVG)	42
3.4	MATERIALS FOR TISSUE ENGINEERING VASCULAR GRAFTS: ELASTIN LIKE POLYMERS AND SILK	45
3.5	<b>BIBLIOGRAPHY</b>	56
<b>4</b>	<b>CHAPTER: MATERIALS AND METHODS</b>	<b>62</b>
4.1	MATERIALS	63
4.2	ELASTIN LIKE POLYMERS	63
4.2.1	PREPARATION OF ELASTIN LIKE POLYMERS SAMPLES	63
4.2.2	ELECTROSPINNING OF ELP SOLUTIONS	64
4.2.1	THICKNESS OF FLAT MONOLAYER AND ELECTROSPUN ELP COATED BALLOON	65
4.2.2	ELP MECHANICAL CHARACTERIZATION	65
4.2.3	DEGRADATION PROFILES OF ELP ELECTROSPUN SCAFFOLDS	66
4.2.4	TUBULAR SCAFFOLD DEVELOPMENT	66
4.2.5	IN VITRO CELL PROLIFERATION ON SCAFFOLDS	67
4.2.6	ELECTROSPINNING CATETHER COATING	67
4.3	CROSSLINK OF ELASTIN LIKE POLYMERS MATRIX	69
4.3.1	CHEMICAL CROSSLINK WITH HEXAMETHYLENDIISOCYANATE(HMDI)	69
4.3.2	CHEMICAL CROSSLINK WITH GENIPIN	69
4.4	SILK-ELP SCAFFOLDS	70
4.4.1	PREPARATION OF SILK-ELP SAMPLES	70
4.4.2	ELECTROSPINNING OF SILK-ELP SOLUTIONS	72
<b>5</b>	<b>CHAPTER: RESULT AND DISCUSSION</b>	<b>73</b>
5.1	ELASTIN LIKE POLYMERS ELECTROSPUN SCAFFOLDS	74
5.1.1	MORPHOLOGICAL ANALYSIS	74
5.1.1	FLAT ELP MECHANICAL CHARACTERIZATION	78
5.1.2	THICKNESS OF FLAT ELP SCAFFOLDS	79
5.1.3	DETERMINATION OF CROSSLINK DEGREE: HMDI	80
5.1.4	CROSSLINK SCAFFOLD'S DEGRADATION PROFILES	84
5.1	SILK-ELP SCAFFOLDS	87
5.1.1	SCANNING ELECTRON MICROSCOPY(SEM)	87
5.2	SCAFFOLD'S INTERACTION WITH HUVEC	89
5.2.1	CELL PROLIFERATION ON ELP SCAFFOLDS	89
5.2.2	CELL PROLIFERATION ON SILK-ELP SCAFFOLDS	90
5.2.3	THICKNESS OF DIRECTLY ELECTROSPUN CATETHERS	95
5.3	IN SITU DEPLOYMENT OF ELP SCAFFOLD	96

**6 CHAPTER: CONCLUSION AND FUTURE PROSPECTS ..... 100**  
**7 *BIBLIOGRAPHY*..... 102**

# Introduzione e scopo del lavoro

---

*L'aterosclerosi è la causa principale di morte nei paesi occidentali per malattia coronarica o ictus; si tratta di una malattia progressiva che tipicamente inizia in tenera età e si esprime clinicamente durante la mezza età e durante la vecchiaia. È una malattia multifattoriale che, per diventare clinicamente evidente, richiede la formazione di una placca fibro-lipidica nella parete di un'arteria che riduce il flusso di sangue. [1]*

*La formazione delle lesioni aterosclerotiche avanzate è la conseguenza di tre processi:*

- 1) l'accumulo di lipidi ed esteri principalmente colesterolo e colesterolo libero, nello spazio sub-endoteliale delle arterie;*
- 2)-la formazione di un infiltrato infiammatorio costituito principalmente da linfociti e macrofagi; i macrofagi accumulatisi continuano a fagocitare lipidi diventando cellule schiumose (cellule schiumose);*
- 3) migrazione e proliferazione delle cellule muscolari lisce (cellule muscolari lisce - SMC)*

*Nonostante il termine "aterosclerosi" derivi dal *âthere* greco, "poltiglia" e sclerosi, "indurimento", è importante sottolineare come il danno possa essere variabile nel tessuto formato a causa della prevalenza di ciascuno dei tre processi. [ 2]*

*Di conseguenza, alcune lesioni aterosclerotiche appaiono prevalentemente dense e fibrose, altre possono contenere grandi quantità di lipidi e detriti necrotici, mentre la maggior parte hanno combinazioni e variazioni di ciascuna di queste caratteristiche. La distribuzione dei lipidi e tessuto connettivo all'interno delle lesioni determina la stabilità, la facilità di rottura e trombosi, con conseguenti effetti clinici.*

*Lo scopo del seguente lavoro di dottorato è parte del progetto europeo "Il Graal" (tessuto in Ingegneria Host guidata Rigenerazione arteriosa intinale strato di Grant nr 278557) il cui scopo è di rigenerare le arterie malate rimuovendo la placca aterosclerotica interna e sostituendola con uno scaffold temporaneo denominato SIL, che porterà alla rigenerazione dello strato intinale.*

*In particolare, il progetto si concentrerà sulla realizzazione di scaffold con una certa porosità che siano riassorbibili e preformati, realizzati tramite Electrosinching, utilizzando come materiale di base polimeri Elastino-simili (Elastin-like-polymers) e un copolimero costituito dalla coniugazione*

*di ELP con seta. Questi due tipi di scaffold saranno impiegati per impianti in vivo, come dispositivi per la rigenerazione dello strato dell'intima dell'arteria.*

## Abstract

---

*Atherosclerosis is the main cause of death in Western countries for coronary heart disease or stroke; the disease process is progressive and typically starts at an early age and is expressed clinically during the middle and old age. It's a multifactorial disease that, to become clinically manifest, requires the formation of a plaque fibro-lipid within the wall of an artery that reduces blood flow.[1]*

*The formation of advanced atherosclerotic lesions is the consequence of three processes:*

- 1) the accumulation of lipids, mainly cholesteryl esters and free cholesterol, in the space sub-endothelium of the arteries;*
- 2) the establishment of an inflammatory infiltration of lymphocytes and macrophages, engulfing lipids accumulated, they become foam cells (foam cells);*
- 3) migration and proliferation of smooth muscle cells (smooth muscle cells – SMC)*

*Despite the term "atherosclerosis" derives from the greek *ãthere*, "mush" and *sclerosis*, "hardening", it is important to emphasize that the injury could be a great variability in tissue formed because of the prevalence of each of the three processes.[2]*

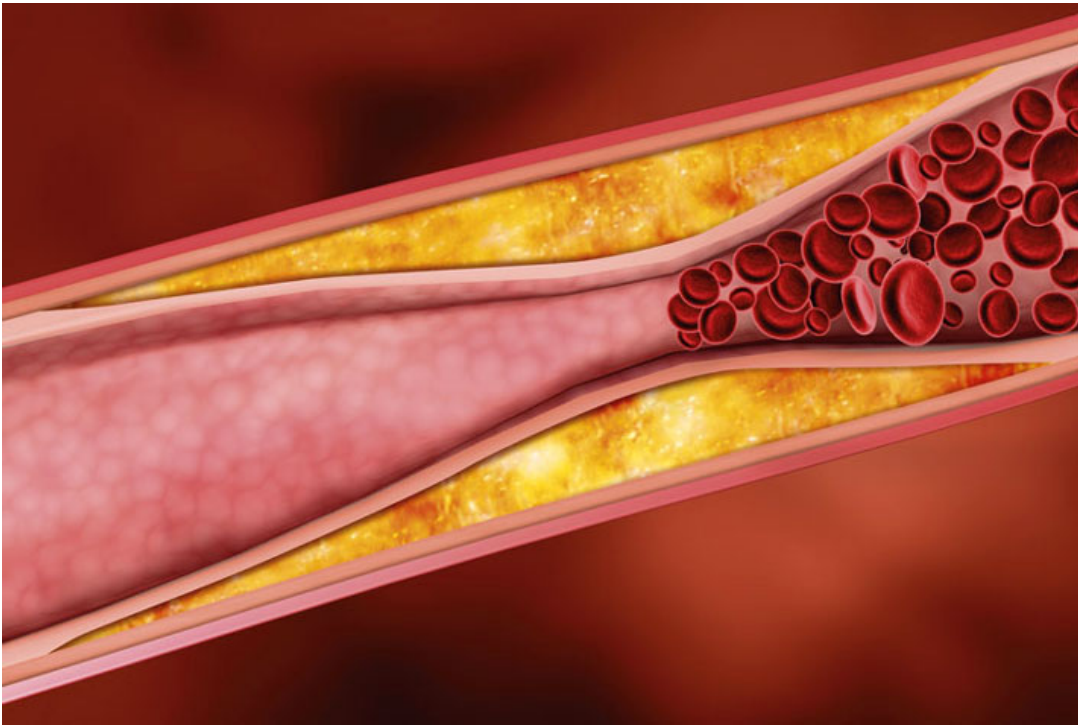
*Consequently, some atherosclerotic lesions appear predominantly dense and fibrous, others can contain large amounts of lipid and necrotic debris, while most have combinations and variations of each of these characteristics. The distribution of lipids and connective tissue within the lesions determines the stability, the ease to rupture and thrombosis, with consequent clinical effects.*

*The purpose of the following doctoral work is part of the European project "THE GRAIL" ( Tissue in Host Engineering Guided Regeneration of Arterial Intimal Layer Grant nr 278557) whose purpose is to regenerate diseased arteries by removing the inner Atherosclerotic plaque and substituting it with a temporary scaffold referred to as Synthetic Intimal Layer(SIL),that will lead to the regeneration of an intimal layer.*

*In particular, the project will be focused on the realization of a selectively porous, resorbable and preshaped scaffold made by Electrospinning, based on recombinant Elastin Like Polymers and a*

*copolymer made by conjugation of ELP with silk. This two types of scaffold will be deployed once in contact with healthy medial layer of arterie as a new internal elastic lamina.*

# 1 CHAPTER: CARDIOVASCULAR DISEASES AND ATHEROSCLEROSIS



## 1.1 STRUCTURE OF ARTERIES

The wall of the arterial vessels is constituted by a series of layers (tunics): from the inside of the vessel lumen to the outside, we observe a tunica intima, a tunica media and tunica adventitia;(1) the intima adjacent to the vessel lumen, which includes the endothelial monolayer that lines the blood vessel and underlying extracellular connective tissue, (2) the smooth muscle containing media, and (3) the outermost adventitia, which consists principally of fibroblasts within collagen bundles surrounded by proteoglycans. in the capillaries(**fig.1.1**).[3]

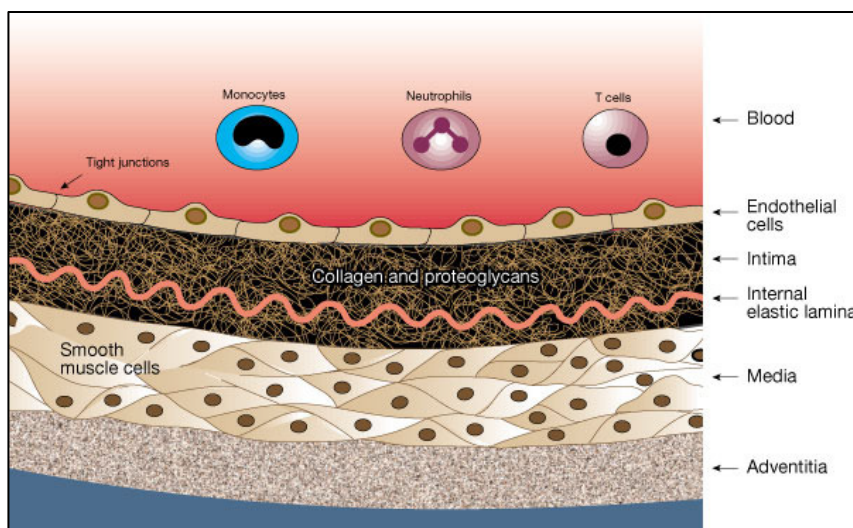


**Figure 1.1 Architecture of arterial vessel**

The tunica intima is composed of a layer-celled, the endothelium, supported by a layer of loose connective tissue, the basal lamina, and an elastic layer sub-endothelial system. The endothelium is a pavement epithelium, simple, pretty fragile but with a great capacity for regeneration and growth; regenerates, in fact, continuously and can be formed of natural or artificial implants inserted surgically. Variations in the diameter of the artery, in the shape of the pot (curvatures and shrinkage) and pulsatory motion of the vessel wall, may have employed to endothelial cells a different form. In fact, the endothelial cells of arteries, in which the blood flow is laminar and uniform, have an elongated shape and are aligned in the flow direction, while those located in the regions of the vessel which have branches or bends, where the flow is turbulent, have a polygonal shape and not take special guidelines. The endothelium plays a critical role in regulating the entry, exit and lipoprotein metabolism and other agents that can participate in the formation of atherosclerotic lesions.[4]

The sub-endothelial layer consists of fibroblasts and collagen fibers by them; finally, in the part of underwear which borders the media, this is the internal elastic lamina, which contributes to the elasticity of the vessel. This foil is fenestrated to facilitate the passage of nutrients from the blood to the tunica media. the intima is the tunic which trains the atherosclerotic lesions. In some cases, the lesions are formed from a thickening or asymmetric generalized intimal invading as the lumen, with the result of a reduction in blood flow. In other cases, the increase in thickness intima is accompanied by a continuous artery dilation (aneurysm) so that the lumen of the vessel changes little actual diameter. In this second case the atherosclerotic lesions appear more symmetrical and concentric. The media is the thickest layer of the wall, typically costs concentric elastin, separated by thin layers of connective tissue, collagen fibers and smooth muscle cells (SMC) and is responsible for maintaining the blood pressure and continuous flow of blood. The SMC contain actin filaments that contract in response to depolarization of the cell membrane and generate voltage. In large arteries, the SMC tend to be aligned longitudinally, are surrounded by a common basal lamina and are associated with collagen fibers closely intertwined. The elastic fibers, that are interposed between the SMC, are relatively extensible and allow contraction and distension of the artery wall in relation to the pressure of the blood flow during the cardiac cycle. The SMC, in addition to synthesize collagen and elastic fibers, determine the mechanical properties of the arterial wall and are actively involved in the metabolic processes that contribute to the tone of the wall; under conditions in which the pressure, motility and increased wall tension, the metabolism of the SMC of the media is incremented. The tunica adventitia, the outermost layer, protects the arteries and allows anchoring to the surrounding tissues. It consists of connective tissue containing scattered fibers of elastin and collagen in which, in the case of large vessels, one can find nerve plexuses and lymphatic vessels. Thanks to the limited elasticity of the collagen fibers, this layer poses a limit to the dilation of blood vessels. Typically, in large arteries adventitia receives nutrients from "vasa-vasorum", a network of capillaries that develops around the vessel.[5]

## *1.2 VASCULAR TISSUE AND PLAQUE FORMATION*

Atherosclerosis is an inflammatory disease that affects mainly the elastic wall of medium-sized arteries. Inflammation is a component of all forms of plaque. Moreover, a topographic relationship among an inflammatory infiltrate, plaque rupture and thrombosis was proved by van der Wall et al, suggesting a pathogenetica role for macrophages at the site of cap rupture with fatal acute myocardial infarction (AMI) as a consequence of this process.[6]

Further observation demonstrated the role of activated macrophage and T-lymphocytes in plaque destabilization. The combination of macrophages and lymphocytes in vulnerable plaque is associated with the secretion of cytokines and lytic enzymes that result in thinning of the fibrous cap, predisposing the lesion to a rupture. [7]

Atherosclerotic lesions, accordingly to the American Heart Association classification, recently modified by Virmani et al. and Naghavi et al., are divided in two groups:

- i. Non atherosclerotic intimal lesions;
- ii. Atherosclerotic progressive lesions

The primary event in the formation of atherosclerotic lesions is the local accumulation of lipids in the sub-endothelial space of the intima of arteries. The lipids are transported in plasma in the form of lipoprotein, complex water-soluble molecules consist of a core of cholesterol esters and triglycerides, and a surface layer of phospholipids, free cholesterol and specific transporter proteins, apolipoproteins. Lipoproteins contribute differently to the development and progression of atherosclerosis: those rich in triglycerides, VLDL and chylomicrons, are not considered atherogenic, but it is believed that they are derivatives from their lipolysis, VLDL remnants and LDL, lipoprotein more high cholesterol. Lipoproteins considered at increased risk for atherosclerosis are the small dense LDL. This fraction of LDL, often characterized by a smaller size and a ratio lipid / protein in favor of lipids, is considered more atherogenic than normal LDL. In fact has an increased plasma half-life that is due to decreased affinity for the apolipoprotein in the LDL receptor. Persisting circulating these lipoproteins continue to yield lipids, increasing density and decreasing in size and are also subject to a greater number of oxidative events becoming oxidized LDL (oxLDL) and then modified LDL (MM-LDL).

The oxidation is considered to be one of the factors of initiation of the atherosclerotic lesion because the oxidized products are able to induce endothelial damage and chemotaxis. The lipoprotein oxidation occurs both at the level of the lipid portion of that protein. The changes include the formation of lipid hydroperoxides, lysophospholipids, oxysterols and aldehyde products resulting from the breaking of the chains of fatty acids. In response to the damage induced by oxidized products and changes in blood flow, endothelial cells are activated by expressing adhesion molecules on the surface and producing chemotactic mediators. Such molecules favor the margination of monocytes and lymphocytes and their subsequent invasion inside the sub-endothelial

space, mainly through mechanisms of diapedesis. The areas in which usually are formed atherosclerotic lesions eg. at points of branching, often are characterized by turbulent flow[8].

The first event of the formation of atherosclerotic plaques is therefore the set of accumulation of lipids, oxidation and endothelial activation and recruitment of leukocytes to the site of injury. Chemotaxis of leukocytes to the site of the lesion and the expression of adhesion molecules are mediated by both the products of lipid oxidation that pro-inflammatory cytokines, a class of mediators of protein nature that are responsible for the chronicism of the disease. Leukocytes are able to adhere to endothelial cells through adhesion molecules and specific receptors expressed on the surface of endothelial cells of the artery. Among these molecules, of particular interest are the VCAM-1 (vascular cell adhesion molecule-1) and ICAM-1 (intercellular adhesion molecule-1) that belong to the families of the immunoglobulin and P-selectin that is part of a distinct family of receptors for leukocytes, known as selectins [9];[10] (fig 1.2).

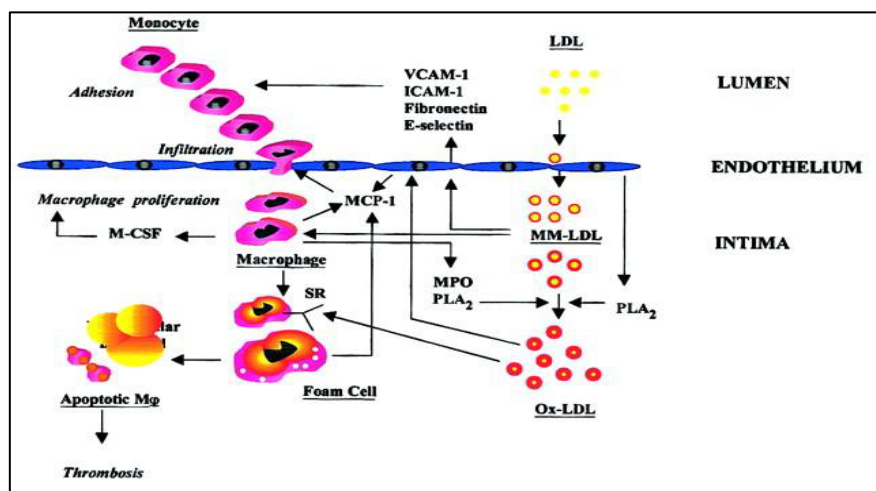


Figure 1.2 Molecular pathways of Monocytes and LDL activation into vessels

After adhering to the surface of endothelial cells of the artery and settle in the intima, the monocytes differentiate into macrophages and subsequently phagocytose large amounts of lipids and are transformed into foam cells. Indeed, oxidized LDL accumulated in the lesion ejaculation are recognized and phagocytized by macrophages via specific receptors, such as the receptor LOX-1, CD36 or the receptor "scavenger" (Scavenger Receptor - SR). Since the expression of these receptors is not inhibited by high levels of intracellular cholesterol, the macrophages can absorb LDL continuously until becoming full and take on the appearance of foam cells (foam cells). These cells can accumulate in the vessel wall and contribute to 'growth of the lesion. on the other hand some of them may undergo death by apoptosis inducing the formation of a nucleus (core) rich

necrotic lipid, a characteristic feature of atherosclerotic plaques. The lesion at this stage is called "lipid industry", because there was only the accumulation of lipids, free or in the form of foam cells.

While the accumulation of lipid engorged macrophage is the characteristic of the stria lipid, the accumulation of fibrotic tissue distinguishes the advanced atherosclerotic lesion. Some growth factors or cytokines produced by mononuclear phagocytes are able to stimulate the migration to the intima and proliferation of the smooth muscle cells of the tunica media.

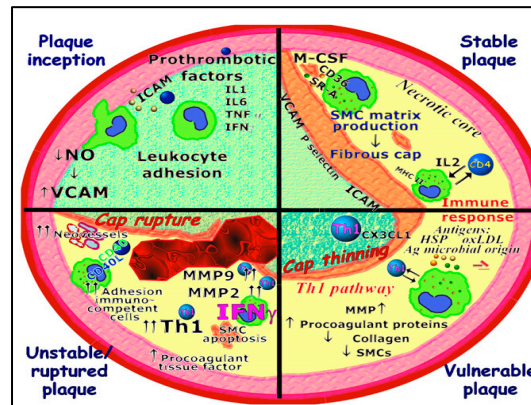


Figure 1.3 Molecular factors involved in plaque evolution.[6]

There is often another phenomenon, that of calcification. Calcification of the arteries is due to the presence, within the atherosclerotic plaques of calcium-binding proteins, such as osteocalcin, osteopontin [6]. Tissue remodeling may also be due to the intervention special enzymes that are found at the level of the plate and which are able to degrade the extracellular matrix of the lamina fibrous part of the plaque. These enzymes include collagenase, gelatinase degrades the different constituents of the plaque. The proinflammatory cytokine production at the level of the lesion favorably intervenes in the production of such enzyme proteins. In this way, the balance of the process becomes unbalanced in favor of continuous degradation of matrix components that increase the risk of plaque rupture and subsequent thrombosis (fig 1.3).

### 1.3 SURGICAL TREATMENT IN ATHEROSCLEROSIS

Atherosclerosis is a disease in which plaque builds up inside arteries. The plaque is made up principally of fat, cholesterol, calcium and other substances that could be found in the blood.

Narrowing of arteries, involving the slowing of blood, leads to serious problems like stroke or AMI (acute myocardial infarction) (fig 1.4).

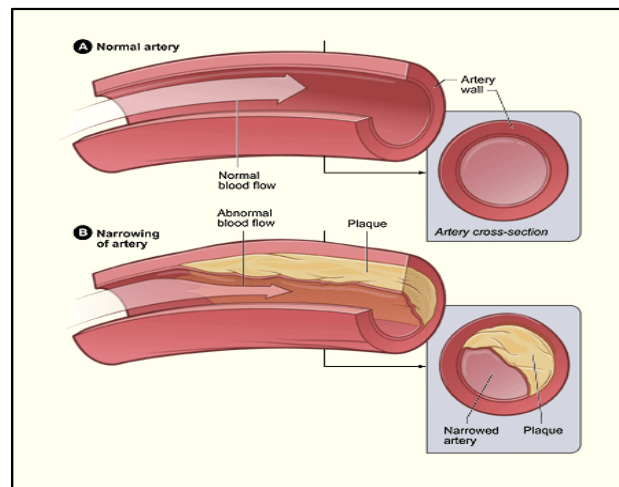


**Figure 1.4 Anatomical view of arterial vessel: a) normal artery with normal blood flow; b) artery with a buildup plaque**

During the initial stages of the disease, usually the plaque grows in the opposite direction with respect to the lumen of the vessel. It is known that, until the plaque does not cover more than 40% of the lamina endothelial, there is no slowing of the blood flow. The clinical events are different, depending on whether the occlusion is partial or total and the effects are more or less severe, depending on whether the supply of oxygen is absent or only reduced.

In the coronary arteries, reducing blood flow due to angina pectoris, while blocking the lumen of the artery causes myocardial infarction. The reduction of blood-flow to the jugular vein, leads to a reduction of the provision of oxygen to the brain; this determines strokes and TIA. When atherosclerosis affects the peripheral circulation, you can have gangrene or claudicatio intermittens.

In this regard, the risk factors fall into two broad categories: risk factors that can not be changed and modified risk factors.

The first category includes sex, age, family history and genetic predisposition. For example, it has been seen that the onset of cardiovascular disease occurs about 10 years earlier in men although the incidence of cardiovascular disease is higher in postmenopausal women

In the category of modifiable factors are covered under the smoking, hypertension, physical inactivity, diabetes mellitus, obesity and dyslipidemia. Each of these factors affects the risk in different ways; cigarette smoking acts by promoting the assembly platelet and acts synergistically in

enhancing other risk factors, dyslipidemia and diabetes favor the increase in the concentration of LDL cholesterol in contrast to the cholesterol HDL, while physical inactivity would favor the thickening of the lamina endothelial vessel

The thickening of the vessel wall and subsequent occlusion are surgically treated for the reopening of the occluded vessel, through the bypass or insertion of a stent. These two invasive procedures with a certain percentage of risk and, for this reason, are mainly used in emergency cases. Percutaneous transluminal coronary angioplasty (PTCA) is a widely used technique that allows you to dilate arteries which spread the blood to the heart (coronary arteries) in the event that these are fully or partially occluded by atherosclerotic plaques. The angioplasty involves the use of a balloon catheter capable of causing vasodilatation and restore the normal blood flow. It's a procedure of mechanical remodeling of the wall of a coronary artery in stenotic segments (restricted). Its use is now more and more frequently, so as to have significantly reduced the use of cardiac surgery. In a traditional angioplastic procedure a catheter equipped with a balloon at the tip is used and is inserted under local anesthesia in the femoral artery or radial and pushed towards the heart up to the headquarters of the stenosis. Then the balloon is inflated up to the diameter of the coronary artery (2 to 5 mm) so dilating the blood vessel restricted. The traditional angioplasty leads to dilatation of the stenosis with success in the great majority of cases.

In recent years the expansion method described above, if they are flanked other. These new methods allow you to treat narrowed coronary hardly can attack with only the balloon catheter. The choice of which method to use is essentially technical and left to the operator's experience. The coronary stent is a metal prosthesis in the form of a small tube that, positioned at the level of the constriction, allows to widen it in a more effective and long lasting than traditional angioplasty. The prosthesis does not meet to rejection, does not cause tumors and absolutely does not move after it has been positioned. After 4-6 weeks the implant is embedded in the wall of the coronary artery, that is covered by the wall cells (endothelium) that isolate it from the blood. Until this process is not completed is required the use of drugs that make the blood more fluid and, in particular, makes the platelets less active. The drugs that are used most frequently are aspirin and ticlopidine. The stent may be decided electively, or to treat a complication such as acute occlusion or dissection.

Angioplasty is however complicated by the restenosis, a wound healing process in exuberant treated point which can lead to the appearance of a new shrinkage after 2-6 months of treatment. The restenosis may occur in about 30% of cases after traditional angioplasty and after rotational atherectomy or directional [11];12]. The stent reduces this risk, which may be less than 10% if they

are treated in the coronary narrowings short and main. However none of these methods can reduce to zero the risk of restenosis. The occurrence of restenosis usually occurs gradually with angina pectoris (chest pain) after 2 or 4 months and usually leads to acute complications dramatic. Often restenosis gives symptoms modest or absent. For this reason the patient must undergo periodic inspections cardiology and all the recommended tests often including a stress test after 3-6 months and above must not underestimate any symptoms appearing in the months following discharge, although with symptoms vanished. When restenosis occurs it can be treated with a new angioplasty or, in some cases, may be required cardiac surgery. The risk of restenosis is related to a remodeling process early (scarring after surgery) and then, after passing the risk period (6-8 months after treatment) the good results can be considered definitive[13].

Although the pathophysiological mechanisms underlying restenosis are not yet fully understood, several experimental evidences both in man and suggest that inflammation plays a central role in this phenomenon[14];[15]. The vascular damage leading to revascularization induces an immediate and progressive release of thrombogenic factors, mitogenic and vasoactive molecules resulting in platelet aggregation, thrombus formation and inflammatory reaction with activation of macrophages and vascular smooth muscle cells (VSMCs)[16];[17].

These events cause the production and release of growth factors and cytokines which in turn signal are for their own synthesis and release from inflammatory cells[18].Consequence of this mechanism is the migration of VSMCs from their usual position in the middle of the vessels, the intima where they experience a change in phenotype that causes their proliferation with formation of a new structure called "neointima" [19];[20]. From this point of view, the phenomenon of restenosis can be considered as an inflammatory-proliferative response to vascular injury [20].

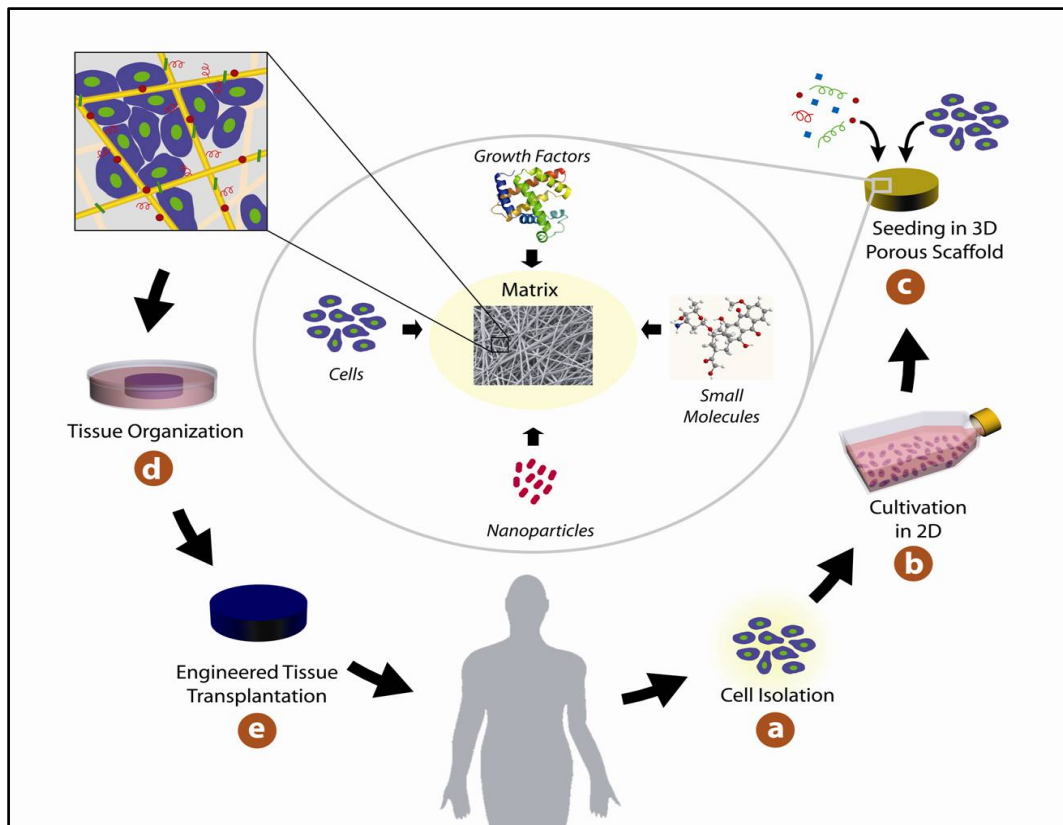
## 1.4 BIBLIOGRAPHY

- [1]- R Rosamond W, Flegal K, Friday G, Furie K, Go A, Greenlund K, Haase N, Ho M, Howard V, Kissela B, Kittner S, Lloyd-Jones D, McDermott M, Meigs J, Moy C, Nichol G, O'Donnell CJ, Roger V, Rumsfeld J, Sorlie P, Steinberger J, Thom T, Wasserthiel-Smoller S, Hong Y; American Heart Association Statistics Committee and Stroke Statistics Subcommittee. Heart disease and stroke statistics-2007 update: a report from the American Heart Association Statistics Committee and Stroke Statistics Subcommittee. *Circulation*. 2007;115:e69-171
- [2]-Stary HC, Chandler AB, Dinsmore RE, Fuster V, Glagov S, Insull W Jr, Rosenfeld ME, Schwartz CJ, Wagner WD, Wissler RW. A definition of advanced types of atherosclerotic lesions and a histological classification of atherosclerosis. A report from the Committee on Vascular Lesions of the Council on Arteriosclerosis, American Heart Association. *Arterioscler Thromb Vasc Biol*. 1995;15:1512-31
- [3]-Gail W. Sullivan, Ian J. Sarembock, and Joel Linden *The role of inflammation in vascular diseases*, *Journal of Leukocyte Biology* Volume 67, May 2000.)
- [4]-Giannotti G, Landmesser U. Endothelial Dysfunction as an Early Sign of Atherosclerosis. *Herz*. 2007;32:568-572
- [5]-Saladin Kenneth S. *Anatomy and Physiology-The unity of form and function*. Fourth Edition 2008
- [6]-Spagnoli LG, Bonanno E, Sangiorgi G, Mauriello A. Role of inflammation in atherosclerosis. *J Nucl Med*. 2007 Nov;48(11):1800-15.
- [7]-Hansson GK. Inflammation, atherosclerosis, and coronary artery disease. *N Engl J Med*. 2005 Apr 21;352(16):1685-95
- [8]-Nakajima K, Nakano T, Tanaka A. The oxidative modification hypothesis of atherosclerosis: the comparison of atherogenic effects on oxidized LDL and remnant lipoproteins in plasma. *Clin Chim Acta*. 2006;367:36-47.
- [9]-Charo IF, Taubman MB. Chemokines in the pathogenesis of vascular disease. *Circ Res*. 2004;95:858-66;24
- [10]-Galkina E, Ley K. Vascular adhesion molecules in atherosclerosis. *Arterioscler Thromb Vasc Biol*. 2007;27:2292-301
- [11]- Suryapranata HI, de Feyter PJ, Serruys PW. Coronary angioplasty in patients with unstable angina pectoris: is there a role for thrombolysis?. *J Am Coll Cardiol*. 1988 Dec;12(6 Suppl A):69A-77A
- [12]-Smith LRI, Harrell FE Jr, Rankin JS, Califf RM, Pryor DB, Muhlbaier LH, Lee KL, Mark DB, Jones RH, Oldham HN, et al. Determinants of early versus late cardiac death in patients undergoing coronary artery bypass graft surgery. *Circulation*. 1991 Nov;84(5 Suppl):III245-53
- [13]-Andrew Farb, MD; Deena K. Weber, MS; Frank D. Kolodgie, PhD; Allen P. Burke, MD; Renu Virmani, MD. Morphological Predictors of Restenosis After Coronary Stenting in Humans. *Circulation*. 2002; 105: 2974-2980
- [14]-Prediman K. Shah, MD. Inflammation, Neointimal Hyperplasia, and Restenosis As the Leukocytes Roll, the Arteries Thicken. *Circulation*. 2003; 107: 2175-2177
- [15]-GA Ferns, EW Raines, KH Sprugel, AS Motani, MA Reidy, R Ross. Inhibition of neointimal smooth muscle accumulation after angioplasty by an antibody to PDGF. *Science* 6 September 1991: Vol. 253 no. 5024 pp. 1129-1132
- [16]-Frederick G.P. Welt, Campbell Rogers. Inflammation and Restenosis in the Stent Era. *Arteriosclerosis, Thrombosis, and Vascular Biology*. 2002; 22: 1769-1776
- [17]-A. W. Clowes, T. R. Kirkman, and M. A. Reidy. Mechanisms of arterial graft healing. Rapid transmural capillary ingrowth provides a source of intimal endothelium and smooth muscle in porous PTFE prostheses. *Am J Pathol*. 1986 May; 123(2): 220-230.
- [18]- Libby PI, Hansson GK. Involvement of the immune system in human atherogenesis: current knowledge and unanswered questions. *Lab Invest*. 1991 Jan;64(1):5-15.

**[19]**-Robert S. Schwartz, MD, FACC; Kenneth C. Huber, MD; Joseph G. Murphy, MB; William D. Edwards, MD, FACC; Allan R. Camrud, RN; Ronald E. Vlietstra, MB, BCh, FACC; David R. Holmes, MD. Restenosis and the proportional neointimal response to coronary artery injury: Results in a porcine model. *J Am Coll Cardiol.* 1992;19(2):267-274. doi:10.1016/0735-1097(92)90476-4

**[20]**- Hidehiko Hara, Masato Nakamura, Julio C. Palmac, Robert S. Schwartz. Role of stent design and coatings on restenosis and thrombosis. *Advanced Drug Delivery Reviews Volume 58, Issue 3, 3 June 2006, Pages 377–386*

## 2 CHAPTER: TISSUE ENGINEERING



## 2.1 INTRODUCTION

*The primary goal of tissue engineering procedures is the generation of “neo-tissues” that could be adapted by the body and that could be used to carry on physiological functions. For this purpose, tissue engineering involves fabrications of three dimensional scaffolds to support cellular growth, proliferation and regeneration of tissues [2].*

*By culturing the cells on the scaffold, the cells will be able to embed themselves into the biomaterial. The main advantages of scaffolds are three:*

- Scaffolds provide biomechanical support for the cells until they produce their ECM;*
- Scaffolds can incorporate signals (GFs), important for maintenance of tissue viability and for inducing scaffold vascularization;*
- Control on tissue formation (shape and size) prior to transplantation.*

## 2.2 TISSUE REGENERATION:SCAFFOLDS AND BIOMATERIALS

By the mid to late 1990's, tissue engineering efforts including one at Yale University, established by Drs. Chris Brewer and Mark Saltzman, were springing-up in virtually every developed country in the world and several privately funded ventures in Tissue Engineering began to arise [1].

In 1994, TES (Tissue Engineering Society) was founded and finally incorporated in the State of Massachusetts in 1996. Tissue engineering was brought to public attentions with the airing of a BBC broadcast exploring the potential of tissue-engineered cartilage when it broadcast images of the now infamous “mouse with the human ear”, fondly referred to as auriculosaurus, from the laboratory of Dr. Charles Vacanti at University of Massachusetts Medical Center [3];[2].

Traditionally tissue engineering strategies typically employ a top-down approach in which cells are seeded on a biodegradable polymeric scaffold, like PLGA scaffold. In top down approaches, the cells are expected to populate the scaffold, usually with the help of growth factor, mechanical stimulation or perfusion. Cells upon the scaffolds will produce a functional extracellular matrix and all the microarchitecture. Despite all the advances in using biofunctionalization techniques and more bioactivated scaffolds, this approach has the disadvantage to not recreate the microstructural characteristics of tissues [4].

Currently, the emerging “bottom-up” method may hold great potential to address this challenge, and focuses on the fabrication of microscale tissue building blocks with a specific microarchitecture and assembling these units to engineer larger tissue constructs from the bottom up. Fabrication of tissue building blocks can be achieved via multiple approaches, including fabrication of cell-encapsulating microscale hydrogels (microgels), self-assembled cell aggregation, generation of cell sheets, and direct printing of cells (**fig 2.1**). These microscale building blocks can be successfully assembled into complex tissue constructs, with control over features such as the shape and composition of individual blocks [5];[6];[7].

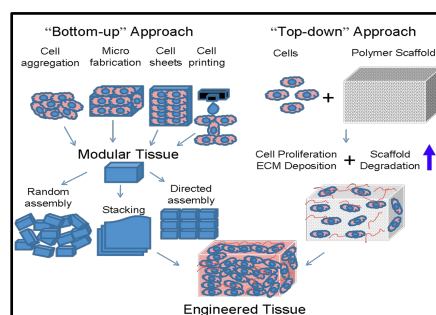


Figure 2.1 Schematic of top-down and bottom up approaches for tissue Engineering.

The possibility of producing scaffolds for tissue regeneration is determined by the ability to use specific materials that can be colonized by cells and allow their growth, without creating immune reactions and / or inflammations. In this regard, biomaterials can be defined, in very general, such materials that are not medicals or foods contained in devices in contact with the tissues or biological fluids [8]. Basic requirements of biomaterials are the biocompatibility and reliability.

The biocompatibility is a basic requirement for a biomaterial; it is considered a measure of the ability of the material to induce a favorable reaction to its presence. Biocompatibility is a function of the mechanical properties and chemical-physical properties of materials, of the geometric characteristics of the devices (size, shape) and the conditions of the host organism (tissue type, location of planting, age, gender, general health and pharmaceutical system) [9]. The problems associated with biocompatibility are associated with the responses that the body generates in the presence of a foreign material. The reliability of a material, instead, indicates how that material is able to ensure a continuity in its function. biomaterials can be classified in different ways: according to the type (natural or synthetic), based on the biological role (toxic, bioinert, bioactive, bioabsorbable), depending on the function and / or duration of use temporary, (media not resorbable and supports biodegradable) and permanent.

The three main classes of biomaterials that are used today are: metals, ceramics and polymers.

The polymeric materials are constituted by molecules with high molecular weight (even higher than 2,000,000 amu = Atomic Mass Unit), generally organic, such macromolecules. The macromolecules originate from the concatenation of individual units (monomers) to form long chains which may be linear, branched or crosslinked. The polymeric materials are constituted by molecules with high molecular weight (even higher than 2,000,000 amu = Atomic Mass Unit), generally organic, such Macromolecules. The polymers can be classified:

- 1) according to their origin: Natural polymers (polysaccharides, proteins ..); Synthetic Polymers (plastics, resins, rubber ..);
- 2) according to the structure: homopolymers: Copolymers: heteropolymers:
- 3) according to the type of polymerization: condensation polymers: Addition polymers (ionic or radical): Polymers of coordination.
- 4) based on the thermal properties: Thermoplastic Polymers: Thermosetting Polymers.

Naturally derived polymers are abundant and usually biodegradable. Their principal disadvantage lies in the development of reproducible production methods, because their structural complexity often renders modification and purification difficult. Additionally, significant batch-to-batch variations occur because of their 'biopreparation' in living organisms (plants, crustaceans)[11]. Polymers used as biomaterials can be synthesized to have appropriate chemical, physical, interfacial and biomimetic (characteristics, which permit various specific applications).

Synthetic polymers are available in a wide variety of compositions with readily adjusted properties. Processing, copolymerization and blending provide simultaneous means of optimizing a polymer's mechanical characteristics and its diffusive and biological properties. The primary difficulty is the general lack of biocompatibility of the majority of synthetic materials, although poly(ethylene oxide) (PEO) and poly(lactic-co-glycolic acid) are notable exceptions.

Polymer biocompatibility refers to the reaction of polymers with blood and tissues, depending on the site and purpose of use. A response in the host organism is generally unfavourable unless vascularization is required to support living cells. For blood-contact applications, biocompatibility is determined largely by specific interactions with blood and its components. For applications not involving blood contact (e.g. dental work), the choice of biomaterial generally depends on its tissue biocompatibility. A material may be biocompatible in one application but bioincompatible in another. Indeed, because the surface of the materials is in direct contact with biological fluids, the interfacial characteristics are significant for impermeable solid device. In all these cases, the interfacial interactions between the biomaterial and the body are responsible for the biological response[11].

The nature of a surface can control its blood compatibility through its interactions between the surface and the negatively charged platelets. Polymer surfaces that do not adsorb any plasma proteins must be considered to be blood compatible, with the additional advantage that a device fabricated from completely blood-compatible materials does not require immune suppression of the patient after implantation. The physical properties (durability, permeability) and degradability may also influence the biocompatibility [11].

The choice of a material for a specific application is mainly based on its physicochemical, interfacial and biomimetic properties, although traditional mechanical properties such as impact strength, elasticity and permeability are also essential for specific applications. Indeed, the choice of the polymer is primarily governed by the end use of the biomaterial and involves selection not only on the basis of physical and chemical properties but also on extensive biochemical characterization

followed by specific preclinical testing of the chosen material.

The selection of polymers for matrices or carriers in controlled-delivery devices requires the consideration of characteristics such as molecular weight, adhesion and solubility, depending on the type of system to be prepared, its action and the target site in the body. For example, high molecular weight polymers cannot cross the blood–brain barrier and are not resorbed after oral administration [10]. Polymeric materials for drug delivery must satisfy additional requirements, such as environmental responsiveness (e.g. pH- or temperature- dependent phase or volume transformations). Hydrophilic and amphiphilic polymers are preferred for certain specialized applications (e.g. ophthalmological and vaginal applications).

Biodegradable polymers containing ‘hydrolysable’ groups in their chains, which are susceptible to biodegradation to low molecular weight, nontoxic products, have also been considered for controlled- drug-delivery systems. Indeed, this appears to be their most widely investigated practical application. Polyesters, polyanhydrides, polyamides and natural polymers, as well as networks, copolymers, blends and microcapsules based on these polymers, have been extensively studied and used as biodegradable matrices for the release of bioactive agents[11];[12];[13].

The fundamental concept behind tissue engineering is to utilize the body’s natural biological response to tissue damage in conjunction with engineering principles [14]. To achieve successful tissue regeneration, three key factors are to be considered: cells, scaffolds, and biomolecules (e.g., growth factor, gene, etc.). Currently, two strategies have emerged as the most promising tissue engineering approaches [14].

One is to implant pre-cultured cells and synthetic scaffold complexes into the defect place. In this approach, the seeded cells are generally isolated from host target tissues, for which they provide the main resource to form newly born tissue. The synthetic scaffolds, on the other hand, provide porous three-dimensional structures to accommodate the cells to form extracellular matrix (ECMs) and regulate the cell growth in vivo [15];[16]. These synthetic scaffolds are biodegradable and degrade in accordance with the tissue regeneration time frame. The other approach is to place acellular scaffolds immediately after injury. The governing principle of this approach is using scaffolds to deliver appropriate biomolecules to the defect area; the biomolecules are released from the scaffolds in a controlled manner and may recruit progenitor cells toward the defect area and promote their proliferation and differentiation, thereby enhancing tissue regeneration [17].

The basic idea of tissue regeneration therapy is to take advantage of the natural healing potentials of patients themselves. Basically, body tissue is composed of two components: cells and the surrounding environment. The latter includes the extracellular matrix (ECM) for cell proliferation and differentiation (natural scaffold) as the living place of cells and biosignalling molecules as the

nutrients of cells. There are some cases where tissue regeneration is achieved by the single or combinational use of the components in an appropriate way. However, since successful tissue regeneration cannot always be expected only by their simple combination, it is necessary to biomedically contrive the way to combine. To this end, proper and positive assistance of biomaterial technology will be practically promising.

Scaffolds for tissue Engineering should be made with specific characteristics. the scaffold should be porous and biodegradable. The pore structure is necessary for the infiltration of cells into the scaffold, the supply of oxygen and nutrients to cells proliferated therein and the washout of cell wastes. Once the cell-induced tissue regeneration is naturally initiated, cells eventually produce the ECM of natural scaffold. The scaffold is a temporary platform of cell activities. The long-term retention of cell scaffold sometimes causes physical hindrance against the natural process of tissue regeneration. It is a key for successful tissue regeneration to control the time profile of scaffold biodegradation at the defect as well as the three-dimensional structure. The cell scaffold developed initially is a physical entity that does not have any functions to positively promote the proliferation and differentiation of cells. However, a new type of cell scaffold has been investigated to combine biomaterials with biological ligands reactive for cell receptors, biosignalling molecules and celladhesive substances for artificially promoted cell-based tissue regeneration [18];[19]. The mechanical property of biomaterial scaffolds is also important. If the mechanical strength is low, the scaffold readily deforms in the body. As a result, the regeneration of bulky tissue cannot be always expected. An appropriate mechanical design is much required. For example, the incorporation of fibres and ceramic granules enabled biomaterial sponges to mechanically reinforce and enhance *in vivo* tissue regeneration following the implantation of sponges combined with stem cells[20];[21]. Tissue engineering for clinical regeneration therapy can be classified as either *in vitro* or **in vivo** depending on the site where tissue regeneration or organ substitution is performed. *In vitro* tissue engineering involves tissue reconstruction by cell culture methods and organ substitution with functional cells-termed bioartificial hybrid organ. If a tissue can be reconstructed *in vitro* in factories or laboratories on a large scale, it can be supplied to patients when required. For example, human skin fibroblasts are cultured in a collagen sponge to prepare an artificial dermis for skin grafting [22];[23]. However, it is difficult to reproduce the **in vivo** event completely *in vitro* by using the basic knowledge of biology and medicine or cell culture technologies currently available. At present, it is difficult to realize *in vitro* tissue engineering because the artificial arrangement of a biological environment to induce cell-based tissue reconstruction is practically impossible. Even if a three-dimensional tissue-like construct is prepared *in vitro*, it is practically difficult to allow the construct to survive and function *in vivo* after grafting. The **in vivo** environment for the construct

implanted should be designed.

Distinct from the *in vitro* tissue engineering, *in vivo* tissue engineering is advantageous from the viewpoint of the environment to induce tissue regeneration. It is likely that most of the biological components necessary for tissue regeneration, such as growth factors and cytokines, are naturally supplied by the body. Based on this advantage, almost all the approaches of tissue engineering have been performed *in vivo* with or without biodegradable cell scaffolds.

### 2.3 SCAFFOLD DEVELOPMENT FOR CARDIOVASCULAR DISEASES

Coronary and peripheral vascular bypass are two procedures that are mostly performed with safenous vein or internal mammary artery on patients with cardiovascular diseaes [24]. Although the use of autogenous vascular substitutes has had a major impact on advancing the field of reconstructive arterial surgery, these tissue sources may be inadequate or unavailable.

The first tissue-engineered blood vessel substitute was created by Weinberg and Bell in 1986 [25]. They generated cultures of bovine endothelial cells, smooth muscle cells (SMCs) and fibroblasts in layers of collagen gel supported by a Dacron mesh. Since then, strategies to create a suitable material for a vascular graft have focused on three areas of research: coatings and surface chemical modifications of synthetic materials, biodegradable scaffolds and biopolymers. Each group can be further organized into tissue-engineering strategies for *in situ* vascular regeneration, in which the body's natural healing response is modulated by material design and fabrication, or strategies for *ex vivo* formation of a blood vessel substitute, whereby *in vitro* culture of human cells on polymer substrates before implantation defines their mechanical and biological properties [26].

Dacron is most commonly used for aortic replacement and to a lesser extent as a conduit for femoropopliteal bypass surgery. Despite some evidence that suggests that platelet deposition and complement activations[27];[28] are lower on ePTFE than Dacron prostheses, the patency rates of Dacron and ePTFE grafts are similar [29].

The use of biodegradable polymers as scaffolds on which layers of cells are grown is an alternate tissue-engineering approach for the development of a functional vascular graft. The scaffold degrades and is replaced and remodeled by the extracellular matrix (ECM) secreted by the cells. Polyglycolic acid (PGA) is commonly used in tissue-engineering applications as it degrades through hydrolysis of its ester bonds, and glycolic acid, in turn, is metabolized and eliminated as water and carbon dioxide.

Another versatile polymer is polycaprolactone (PCL) that slowly degrades by hydrolysis of ester linkages, with elimination of the resultant fragments by macrophages and giant cells. Shin'oka et al. reported the use of PCL-based scaffolds to engineer venous blood vessels [30];[31]. The PCL–polylactic acid copolymer was reinforced with woven PGA and seeded with autologous smooth muscle and endothelial cells harvested from a peripheral vein. After 10 days, the construct was implanted as a pulmonary bypass graft into a 4-year-old child [31].

An alternative strategy to synthetic and degradable scaffold-based vascular grafts is the manipulation of proteins that constitute the architecture of native ECM. One such protein is type I collagen, a major ECM component in the blood vessel. Collagen fibers function to limit high strain deformation, thereby preventing critical rupture of the vascular wall [32]. Collagen gels and fibers reconstituted from purified collagen are ideal in artificial blood vessel development due to their low inflammatory and antigenic responses. Furthermore, integrin-binding sequences in collagen allow for cell adhesion during fibrillogenesis [33]. Collagen and Elastin have been used for the preparation of scaffolds. Qijin et al selectively removes elastin and collagen from decellularized aortas in order to obtain a scaffold with adequate size and shape of pores for cell infiltration and repopulation. They characterize scaffolds and demonstrate that both the two types exhibit adequate mechanical characteristics, porosity, biodegradability and toxicity [34].

The shortcomings of a stiff collagen-based scaffold have motivated researchers to explore the potential of more elastic fibrin gels in vascular tissue engineering [35]. Fibrin is formed when fibrinogen polymerizes into a fibrillar mesh with the addition of thrombin. An advantage of this biopolymer is the ability to produce it with the patient's own blood, thereby preventing an inflammatory response upon implantation [36]. Fibrin also binds to critical proteins that direct cell fate, such as fibronectin and VEGF . In vivo degradation can be controlled with the proteinase inhibitor aprotonin and crosslinking agents, although there are concerns that the concentrated presence of these natural proteins may interfere with local coagulation cascades [37].

The elasticity afforded by fibrin-based grafts is a critical factor in vascular tissue-engineering design. Researchers have also explored the potential of incorporating scaffolds with more extensible proteins such as elastin, a key structural element in native vasculature. Crosslinked elastic fibers form concentric rings around the medial layer of arteries, providing elasticity to the vascular graft by stretching under a stress and recoiling back to the original dimensions as the load is released [38];[39]. In addition, elastin regulates vascular SMC activity by inhibiting SMC proliferation.

Unlike collagen, the stable crosslinked fiber network of native elastin makes isolation and purification techniques difficult.

Recently, the development of recombinant genetic and protein engineering has enabled the synthesis of bioinspired protein polymers that not only mimic structural proteins but also direct cellular fate by emulating the ECM in vivo. Specifically, polymers with pentapeptide repeat motifs similar to VPGVG exhibit elastic behavior with features that are consistent with native elastin, including a mobile backbone and the presence of  $\beta$  turns [40];[41]. The biosynthetic machinery of microorganisms can be exploited to produce significant quantities of these recombinant protein polymers that have been designed from primary amino acid sequences and self-assemble into a distinct 3D folded structure [42]. These elastin- mimetic biopolymers, in turn, can be cast as hydrogels or electrospun into nanofibrous scaffolds [43].

## 2.4 BIBLIOGRAPHY

- [1]-J. Lannutti, D. Reneker, T. Ma, D. Tomasko, D. Farson. *Electrospinning for tissue engineering scaffolds. Materials Science and Engineering:Volume 27, Issue 3, April 2007, Pages 504–509*
- [2]- Pinar Zorlutuna, Nasim Annabi, Gulden Camci-Unal, Mehdi Nikkhah, Jae Min Cha, Jason W. Nichol, Amir Manbachi, Hojae Bae, Shaochen Chen and Ali Khademhosseini. *Microfabricated Biomaterials for Engineering 3D.Tissues. Advanced Materials Volume 24, Issue 14, pages 1782–1804, April 10, 2012*
- [3]-Napolitano AP, Ch P, Dean DM, Morgan JR. *Dynamics of the self-assembly of complex cellular aggregates in micromolded nonadhesive hydrogels. Tissue Eng. 2007;13:2087–2094, Tavana H, Mosadegh B, Takayama S. Polymeric aqueous biphasic systems for non-contact cell printing on cells: engineering heterocellular embryonic stem cell niches. Adv Mater. 2010;22:2628–2631*
- [4]-Tavana H, Mosadegh B, Takayama S. *Polymeric aqueous biphasic systems for non-contact cell printing on cells: engineering heterocellular embryonic stem cell niches. Adv Mater. 2010;22:2628–2631*
- [5]-Tingli Lu Yuhui Li Tao Chen, *Techniques for fabrication and construction of three-dimensional scaffolds for tissue engineering. International Journal of Nanomedicine 2013;8 337–350*
- [6]-II *International Consensus Conference on Biomaterials, Chester, Great Britain, 1991*
- [7]-Heidi M. Mansour, MinJi Sohn, Abeer Al-Ghananeem and Patrick P. DeLuca. *Materials for Pharmaceutical Dosage Forms: Molecular Pharmaceutics and Controlled Release Drug Delivery Aspects. Int. J. Mol. Sci. 2010, 11, 3298-3322*
- [8]-Dimitriu, S. (1994) *Polymeric Biomaterials, Marcel Dekker, Hubbel, J. A. (1994) Trends Polym. Sci. 2, 20–25*
- [9]-Atala, A. and Mooney, D. J. (1997) *Synthetic Biodegradable Polymer Scaffolds, Birkhauser Boston, Leuschner, J. (1992) Clin. Mater. 10, 51–57).*
- [10]-Plate, N. and Vasilev, A. (1986) *Fiziologiczeski Activnie Polimeri, Himija, Moskva, Russia*
- [11]-Birkhauser Boston, Tarcha, P. J. (1991) *Polymers for Controlled Drug Delivery, CRC Press, Boca Raton, FL, USA*
- [12]-Porter JR, Ruckh TT, Popat KC. *Bone tissue engineering: a review in bone biomimetics and drug delivery strategies. Biotechnol Prog. 2009;25(6):1539–60*
- [13]-Langer R, Vacanti JP. *Tissue engineering. Science. 1993;260 (5110):920–6*
- [14]-Rosenberg MD. *Cell guidance by alterations in monomolecular films. Science. 1963;139:411–2*
- [15]-Ma Z, Kotaki M, Inai R, Ramakrishna S. *Potential of nanofiber matrix as tissue-engineering scaffolds. Tissue Eng. 2005;11(1– 2):101–9*
- [16]-Wei Ji & Yan Sun & Fang Yang & Jeroen J. P. van den Beucken & Mingwen Fan & Zhi Chen & John A. Jansen, *Pharm Res (2011) 28:1259–1272*
- [17]-M P Lutolf, J A Hubbell. *Synthetic biomaterials as instructive extracellular microenvironments for morphogenesis in tissue engineering. Nature Biotechnology 23, 47 - 55 (2005)*
- [18]-Gail Chan, David J. Mooney. *New materials for tissue engineering: towards greater control over the biological response. Trends in Biotechnology. Volume 26, Issue 7, July 2008, Pages 382–392*
- [19]-Yosuke Hiraoka, Yu Kimura, Hiroki Ueda, and Yasuhiko Tabata. *Fabrication and Biocompatibility of Collagen Sponge Reinforced with Poly(glycolic acid) Fiber. Tissue Engineering. December 2003, 9(6): 1101-1112.*
- [20]-Yoshitake Takahashi, Masaya Yamamoto, Yasuhiko Tabata. *Enhanced osteoinduction by controlled release of bone morphogenetic protein-2 from biodegradable sponge composed of gelatin and  $\beta$ -tricalcium phosphate. Biomaterials Volume 26, Issue 23, August 2005, Pages 4856–4865*

[21]-Kuroyanagi YI, Yamada N, Yamashita R, Uchinuma E. Tissue-engineered product: allogeneic cultured dermal substitute composed of spongy collagen with fibroblasts. *Artif Organs*. 2001 Mar;25(3):180-6.

[22]-Shigeru Ichioka, Sachio Kouraba, Naomoi Sekiya, Norihiko Ohura, Takashi Nakatsuka. Bone marrow-impregnated collagen matrix for wound healing: experimental evaluation in a microcirculatory model of angiogenesis, and clinical experience. *British Journal of Plastic Surgery Volume 58, Issue 8, December 2005, Pages 1124–1130*

[23]- Atsushi Urakami, Tsukasa Tsunoda, Tadahiko Kubozoe, Tomoyuki Takeo, Kazuki Yamashita and Hiroyuki Imai. Rupture of a bleeding pancreatic pseudocyst into the stomach. *Journal of Hepato-Biliary-Pancreatic Surgery Volume 9, Issue 3, pages 383–385, September 2002*

[24]- Association AH. *Hearth Diseases and Stroke Statistics-2008 update*. [www.americanheart.org](http://www.americanheart.org)

[25]-Weinberg CB, Bell E. A blood vessel model constructed from collagen and cultured vascular cells. *Science* 1986;231(4736):397–400

[26]-Swathi Ravi, Elliot L Chaikof. Biomaterials for vascular tissue engineering. *Regen Med*. 2010 January ; 5(1): 107. doi:10.2217/rme.09.77

[27]-Allen BT, Mathias CJ, Sicard GA, Welch MJ, Clark RE. Platelet deposition on vascular grafts. The accuracy of in vivo quantitation and the significance of in vivo platelet reactivity. *Ann Surg* 1986;203 (3):318–328

[28]- Shepard AD, Gelfand JA, Callow AD, O'Donnell TF Jr. Complement activation by synthetic vascular prostheses. *J Vasc Surg* 1984;1(6):829–838

[29]-Abbott W, Green R, Matsumoto T, et al. Prosthetic above-knee femoropopliteal bypass grafting: results of a multicenter randomized prospective trial. Above-Knee Femoropopliteal Study Group. *J Vasc Surg* 1997;25(1):19–28

[30]-Kim BS, Mooney DJ. Engineering smooth muscle tissue with a predefined structure. *J Biomed Mater Res* 1998;41(2):322–332

[31]-Shinoka T, Shum-Tim D, Ma PX, et al. Creation of viable pulmonary artery autografts through tissue engineering. *J Thorac Cardiovasc Surg* 1998;115(3):536–545. discussion 545–546

[32]-Watanabe M, Shin'oka T, Tohyama S, et al. Tissue-engineered vascular autograft: inferior vena cava replacement in a dog model. *Tissue Eng* 2001;7(4):429–439

[33]-Ennett AB, Kaigler D, Mooney DJ. Temporally regulated delivery of VEGF in vitro and in vivo. *J Biomed Mater Res A* 2006;79(1):176–184

[34]-Qijin Lu, Kavitha Ganesan, Dan T. Simionescu, Narendra R. Vyavahare. Novel porous aortic elastin and collagen scaffolds for tissue engineering. *Biomaterials Volume 25, Issue 22, October 2004, Pages 5227–5237*

[35]-Cummings CL, Gawlitta D, Nerema RM, Stegemann JP. Properties of engineered vascular constructs made from collagen, fibrin, and collagen–fibrin mixtures. *Biomaterials* 2004;25(17):3699–3706

[36]-Ye Q, Zünda G, Benedikta P, et al. Fibrin gel as a three dimensional matrix in cardiovascular tissue engineering. *Eur J Cardiothorac Surg* 2000;17(5):587–59

[37]-Jockenhoewel S, Zund G, Hoerstrup SP, et al. Fibrin gel advantages of a new scaffold in cardiovascular tissue engineering. *Eur J Cardiothorac Surg* 2001

[38]-Patel A, Fine B, Sandig M, Mequanint K. Elastin biosynthesis: The missing link in tissue-engineered blood vessels. *Cardiovasc Res* 2006;71(1):40–49

[39]-Silver FH, Snowhill PB, Foran DJ. Mechanical behavior of vessel wall: a comparative study of aorta, vena cava, and carotid artery. *Ann Biomed Eng* 2003;31(7):793–803

[40]-Chang DK, Urry DK. Molecular dynamics calculations on relaxed and extended states of the polypentapeptide of elastin. *Chem Phys Lett* 1988;147

**[41]**-Urry DW. *Five axioms for the functional design of peptide-based polymers as molecular machines and materials: principles for macromolecular assembly.* *Biopolymers* 1998;47:167–178

**[42]**-Nagarsekar A, Crissman J, Crissman M, Ferrari F, Cappello J, Ghandehari H. *Genetic engineering of stimuli-sensitive silkelastin-like protein block copolymers.* *Biomacromolecules* 2003;4(3):602–607

**[43]**-Wright ER, Conticello VP. *Self-assembly of block copolymers derived from elastinmimetic polypeptide sequences.* *Adv Drug Deliv Rev* 2002;54(8):1057–1073.

## 3 CHAPTER: ELECTROSPINNING



### 3.1 INTRODUCTION

*A possible application of electrospinning technique is related to the field of biomedical tissue engineering for the manufacture of three-dimensional scaffolds. In particular, by subjecting a system polymer/solvent with a suitable concentration to the action of an electric field of some Kv, it is possible to realize polymeric fibers with diameters of the order of nanometers from which are obtained by superposition of the systems 3d characterized by a structure called woven not woven; the overlap of these tissues fact makes possible the manufacture of so-called woven not woven tissues in which the fibers are arranged randomly [1]. The main advantage of these types of scaffolds lies in the possibility of cultivating the cells of different morphology (depending on the application) to their inside, through the interstices between adjacent fibers that have the same function of the porosity and which, in contact with the polymer matrix have the ability to differentiate and proliferate without encountering phenomena of apoptosis and/or cell death.*

*Up to now, a range of techniques such as drawing, template synthesis, phase separation, self-assembly, and electrospinning, etc. have been adopted to prepare nanofibers based on polymers, metals, ceramics and glass, etc [4];[5], as well as their further assemblies into two dimensional (2D) and three-dimensional (3D) nano structures for practical applications [6]. Among these techniques, electrospinning is regarded as a simple and versatile top-down approach for fabricating uniform ultrafine fibers in a continuous process and at long length scales. Since electrospinning has some advantages, such as the easy control of porosity, fiber size, and morphology, much effort has been taken to fabricate micro/nanofibers with desired morphologies, such as aligned fibrous array, fibrous patterns [7];[8].*

*Nevertheless, scalable and controllable assembly of nanofibers for 3D fibrous structures still presents a major challenge because most of the electrospun nanofibers are limited to the*

*conventional 2D membranes. In general, there are four main strategies for the fabrication of 3D electrospun fibrous macro-structures: (a) increasing spinning time; (b) assembly by post-processing of 2D electrospun fibrous structures (e.g., folding, layer-by-layer electrospinning, sintering, mechanical expansion); (c) direct assembly by an auxiliary factor (e.g., a 3D template, liquid collector); (d) self-assembly. These 3D electrospun fibrous macro-structures demonstrate many promising potential and practical approaches to the field of tissue engineering.*

### 3.2 TECHNIQUE PRINCIPLES

Electrospinning is one of the main technologies used for the creation of fibers of micrometer and nanometer scale in various fields of engineering and not only. Contrary to other spinning techniques, such as melt spinning, wet and dry spinning, which exploit the mechanical stresses resulting from the nature of the process (extrusion of the molten polymer, fiber board after solidification of polymer solutions), the electrospinning uses electrostatic forces. The principle of electrospinning operation is based on the application of a high potential difference (Kilovolt) between two electrodes; such electrodes are respectively constituted by a capillary metal (cathode) that contains the molten polymer to be processed and a plate of copper or aluminum (anode) on which takes place the collection of the fibers.

A typical electrospinning setup consists of a capillary through which the liquid to be electrospun is forced; a high voltage source with positive or negative polarity, which injects charge into the liquid; and a grounded collector. Syringe pump, gravitational forces, or pressurized gas are typically used to force the liquid through a small-diameter capillary forming a pendant drop at the tip (**fig 3.1**). An electrode from the high voltage source is then immersed in the liquid or can be directly attached to the capillary if a metal needle is used. The voltage source is then turned on and charge is injected into the polymer solution. Increasing the electric field strength causes the repulsive interactions between like charges in the liquid and the attractive forces between the oppositely charged liquid and collector to begin to exert tensile forces on the liquid, elongating the pendant drop at the tip of the capillary. As the electric field strength is increased further a point will be reached at which the electrostatic forces balance out the surface tension of the liquid leading to the development of the Taylor cone. If the applied voltage is increased beyond this point a fiber jet will be ejected from the apex of the cone and be accelerated toward the grounded collector [9]. While the fiber jet is accelerated through the atmosphere toward the collector it undergoes a chaotic bending instability, thereby increasing the transit time and the path length to the collector and aiding in the fiber thinning and solvent evaporation processes.

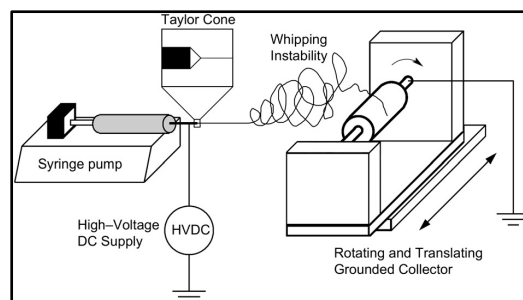


**Figure 3.1 Schematic of Electrospinning Set-Up**

The electrospinning process presents an electrified fluid dynamics related problem. In order to control the morphology, structure, and mass production of the electrospun nanofibers, it is necessary to understand quantitatively how the electrospinning process transforms the fluid solution through a millimeter diameter capillary tube into solid micro/nanofibers which are four to five orders of magnitude smaller in diameter. Recent theoretical and experimental studies have demonstrated that the electrospinning process generally consists of three stages: (1) jet initiation and elongation of the charged jet along a straight line; (2) growth of electrical bending instability (also known as whipping instability) and further elongation of the jet, which may or may not be accompanied with the jet branching and/or splitting; (3) solidification of the jet into micro/nanofibers and deposition on collector.

As what concerns the jet initiation and straight elongation, the electric force has been identified as the driving force for initiating an electrospinning process. In needle electrospinning, under the influence of electric force, the charged solution droplet at the needle tip reduces its size so that the force balance is maintained. With an increase in the applied voltage, the shape of the solution droplet evolves from the hemisphere to a cone shape (Taylor cone) with a high electric force concentrated at the tip of the Taylor cone [10]. When the electric field reaches a critical voltage  $V_c$ , the droplet at the cone tip overcomes its surface tension to eject into the electric field, and a solution jet is thus generated. According to Taylor's calculation, the critical voltage  $V_c$  (expressed in kilovolts) for electrospinning is given by:

$$V^2 c = 4 \frac{H^2}{h^2} \left( \ln \left( \frac{2H}{R} \right) - 1.5 \right) \left( \frac{1}{3} \pi R \gamma \right) \quad (0.09)$$

where  $H$  is the distance from the needle tip to the collecting screen,  $h$  is the length of the liquid column,  $R$  is the needle outer radius, and  $\gamma$  is the surface tension of the solution (units:  $H$ ,  $h$  and  $R$  in cm,  $\gamma$  in dyn per cm); the factor 0.09 is inserted to express the voltage in kilovolts [10].

The critical electric field intensity for electrospinning nanofibers was proposed as:

$$E_c = \sqrt[4]{4\gamma\rho g / \epsilon^2}$$

where  $\rho$  is the liquid mass density,  $g$  is the gravity acceleration,  $\gamma$  is the surface tension of the solution,  $\epsilon$  is the permittivity. In both the models, electric force plays a crucial role in the jet initiation. Before the growth of electrical bending instability, the straight, tapered segment of the jet leaving the tip is accelerated as the Coulomb forces, acting on the charges carried with the leading

segments, pull the jet toward the collector. The velocity of the electrospinning jet has been estimated using a moving substrate and high-speed camera to be about 1–15 m s<sup>-1</sup> [10]; [11]. The critical length of the straight jet (L) in electrospinning also can be estimated by the following equation proposed by He et al. [10]; [12]:

$$L = \frac{4kQ^3}{\pi\rho^2I^2} (R_0^{-2} - r_0^{-2})$$

where  $R_0 = (2Q/kE)^{1/3}$ , Q is the flow rate,  $\sigma$  is the surface charge, k is the dimensionless conductivity, E is the applied electric field, I is the current passing through the jet,  $\rho$  is the liquid density and  $r_0$  is the initial radius of the jet. It is found that the theoretic prediction was in well agreement with the experimental observations for poly(hydroxybutyrate-co-valerate) (PHBV) and cellulose solutions.

As the diameter of the jet, in the straight segment, decreases monotonically with distance from the tip, the jet becomes very long and thin, and the characteristic time required for excess charge to redistribute itself along the full length of the jet becomes longer. The location of excess charge, within or on the fluid, then tends to change with the elongation, bending and otherwise deforming the jet. That means the long jet becomes unstable due to the growth of various instabilities. Recent studies have demonstrated that the key role in reducing the jet diameter from a micrometer to a nanometer is played by a non axisymmetric or electrically driven bending instability, which causes bending and stretching of the jet at very high frequencies.

These studies investigate mathematical exposition and asymptotic analysis to model the instabilities. It was found that there are three types of instability. The first one is the classical Rayleigh instability; it concerns asymmetric instability dominated by the surface tension and suppressed at high electrical field  $E_0$  and the surface charge density  $\sigma$  exceed a threshold given by:

$$(\varepsilon - \varepsilon')E_0^2 + \frac{4\pi^2\sigma^2}{\varepsilon'} = 2\pi\gamma/h$$

where  $\gamma$  is the surface tension, h is the radius of the jet,  $\varepsilon$  and  $\varepsilon'$  are the dielectric constant inside and outside the jet separately, and  $\varepsilon/\varepsilon'$ . The second type of instability is another asymmetric instability that occurs at high electric field than the Rayleigh instability. The third type of instability is referred to the long wave perturbation of a liquid column driven by the electrical force and aerodynamic interaction at high electric field [10].

Other two instabilities are due to the fluctuations in the dipolar component of the charge distribution. They are electrically driven and essentially independent of the surface tension of the liquid. It is

noted that the electric field strength will be proportional to the instability level. Namely, the Rayleigh instability occurs when the electric field is the lowest, whereas the bending instability corresponds to the highest electric field [10];[13].

Although electrospinning is relatively simple to use, there are many parameters that can greatly influence the transformation of the polymer solution into nanofibers. These parameters could be divided into two groups:

- Parameters that are related to the polymer/ solvent chemical properties
- Parameters related to the process

Parameters related to polymer and solvent properties include viscosity, conductivity, surface tension, molecular weight of the polymer, boiling point while parameters that are related to the process are working voltage applied, distance between the tip and the collector surface and polymer flow rate. There is another category of parameters that influences the obtaining of fibers: this category is related to the ambient parameters such as solution temperature and humidity. The effects of electrospinning parameters are a key aspect for the obtaining and the optimization of fiber morphology. All the parameters have been widely explored for different systems. For example, Zheng et al. [14] carried out a series of experiments to study the influence of processing variables (solution concentration, spinning distance, collecting position and humidity) on the formation of near-field electrospun polyvinyl pyrrolidone (PVP) with a working voltage of less than 2.8 kV and a spinning distance of less than 10 mm. They found that no fibers were collected when the PVP concentration was too low (<20 wt%) to attach to the spinning tip or the PVP concentration was too high (>40 wt%) to produce a spinning jet electrospinning [15].

In addition to viscosity (solution concentration), the effects of other parameters such as flow rate, distance from nozzle to collector, initial jet/orifice radius, electric potential, relative humidity, etc. on nanofiber diameter have been explored systematically by Thompson et al. [16].

- a. Initial jet/orifice radius: decreasing orifice radius tends to decrease the average fiber diameters (e.g., average fiber diameters of 250, 150 and 125 nm for orifices of radii 0.59, 0.42 and 0.29 mm, respectively) [17].
- b. Flow rate: increasing flow rate tends to increase fiber diameter [18];[19].
- c. Distance from nozzle to collector: average fiber diameters tend to decrease with increase in collector distance [18];[19];[20]. For example, Nylon-6 fiber diameters decrease from 230

to 140 nm with spinning distance changing from 4 to 18 cm, holding other parameters constant [20].

- d. Polymer concentration: Nylon-6 fiber diameters increase from 80 to 230 nm when increasing initial polymer concentration from 10 to 25%
- e. Applied voltage: in general, a higher applied voltage ejects more fluid in a jet, resulting in a larger fiber diameter [21];[22].
- f. Vapor diffusivity: lower evaporating solvent allowing for longer stretching process before jet solidification taking place, and thus for thinner fibers
- g. Relative humidity: as the relative humidity increases, the solidification process becomes slower, allowing elongation of the charged jet to continue longer and thereby to form thinner fibers. For example, as the relative humidity increases from 5.1% to 48.7%, the diameter of the solidified PEO fibers decreases from 253 to 144 nm [23].
- h. Solution conductivity: increasing solution conductivity tends to decrease fiber diameter due to increase in electrical charge carried by the jet and thus tensile force in the presence of an electric field. For example, by adding increasing concentrations of NaCl (ranging from 0.05 to 0.2%, the corresponding solution conductivity increased from 1.53 to 10.5 mS/cm), Zhang et al. were able to decrease the mean fiber diameter from  $214 \pm 19$  to  $159 \pm 21$  nm.
- i. Surface tension: the effect of surface tension is negligibly small for most properly chosen electrospun solutions, where the viscoelastic forces completely dominate the surface tension [16]. However, for higher surface tension solvents like water, low viscosity and low conductivity/charge density systems beaded fibers tend to form.

Several approaches to electrospinning 3D fibrous macro-structures have been realized. As shown in Fig. , one simple way is sequential electrospinning or multilayering electrospinning. In this way, electrospun fiber membrane with a certain thickness will be obtained, which can reach hundreds of microns and become a 3D fibrous structure, although these methods may take a long time (for example, from 20 min to 20 h) till it grows to a sufficient 3D structure. Another way is post-processing of the electrospun fibers, such as peeling off the thin film from the collector, and then bending/folding or stacking the fiber layers into a 3D fibrous structure like pipe or thick mat. In addition, 3D fiber structures can be also successfully obtained through modification of the collector, for example, replacing the conventional 2D flat collector by a 3D collecting template). In addition, other method such as using liquid collection and removing microparticles filled between nanofibers have been reported, although a subsequent treatment to dry the as-prepared 3D structures or handle with the porogen is usually needed. Furthermore, by controlling some parameters during the

electrospinning process (e.g., the solution concentration/viscosity, electrostatic field, ambient humidity), a rapid growth (or self-assembly) of 3D fibrous macro-structures has been achieved without any additional assistance (e.g., fibrous yarns or spongiform fiber stacks), as shown in **fig. 3.2**.

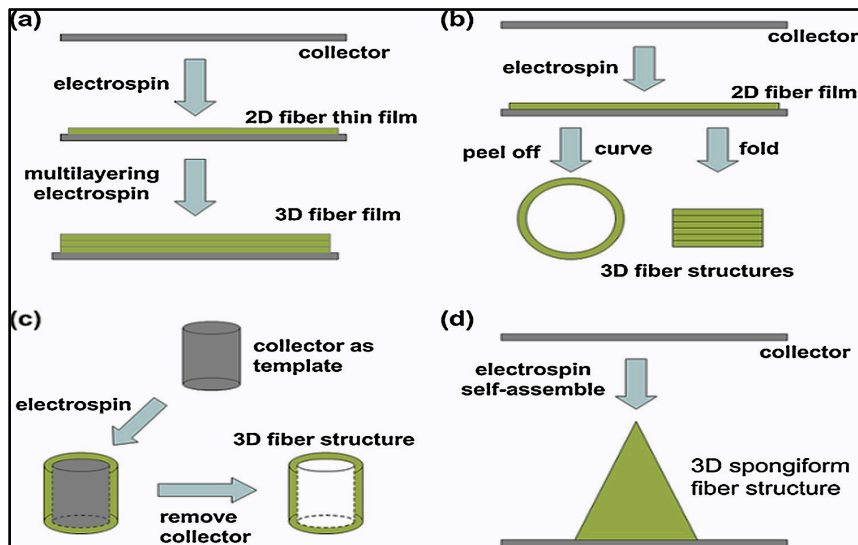


**Figure 3.2** Schematic illustration of several approaches to fabricate 3D nanofibrous structures via electrospinning: (a) multilayer electrospinning; (b) folding or stacking 2D fiber films; (c) using a 3D collecting template; (d) self-assembly.

### *3.3 ELECTROSPINNING SCAFFOLD PRODUCTION: TISSUE ENGINEERING VASCULAR GRAFTS (TEVG)*

Nowadays, biomaterials are commonly used in various medical devices and systems: synthetic skin, drug delivery systems, tissue cultures, hybrid organs, synthetic blood vessels, artificial hearts, cardiac pacemakers, screws, plates, wires and pins for bone treatments, total artificial joint implants, skull reconstruction, and dental and maxillofacial applications [24].

The use of cardiovascular biomaterials (CB) is subjected to its blood compatibility and its integration with the surrounding environment where it is implanted [25]. Whenever, CB is used, two important considerations should be weighed equally; namely, (1) physical and mechanical features such as strength and deformation, fatigue and creep, friction and wear resistance, flow resistance and pressure drop, and other characteristics to be engineered must be considered and (2) biocompatibility or compatibility refers to material and tissue interactions are also to be considered. These characteristics have to be tested and appraised in an array of in vivo and in vitro experiments [26]. The first aspect mentioned is almost predetermined depending on the material chosen and its inherent properties. However, the second aspect biocompatibility is of immense interest for every cardiac implant material chosen and it decides the patency of the same [27].

Cardiovascular biomaterials are used in two modes, namely, temporary and permanent [10]. Based upon mode of use, cardiovascular devices can be classified as temporary internal, temporary external, and permanent internal devices [28]. Testing of compatibility of cardiovascular devices largely depends upon the mode of use. All CB comes with contact with blood and this duration of contact further determines the testing parameters. Contact duration may be limited (less than 24 h), prolonged (>24 h to 30 days), and permanent (>30 days). Blood compatibility is to be evaluated for all blood contacting devices irrespective of the contact duration. According to ISO-10993, thrombogenicity, hemolysis, and immunology (complement activation) testing has to be performed for these devices [29]. One of the leading causes of cardiac biomaterial failure is the initiation of thrombosis formation by the blood contacting devices [30]. The mechanism underlying thrombus formation is discussed briefly for understanding the reason behind the cardiac device failure. Adsorption of proteins on the surface of implanted cardiac biomaterial through intrinsic pathway or through the release of tissue factor from the damaged cells at the site of injury (extrinsic pathway) is the initial event leading to thrombosis. The intrinsic pathway (Fig 3.3) is independent of injury and the adsorbed surface proteins form a complex comprising collagen, highmolecular weight kininogen

(HMWK), prekallikrein, and factor XII. Cardiovascular application of biomaterials includes metals and their alloys, polymers, and some biological materials [32].

Cardiovascular stents are synthetic materials scaffolds used to expand and/or support blood carrying vessels. The first clinical application of a metallic stents was performed in 1986 by Sigwart [34]. Since then, stents have been used in a majority of percutaneous coronary interventions because they can be delivered via minimally invasive surgery resulting in rapid recovery times and with less surgical risk. So far, stents have been made of metals such as stainless steel, tantalum, nitinol, cobalt alloy and platinum iridium; however they suffer from limited flexibility, stiffness mismatch, compliance mismatch, thrombogenicity and intima proliferation etc. [35]. Therefore a polymer coating on metal stents is usually used to improve its biocompatibility and/or load drugs to improve restenosis complications. Small-diameter vascular grafts (SMVGs) ( $D < 6$  mm) are increasingly needed in the clinic for coronary disease and hemodialysis. Unfortunately, the acute thrombosis and subsequent occlusion often lead to the failure of the transplantation when commercialized poly(ethylene terephthalate) (Dacron) or expanded poly(tetrafluoroethylene)(e-PTFE) vascular grafts were used

Tissue Engineering is an alternative approach for creating new vascular grafts. Tissue Engineering Vascular Grafts are a particular type of grafts, mainly made of biodegradable polymers that can be seeded with cells. In this regard, development of vascular grafts with slow degradation and controlled regenerative process has become a new concept and direction. These grafts provide a favorable environment for the recruitment of autogenous vascular cells. After a full degradation of the polymer scaffold, “neo-artery” could be generated [36].

It is crucial that TEVG functions, i.e. gets integrated to the adjacent blood vessels, sustains the load from blood pressure and allows blood flow without leakage, immediately after implantation. Biocompatibility and bioactivity are other primary requirements for engineering vascular grafts. In addition, the mechanical properties, adhesive ligands, growth factor presentation, transport and degradation kinetics of the materials used for the scaffold should mimic the relevant ECM environment to a reasonable extent. It is favorable to use cost-effective and cytocompatible materials with tunable properties for a particular tissue.

The most promising type of vascular grafts are degradable electrospun grafts which have good biocompatibility and mechanical properties. Electrospinning offers the ability to fine-tune mechanical properties during the fabrication process, while also controlling the necessary biocompatibility and structure of the tissue engineered grafts. The ability of the electrospinning

technique to combine the advantages of synthetic and natural materials makes it particularly attractive for TEVG, where a high mechanical durability, in terms of high burst strength and compliance (strain per unit load), is required. In addition, the incorporation of natural polymers, with an abundance of cell binding sites, can promote the formation of a continuous monolayer of EC in the lumen and proliferation of other cell types in the matrix of the graft's wall [37].

The electrospinning technique also offers precise control over the composition, dimension and alignment of fibers that have impact on the porosity, pore size distribution and architecture of scaffolds. This method allows for engineering of a wide range of tunable structural and mechanical properties as required for specific applications. Moreover, aligned nanofibers can be used for orienting cells in a specific direction necessary to provide the anisotropy encountered in certain organs including blood vessels. Companies have recently commenced the fabrication of electrospun grafts for transplantation of trachea, and other tissue engineered conduit. The world's first tissue engineered tracheal transplant was successfully used in a clinical trial in Sweden in June 2011 [38];[39].

Electrospun vascular grafts can be obtained using various polymers that can allow cellular infiltration and revascularization of the vessel. Cellularization of the vascular graft, also known as engraftment, is a key factor for the tissue regeneration and remodeling. However, one major problem associated with electrospinning is the small pores, which often result in insufficient cell infiltration. To solve this problem, various techniques have been tested to increase pore size and overall porosity, including the salt/ polymer leaching [40];[41], modification of collector apparatus, post treatment by laser radiation [42]. In addition, adjusting the electrospinning parameters can control the scaffold porosity. It has been reported that the pore size is closely related to the fiber diameter of electrospun mats, which means that the pore size increases with the increase of the fiber diameter. During electrospinning, the fiber diameter can be readily controlled by changing the parameters, such as the concentration of the polymer solution, voltage, solvent, etc

### *3.4 MATERIALS FOR TISSUE ENGINEERING VASCULAR GRAFTS: ELASTIN LIKE POLYMERS AND SILK*

Regenerative medicine aims to treat patients through the use of materials that do not cause toxic or inflammatory reactions; in this context, numerous synthetic biodegradable polymers, such as PCL or PLGA have been used for the production of scaffolds. One of the most common disadvantages due to use of these scaffolds lies in the fact that, despite being degraded within the body, they are hardly recognized by the cells and, consequently, do not allow the infiltration inside them. For this reason, recently the production of scaffolds for regenerative medicine mainly focuses on the use of fibrous proteins that mimic the structure of the extracellular matrix.

One of the most abundant proteins present in the body and used as material for the manufacture of scaffold is elastin. Elastin is a structural protein that is found in all connective tissues of vertebrates. It has many functions, among which the main is to give elastic resistance to the tissues that contain it, such as large elastic blood vessels(aorta), elastic ligaments, lungs and skin which are subjected to repetitive and reversible deformation. [43];[44];[45] The ability to go to meet different types of deformations and stresses that are not able to cause breakage, makes it one of the most suitable candidate in the field of tissue regeneration and wound healing.

Elastin is an insoluble, polymeric, extracellular matrix protein that provides tissues, including the lungs, the skin, and the arteries, with the properties of extensibility and elastic recoil. Mechanically, the polymeric elastin matrix is extremely durable. For example, in the large arteries elastin can undergo billions of loading and unloading cycles without failure [46].

Elastin is synthesized as tropoelastin, the 70 kDa soluble precursor to insoluble elastin.

The formation of elastin from the tropoelastin, is a complex process that involves a great number of factors and it's suggested begins as tropoelastin is escorted through the intracellular compartments and presented on the cellular surface of elastic binding proteins. [47];[48].

Tropoelastin is synthesised in the rough endoplasmatic reticulum and undergoes few intracellular post translational modifications, including release of the signal peptide and hydroxylation of some Pro residues by the enzyme prolyl-hydroxylase. Intracellularly, tropoelastin is immediately bound to the 67 kDa elastin-binding protein to prevent intracellular aggregation [48]. This chaperone is also a subunit of the elastin–laminin receptor and is present on many cell types, including

fibroblasts, vascular smooth muscle cells, endothelial cells, chondrocytes, monocytes, lymphocytes and polymorphonuclear leukocytes [49]. The receptor is composed of two transmembrane subunits of 61 and 55 kDa and the 67 kDa elastin binding protein and has a binding site for elastin or laminin and for a galactoside (e.g. lactose or a glycosaminoglycan like chondroitin sulphate or dermatan sulphate) [50];[47]. The elastin-binding protein only releases tropoelastin upon binding of the galactosugars of the microfibrillar component in the extracellular space. The binding for both tropoelastin and its membrane-bound 55 kDa subunit is then reduced resulting in the release of tropoelastin from the elastin-binding protein and the release of the elastin binding protein from the transmembrane subunit after which this is recycled [48];[51]. Outside the cell, the extracellular components acts like scaffolds for the deposition of elastin; the microfibrils ending up and around the elastic fibers. The tropoelastin is crosslinked by an enzyme, the Lysyl-Oxidase with the involving of vitamin B6 and copper; this result in the formation of specific interchain links like (iso)desmosine (**fig 3.3**). The crosslink procedure result in the formation of the insoluble and stable elastin.

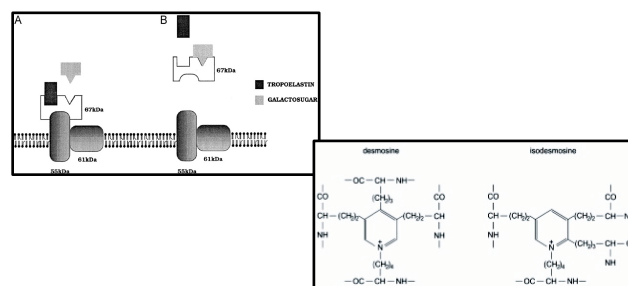
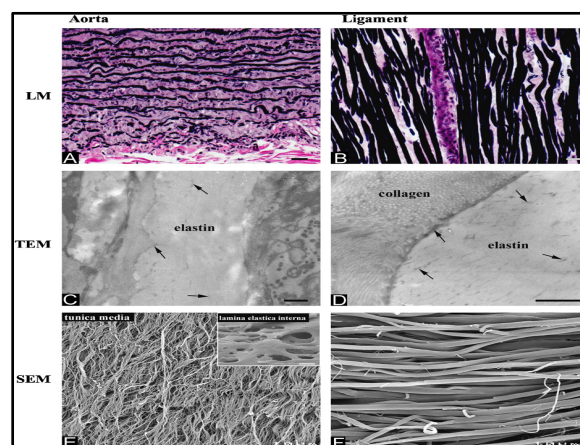


**Figure 3.3 Crosslink mechanism and formation of Desmosine and (Iso)Desmosine [48];[51]**

Elastin is differently distributed in tissues (e.g. up to 70% in elastic ligaments, 50% in large arteries, 30% in lungs) and is present as rope like structures in the media of elastic arteries and skin (**fig 3.4**) [52];[53].Figure 3.4



**Spatial distribution of Elastin in tissues [52];[53]**

Elastin is a very hydrophobic protein, where 75% of its sequence consists of four non-polar amino acids such as Gly (Glycine), Ala (Alanine), Val (Valine), Pro (Proline) [54]. Elastin can be used as biomaterial in different forms (including insoluble elastin, but is not widely used like other proteins such as silk or collagen. It is also potentially used in all the applications where the elasticity and resilience are basic requirements.

Historically, elastin was very difficult to isolate, purify and characterize. First of all, elastin is synthesized as monomer, Tropoelastin, which undergoes chemically crosslink by Lysyl-Oxidase that generates two stable molecules, Desmosine and (iso)Desmosine. These crosslinked structures are stable and it means that mature elastin is insoluble in all reagents except those that hydrolyze peptide bonds. Elastin interacts even with glycosaminoglycans through its C-terminal, GRKRRK [55]. Moreover, elastin has a great number of binding sites for other molecules: it interacts with elastic binding proteins (a transmembrane receptor mainly involved in cellular behaviour like migration, proliferation and differentiation) [56].

Another important aspect is given by the process of calcification, a process that often occurring with cardiovascular prosthetic implants [57].

To overcome these problems, from the mid of 1990 with the help provided by biotechnology, human elastin was achieved using a Bacterial system, lysogenic *E. coli* host AR120 [58] but the product was not stable. Even introducing some modifications in the manufacturing procedure, the yield of protein expression was really poor (2-4 mg x L).

A new approach, was that, rather than using the native coding sequence for the human elastin gene, a fully synthetic gene of 2100 bp was constructed that coded for the same protein sequence but had a different codon distribution optimized for expression in *E. coli* [59]. The key feature of this approach was to match the synthetic gene codon usage pattern to the *E. coli* host, since in the human sequence at least one-third of the codons are rare, expression-limiting codons in *E. coli*.

Recombinant technology allows for the production of many different materials. In particular, the repetitive structure of Elastin has led to development of polymers based on hydrophilic-hydrophobic short peptides derived from the native sequence [60];[61].

The elastin like polypeptides found very useful in the field of tissue engineering not only because biodegradable and biocompatible but also because, thanks to biotechnology techniques with which they are produced, their structure can be precisely defined, affording exquisite control over final protein functionality [62].

Elastin-like polypeptides are artificial repetitive peptides derived from mammalian elastin. They consist of a repeating pentapeptide, VAL-PRO-GLY-Xaa-GLY, where Xaa termed guess residue is any natural aminoacid, except [63]. Elastin-like polypeptides (ELP) are environmentally responsive polymers that exhibit phase separation in response to external stimuli such as temperature, pH, light, and ionic strength. It has been shown that the sequence of the pentapeptide, its length, and the solution concentration are very important in the transition of the molecules from soluble to insoluble.

ELPs are of considerable interest as scaffolds for tissue engineering as they possess unique characteristics. An advantage unique to ELPs and other repetitive polypeptides is the ability to design the peptide sequence at the genetic level. Incorporation of genetically encoded moieties for chemical or physical crosslinking to form networks as well as sites for controlled degradation or ligand presentation both add to the functionality of ELP for tissue engineering [64];[65];[66]. These attributes of ELPs have led to their use in tissue engineering and regenerative medicine for cartilage and intervertebral disc tissue repair, small-diameter vascular grafts, urinary bladders, stem cell matrices, neural guides, post-surgical wound treatment, and generation of stem cell sheets [67];[68]. In addition, multimeric blocks of ELPs with various integrin binding domains have shown promise as an artificial extracellular matrix (ECM) for small diameter vascular grafts[69].

One of the most important properties of these molecules that determines their “smart” nature is the lower critical solution temperature (LCST). The LCST is such that, below it, the polypeptides are soluble, while above it, become insoluble and form coacervates.

Urry and coworkers first studied small elastin like polypeptides (GVGVP)<sub>n</sub>.(GVGVP)<sub>251</sub>. These molecules are soluble and disordered in water at temperatures below 25 °C. In this dissolved state in water the aliphatic side chains are completely surrounded by hydrophobic hydration. On raising the temperature above a critical value, called T<sub>t</sub>, (GVGVP)<sub>n</sub> phase separates and self-assembles by hydrophobic association to form a state that is 63% water/37% polypentapeptide by weight(B). On standing at 70 °C the hydrophobically self-assembled state slowly denatures [70].

The transition temperature of the ELP mainly depends on the chain length, by the concentration of the solution and the structure of the polypeptides. The combination of these three factors is used for the synthesis of specific molecules. The production of this type of molecules is in response to factors such as pH, temperature, ionic concentration and light. One of the first studies by Urry et al. focused on the relationship between the change in transition temperature of ELP and the hydrophobicity of the aminoacid residue in the sequence –VPGXG [71]. This work shows that there

is a predictable relation between the temperature transition and the hydrophobicity of the guest amino acid. The chemical nature of this residue influences the transition temperature reverse; the more hydrophobic residue, the more the transition temperature decreases.

The change in the transition temperature results in a change of the molecular arrangement of ELP.

In particular, Urry and Cabello conducted a study on the thermal properties of these polymers demonstrating that the change in temperature determines a new molecular arrangement [72]. In particular, based on the model proposed by Urry, the change of the structure that has not just the polymer approaches its temperature transition, determines the transition from a  $\beta$ -turn structure to a  $\beta$ -spiral structure (helical arrangement typical of the  $\beta$ -turn). These same structures are further stabilized by the formation of trimers, said twisted coils [73].

Numerous studies have been conducted in order to investigate the phenomenon, especially using CD and FTIR. It was seen that at high temperatures, the structure of the polypeptides is mainly formed by  $\beta$ -turn. Still, in agreement with the model proposed by Urry, it has been shown that increasing the temperature above the transition temperature, the molecules organize themselves to form  $\beta$ -sheets [74].

Subsequently it was shown that for small ELP in a temperature range between 0 and 42 degrees, there are numerous structures of type  $\beta$ -turn, below and above this temperature, and that even in the presence of the other polymer chains, only a small of these has an arrangement II- $\beta$  beta strand type [75].

Some researchers used elastin-like polypeptide sequences other than VPGVG to study the conformational change of the chains through the transition. One of this molecule was (LGGVG)<sub>n</sub> that was studied by Martino et al [76]. They first studied this ELP using CD spectroscopy and transmission electron microscopy. They suggested that the sequence XGGXG better represent elastin molecules as it illustrates what they called “sliding  $\beta$ -turn” [77]. They showed that a simultaneous presence of different conformations can be observed for this construct which includes type II  $\beta$ -turns, type I  $\beta$ -turns, and unordered structure and makes this ELP a structurally heterogeneous biopolymer. Making TEM analysis, they have also demonstrated, albeit in organic solvents and not in water, the presence of different structures twisted rope aggregates [78]. The use of organic solvents such as TFE and HFP has been shown to influence the structure to form structures of type II  $\beta$ -turns [78].

Although many of the studies conducted by Urry et al. have been carried out on small cyclic peptides, it is evident that within the same sample there is a heterogeneity of species with different molecular arrangement, in response to temperature changes. In particular, II- $\beta$ -turns, III- $\beta$ -turns and  $\beta$ -strand are present in the sample that has not yet reached the transition temperature. As the temperature increases, and above the transition temperature there is an increase of the III- $\beta$ -turns species [79].

In determining the molecular arrangement of the polypeptides ELP, a crucial role is played by water. The more hydrophobic polypeptides, in fact, are surrounded by water molecules, named water of hydrophobic hydration. At low temperatures, the water of hydration hydrophobic form shells around the surface of the molecules; increasing the temperature, these structures are broken and part of the molecule is exposed to water [80]. The hydrophobic residues that are in contact with the water guide the process of formation of the aggregates, as soon as it reaches the transition temperature. The fact that the transition of biomolecules from soluble to insoluble correlates with the reordering of waters around the molecules was used to relate the transition temperature of ELPs to the water of hydrophobic hydration. It has been suggested that even the thermal characteristics of the water of hydrophobic hydration is different from that of the bulk water [71].

The water of hydrophobic hydration and its role in changing the transition temperature of ELP polymers has been subjected to many type of studies. For example, Cabello et al. studied a small polypeptide (VPGVG) with the aim of better understanding the folding and the structure of this protein. Using differential scanning calorimetry studies they study the structure of clathrate-like structure that are present in conditions of water deficiency and in excess of water. They show that these clusters of water are distributed in a non homogeneous fashion with a broad range of energy distribution [81].

Not only the water around the small polypeptide have a big role in affecting the reverse transition temperature but even the presence and concentration of salt within the ELP solution. Salts in general affect the solubility of these proteins following the Hofmeister series [82]. Traditionally these salts cause changes in hydrogen bonding among the bulk water molecules; more recent investigations suggest that the ions interacts with the biomolecules itself which results in an interfacial change between these molecules and their surrounding water molecules [83]. This different interaction causes the water molecule clusters around the biomolecule to arrange differently and so in the case of ELP molecules these interfacial waters affect the transition temperature of the polypeptides [83].

Shortly, there are abundant evidence that the water affects the transition temperature, the stability and the molecular arrangement of ELP molecules, both below and above their reverse transition temperature. Many other factors, like the salt concentration and the identity of the molecule affects the structure stability of water molecules around the ELP chains [84].

The structural study of polypeptides ELP carried out by Urry et al. first allowed to study the properties of these polymers in response to temperature change. He was the first, in fact, determined the physical transformation which undergo polypeptides, taking as model a small molecule peptide comprising the aminoacids -VPGVG. Using this molecule model, they first showed the physical transformation of the ELP from low temperatures to temperatures above its transition and based on that that these molecules which are highly hydrated below their transition temperature, start to lose water above  $T_t$  and make a coacervate of about 37% polypeptide but then at even higher temperature there is a denaturation process that ends up losing more water to the point that the coacervate consists of about 68% protein [85].

In general two methods are used for the production of Elastin-like-polypeptides; the first one is the chemical synthesis and the latter is the biotechnological synthesis [84].

The solid state chemistry is the chemical method employed to obtain the elastin-like-peptides. In particular, F-Moc and Boc protected solid state chemistry have been used for the manufacturing of the polypeptides [86]. The disadvantage of this method was the difficulty to produce long peptides molecules.

Thanks to molecular biology and the ability to manipulate genes, the researchers had the ability to design molecules with specific characteristics and the desired length. As regards the elastin like polymers, due to their repetitive structure, they lend themselves easily to being synthesized biotechnologically. The main two approaches are: concatemerization and directional ligation.

In the concatemerization, a double stranded DNA sequence with two well-defined identical sticky ends is constructed using two single stranded forward and reversed sequence DNAs. The existence of the same sticky ends on both sides of the gene causes the ligation process to result in a random distribution of different lengths of the gene. The ligated DNA sequences with different lengths would then be used as the insert into a vector DNA digested at the same recognition cut sites as the two sticky ends of the annealed insert. The genes should then be separated based on their molecular weight. This is a random process and would result in a range of gene sequences with different molecular weights. This process can be specifically useful if different lengths of the gene is needed

at once but there would be little to no control over what fraction of the end product would have a specific molecular weight [87];[84].

The other gene engineering approach is directional ligation. This method became popular when Capello et al. showed that it was applicable on silk-elastin like proteins [88]. a double stranded DNA sequence with two different sticky ends is inserted into a linear vector which is doubly digested with the same two restriction enzymes of the insert DNA sequence. This plasmid is then amplified in vivo in a host bacterial cell. For the next step, two populations of the same plasmid would be used such that one population is cut at both sides of the insert and the other population is cut only at one side such that it provides proper sticky ends for the insert DNA to be ligated to this linear plasmid. The result of the ligation of these two pieces of DNA would be a plasmid DNA of twice the size of the original DNA sequence. In theory this process can be repeated as many times as desired to result in long DNA sequences [89]. The most important features of this technique is the absolute control over the chemical identity and the length of the genes. Even the monodispersity of the product is another important advantage while the main disadvantage is the expensiveness to scale up the process [84].

Elastin in tissue engineering can originate from naturally occurring matrices like the elastin in autografts, allografts, xenografts, and decellularized extracellular matrices or from synthetic sources like elastin-like polypeptides [90] and they have been used in a range of applications like skin substitutes and wound healing [91];[92], vascular grafts [93];[94] liver tissue repair [95], and artificial extracellular matrices [96].

Previous work mainly made by Urry et al. shows the possibility to insert cell recognition sequence to enhance the adhesion and proliferation of cells. They first use and insert an RGD peptide into the molecular ELP chain and did the first in vitro study [97]. Although in many cases the elastin like polymers are used in their uncrosslinked form, for a proper cell growth within the scaffold is necessary to synthesize the scaffold that will then be modified in order to allow the penetration of the cells inside and their growth. For this reason, the ELP scaffolds have been widely fabricated with different crosslinking methods in forms of gels [98], fibers [99], and films [100].

ELP are good candidates for the design of small vascular grafts, thanks to their tunable characteristics and their biocompatibility. In fact, all the vascular grafts and blood vessels have been synthesized with the use of biomaterials but most of all are synthetic biomaterials that leads to immunogenic response, thrombogenicity, inflammations and platelet activation [101];[102].

To overcome all these problems, Tirrell et al. first synthesized ELP molecules containing RGD and CS5 to be used as artificial extra cellular matrix and studied endothelial cell adhesion for vascular graft applications [103]. They show that the RGD sequence was a good choice to improve cell adhesion.

To combine different characteristics such as elasticity and strength in a single material, some groups produced elastin scaffolds using electrospinning. Wise et al., in 2011, synthesized a scaffold by electrospinning human tropoelastin and polycaprolactate. They show an enhanced endothelial recognition and low thrombogenicity [104]. Girotti et al. realized an electrospun scaffold using ELP with a bioactive RGD sequence. They cultured fibroblasts upon films with RGD and with a non-bioactivated control (IKA<sub>24</sub>); for the RGD one they found a good biocompatibility and low mortality of cells [105].

In order to obtain a small TEVG, as reported in previous work by..., we use two different polymers synthesized in Valladolid by BIOFORGE, UVA-TPNTB. The recombinants used in this work are the biofunctionalized ELR known as RGD6 and REDV. RGD6 (**fig 3.5**) contains six equally spaced units of the fibronectin-derived RGD domain along the recombinant chain, which represent the primary integrin-binding sequence and the amino acids that maintain the optimal conformation for interacting with integrins. These cell binding domains are escorted by VPGIG/VPGKG pentapeptide block repeats that confer elastomeric properties on the resulting polymer and crosslinking through lysine residues [105].



**Figure 3.5 Amino acid sequence of Elastin like polypeptides: a) RGD bioactivated polypeptide; b) REDV bioactivated polypeptide**

The other polypeptide include the CS5 cell-binding domain from fibronectin, which contains the REDV domain that has been shown to be important for endothelial cell binding. The CS5 domain is incorporated into the recombinant polymer that included ELP sequences.

It's known that wound healing and tumor growth require active endothelial proliferation, a process referred as neo-angiogenesis. Neoangiogenesis involves the recruitment of endothelial cells to the site of injury or to the tumor vascular bed. Two possible sources of endothelial cells are: endothelial migration and sprouting from preexisting endothelial cells or the recruitment of endothelial precursor cells from the circulation. In order to facilitate their recruitment, cells possess integrin on their surface. Integrins are heterodimeric proteinaceous molecules consist of alpha and beta

monomers covalently linked not the function of which is to mediate cell adhesion and adjust some of signaling processes. Some integrins have been unequivocally linked to diseases such as cancer, infections, certain autoimmune diseases and processes of thrombosis. The integrin alpha 4 beta 1 is primarily known to be expressed on leukocytes and is known to be the receptor VCAM-1, fibronectin and osteopontin. This integrin plays an essential role in the recruitment, migration and attachment of leukocytes and has an important function during inflammation. In previous studies it was shown that integrin alpha 4 beta 1 is produced at the level of hematopoietic stem cells. The adjustment is given by the binding of integrins with their ligands, VCAM-1, osteopontin that are expressed and / or secreted by endothelial cells and bone marrow [106].

Some studies showed that endothelial cells attached to aECMs when the entire CS5 domain was incorporated into the biopolymer, in contrast to low cell attachment when only the REDV sequence from CS5 was incorporated into the biopolymer [107].

Another biomaterial useful for tissue applications is silk. Silk, popularly known in the textile industry for its luster and mechanical properties, is produced by cultured silkworms. Silks are produced by members of the class Arachnida (over 30,000 species of spiders) and by several worms of the order Lepidoptera, which includes moths, butterflies and silkworms. Silks are fibrous proteins synthesized in specialized epithelial cells that line glands in these organisms [108]. Silks provide structural roles in cocoon formation, nest building, traps, web formation, safety lines and egg protection [108];[109]. Silks are generally composed of  $\beta$ -sheet structures due to the dominance of hydrophobic domains consisting of short side chain amino acids in the primary sequence. These structures permit tight packing of stacked sheets of hydrogen bonded anti-parallel chains of the protein. Large hydrophobic domains interspaced with smaller hydrophilic domains foster the assembly of silk and the strength and resiliency of silk fibers [110].

Silks have been investigated as biomaterials due to the successful use of silk fibers from *B. mori* as suture material for centuries [111]. Functional differences among silks of different species and within a species are a result of structural differences due to differences in primary amino acid sequence, processing and the impact of environmental factors [112]. Silks represent a unique family of structural proteins that are biocompatible, degradable, mechanically superior, offer a wide range of properties and are amenable to aqueous or organic solvent processing and can be chemically modified to suit a wide range of biomedical applications [113].

During the past 10 years a great deal of progress has been made in understanding silk genetic and protein structures. Cloning and expression of native and synthetic silks has been achieved in a variety of host systems. The sequences of cDNAs and genomic clones encoding spider silks illustrate the highly repetitive structures [114] which can be readily exploited to construct

genetically engineered spider silk-like proteins using synthetic oligonucleotide versions of the consensus repeats or variants of these repeats. This highly repetitive sequence was also recently fully described for the fibroin heavy chain from the silkworm, *B. mori* [115].

The enhanced environmental stability of silk fibers in comparison to globular proteins is due to the extensive hydrogen bonding, the hydrophobic nature of much of the protein, and the significant crystallinity. Silks are insoluble in most solvents, including water, dilute acid and alkali [116].

Liquid crystalline phases and conformational polymorphism have been implicated in the biological processing of these proteins to contribute to the architectural features within the fibers [117].

These nanoscale features, factoring in the small, orientated and numerous  $\beta$ -sheet crystals, a fuzzy interphase between these crystals and the less crystalline domains, and the shear alignment of the chains, provides a basis for the origin of the novel mechanical properties exhibited by silk fibers. A comparison of mechanical properties combination of strength and toughness. The distinguishing features of the spider silks are the very high strength in combination with excellent elasticity in comparison with these other biomaterials [116].

Silk fibroin offers versatility in matrix scaffold design for a number of tissue engineering needs in which mechanical performance and biological interactions are major factors for success, including bone, ligaments, tendons, blood vessels and cartilage. Silk fibroin can be processed into foams, films, fibers and meshes [116].

Inouye et al. demonstrated the utility of a silk fibroin film in culturing animal cells (SE1116, human colon adenocarcinoma; KB, human mouth epidermoid carcinoma; Colo201, human colon adenocarcinoma; QG56, human lung carcinoma) in comparison to a collagen matrix. Films of both fibroin and collagen supported equivalent cell growth after 5 days in cell culture conditions.

$\text{[MESLLP-}\{[(\text{VPGVG})_2\text{-VPGEG-(VPGVG)}_2]_{10}\text{-(VGIPG)}_{60}\text{-V(GAGAGS)5G}\}_2\text{-[(VPGIG)}_5\text{ AVTGRGDSPASSV]}_6\text{]}$

**Figure 3.6 Amino acid sequence of SILK-Elastin like polypeptides**

Recently, fibrous matrices copolymers silk-elp were electrospun and have been used in tissue engineering and wound healing. These copolymers contain the properties of tensile strength of silk and the elasticity typical of elastin in a single molecule (**fig 3.6**).

Ner et al described the electrospinning of nanoribbons from a SELP-47K aqueous solution [117] and spun microdiameter polydisperse fibres (less than 10  $\mu\text{m}$  to over 60  $\mu\text{m}$ ) were obtained by wet-spinning a solution of SELP-47K in formic acid [117]. More recently, the fabrication of a biocompatible tissue scaffold by electrospinning a solution of 15 wt% SELP-47K in formic acid producing a polydisperse population of fibres with diameters ranging from 50 to 600 nm was reported [117]

### 3.5 BIBLIOGRAPHY

- [1]-D.H Reneker, W. Kataphinan, A. Theron, E.Zussmann, A.L. Yarin, nanofiber garlands of Polycaprolactone by Electrospinning, *Polymer* 43 2002 6785-679
- [2]-Xia YN, Yang P, Sun Y, Wu Y, Mayers B, Gates B, Yin Y, Kim F, Yan H. One-dimensional nanostructures: Synthesis, characterization, and applications. *Advanced Materials* 2003;15:353-89-Yu
- [3]-Long YZ, Sun B, Fan Z. Recent advances in solar cells based on one-dimensional nanostructure arrays. *Nanoscale*. 2012 Apr 28;4(9):2783-96.
- [4]-Huang ZM, Zhang YZ, Kotaki M, Ramakrishna S. A review on polymer nanofibers by electrospinning and their applications in nanocomposites. *Composites Science & Technology* 2003;63:2223-53
- [5]-Lu XF, Wang C, Wei Y. One-dimensional composite nanomaterials synthesis by electrospinning and their applications. *Small* 2009;5:2349-70
- [6]-B. Sun, Y.Z. Long, H.D. Zhang, M.M. Li J.L. Duvail, X.Y. Jiang H.L. Yinfa College of Physics, Qingdao University, Qingdao, Advances in three-dimensional nanofibrous macrostructures via electrospinning, *Progress in Polymer Science* 39 (2014) 862-890
- [7]-Long YZ, Yu M, Sun B, Gu CZ, Fan Z. Recent advances in large-scale assembly of semiconducting inorganic nanowires and nanofibers for electronics, sensors and photovoltaics. *Chemical Society Reviews* 2012;41:4560-80
- [8]-Teo WE, Inai R, Ramakrishna S. Technological advances in electrospinning of nanofibers. *Science & Technology of Advanced Materials* 2011;12, 013002/1-19
- [9]-Travis J. Sill, Horst A. von Recum, *Electrospinning: Applications in drug delivery and tissue engineering*, *Biomaterials* 29 (2008) 1989,2006
- [10]- B. Sun, Y.Z. Longa, H.D. Zhang, M.M. Li, J.L. Duvail, X.Y. Jiang, H.L. Yin. Advances in three-dimensional nanofibrous macrostructures via electrospinning. *Progress in Polymer Science* 39 (2014) 862-890
- [11]-Reneker DH, Kataphinan W, Theron A, Zussman E, Yarin AL. Nanofiber garlands of polycaprolactone by electrospinning. *Polymer* 2002;43:6785-94
- [12]-He JH, Wu Y, Zuo WW. Critical length of straight jet in electrospinning. *Polymer* 2005;46:12637-40
- [13]-Shin YM, Hohman MM, Brenner MP, Rutledge GC. Electrospinning: A whipping fluid jet generates submicron polymer fibers. *Applied Physics Letters* 2001;78:1149-51
- [14]-Zheng J, Long YZ, Sun B, Zhang ZH, Shao F, Zhang HD, Zhang ZM, Huang JY. Polymer nanofibers prepared by low-voltage near-field electrospinning. *Chinese Physics B* 2012;21, 048102/1-6
- [15]-B. Sun, Y.Z. Longa, H.D. Zhang, M.M. Lia, J.L. Duvaile, X.Y. Jiangd, H.L. Yin, Advances in three-dimensional nanofibrous macrostructures via electrospinning, *Progress in Polymer Science* 39 (2014) 862-890
- [16]-Thompson CJ, Chase GG, Yarin AL, Reneker DH. Effects of parameters on nanofiber diameter determined from electrospinning model. *Polymer* 2007;48:6913-22
- [17]-Katti DS, Robinson KW, Ko FK, Laurencin CT. Bioresorbable nanofiber based-system for wound healing and drug delivery: optimization and fabrication. *Journal of Biomedical Materials Research Part B: Applied Biomaterials* 2004;70:286-289
- [18]-Fhong H, Chun I, Reneker DH. Beaded nanofibers formed during electrospinning. *Polymer* 1999;40:4585-92
- [19]-Zuo W, Zhu M, Yang W, Yu H, Chen Y, Zhang Y. Experimental Study on relationship between jet instability and formation of beaded fibers during electrospinning. *Polymer Engineering & Science* 2005;45:70-49
- [20]-Chase GC, reneker DH. Nanofibers in filter media. *Fluid/Particle separation Journal* 2004;16:105-17

- [21]-Demir MM, Yilgor Y, Yilgor E, Erman B. *Electrospinning of Polyurethane fibers* *Polymer* 2002;43:3303-9
- [22]-Meechaiuse C, Dubin R, Supaphol P, Hoven VP, Kohn J. *Electrospun mat of tyrosine-derived polycarbonate fibers for potential use as tissue scaffolding material. Journal of Biomaterial Science, Polymer edition* 2006;17:1039-56
- [23]-Tripatanasuwan S, Zhong ZX, Reneker DH. *Effect of evaporation and solidification of the charged jet in Electrospinning of poly(ethylene oxide) aqueous solution. Polymer* 2007;48:5742-6
- [24]-A Roadmap of Biomedical Engineers and Milestones," <http://users.ox.ac.uk/~exet0249/biomaterials.html#biomat> "Tiger International (Shanghai) BioMetals Co., Ltd," <http://www.biomedicalalloys.com/home.html>
- [25]-C. M. Agrawal, "Reconstructing the human body using biomaterials," *The Journal of Minerals, Metals and Materials Society*, vol. 50, no. 1, pp. 31–35, 1998
- [26]-M. N. Helmus and J. A. Hubbell, "Materials selection," in *Cardiovascular Pathology*, vol. 2, no. 3, chapter 6, pp. 53S–71S, Elsevier Science Publication, 1993
- [27]-Saravana Kumar Jaganathan, I Eko Supriyanto, Selvakumar Murugesan, Arunpandian Balaji, and Manjeesh Kumar Asokan; *MBiomaterials in Cardiovascular Research: Applications and Clinical Implications, BioMed Research International Volume* 2014, Article ID 459465
- [28]-M. W. Curtis and B. Russell, "Cardiac tissue engineering," *Journal of Cardiovascular Nursing*, vol. 24, no. 2, pp. 87–92, 2009
- [29]-Biological evaluation of medical devices—Part 1: Evaluation and testing within a risk management process," <http://www.fda.gov/downloads/MedicalDevices/DeviceRegulationandGuidance/GuidanceDocuments/UCM348890.pdf>, "Biological evaluation of medical devices—Part 12: Sample preparation and reference materials," ISO 10993-12:2012
- [30]-Y. Weng, J. Chen, Q. Tu, Q. Li, M. F. Maitz, and N. Huang, "Biomimetic modification of metallic cardiovascular biomaterials: from function mimicking to endothelialization in vivo," *Interface Focus*, no. 2, pp. 356–365, 2012
- [31]-M. B. Gorbet and M. V. Sefton, "Biomaterial-associated thrombosis: roles of coagulation factors, complement, platelets and leukocytes," *Biomaterials*, vol. 25, no. 26, pp. 5681–5703, 2004, C. Pallister and M. Watson, *Haematology*, Scion Publishing, 2010
- [32]-R. C. Eberhart, H. Huo, and K. Nelson, *Cardiovascular Materials*, *MRS Bulletin*, 17th edition, 1991; R. E. Marchant and I. Wang, "Physical and chemical aspects of biomaterials used in humans," in *Implantation Biology: The Host Response and Biomedical Devices*, pp. 13–38, 1994
- [33]-Allan S. Hoffman. *Stimuli-responsive polymers: Biomedical applications and challenges for clinical translation. Advanced Drug Delivery Reviews Volume* 65, Issue 1, January 2013, Pages 10–16
- [34]-Sigwart U, Puel J, Mirkovitch V, Joffre F, Kappenberger L. *Intravascular stents to prevent occlusion and restenosis after transluminal angioplasty. N Engl J Med* 1987;316:701-6.
- [35]-Serrano MC & Ameer GA, *Recent insights into the biomedical applications of shape-memory polymers. Macromolecular Bioscience* 2012, 12(9), 1156-1171
- [36]-Garg K, Sell SA, Madurantakam P, Bowlin GL. *Angiogenic potential of human macrophages on electrospun bioresorbable vascular grafts. Biomed Mater* 2009;4:031001
- [37]-Ramakrishna S, Fujihara K, Teo WE, Yong T, Ma Z, Ramaseshan R. *Electrospun nanofibers: solving global issues. Mater Today* 2006;9:40–50
- [38]-Jungebluth P, Alici E, Baiguera S, Blanc KL, Blomberg P, Bozoky B, et al. *Tracheobronchial transplantation with a stem-cell-seeded bioartificial nanocomposite: a proof-of-concept study. The Lancet* 2011;378: 1997–2004
- [39]-Anwarul Hasan, Adnan Memic, Nasim Annabi, Monowar Hossain, Arghya Paul, Mehmet R. Dokmeci, Fariba Dehghani, Ali Khademhosseini. *Electrospun scaffolds for tissue engineering of vascular grafts Acta Biomaterialia* 10 (2014) 11–25

- [40]-Baker BM, Gee AO, Metter RB, Nathan AS, Marklein RA, Burdick JA, et al. The potential to improve cell infiltration in composite fiber-aligned electrospun scaffolds by the selective removal of sacrificial fibers. *Biomaterials* 2008;29:2348e58
- [41]-Wang K, Xu M, Zhu MF, Hong Su, Wang HJ, Kong DL, et al. Creation of macropores in electrospun silk fibroin scaffolds using sacrificial PEO microparticles to enhance cellular infiltration. *J Biomed Mater Res A* 2013;101:3474e81
- [42]-Lee BLP, Jeon H, Wang A, Yan Z, Yu J, Grigoropoulos C, et al. Femtosecond laser ablation enhances cell infiltration into three-dimensional electrospun scaffolds. *Acta Biomater* 2012;8:2648e58
- [43]-Keeley, F.W. et al. (2002) Elastin as a self-organizing biomaterial: Use of recombinantly expressed human elastin polypeptides as a model for investigations of structure and self-assembly of elastin. *Philos. Trans. R. Soc. Lond. B Biol. Sci.* 357, 185–189;
- [44]-Rosenbloom, J. et al. (1993) Extracellular matrix 4: The elastic fiber. *FASEB J.* 7, 1208–1218
- [45]- Doreen M. Floss, Kai Schallau, Stefan Rose-John, Udo Conrad and Jurgen Scheller. Elastin-like polypeptides revolutionize recombinant protein expression and their biomedical application; *Trends in Biotechnology* Vol.28 No.1
- [46]-Catherine M. Bellingham<sup>1,2</sup> Margo A. Lillie John M. Gosline Glenda M. Wright Barry C. Starcher Allen J. Bailey Kimberly A. Woodhouse Fred W. Keeley. Recombinant Human Elastin Polypeptides Self-Assemble into Biomaterials with Elastin-Like Properties *Biopolymers*, Vol. 70, 445–455 (2003)
- [47]-Hinek, A.; Wrenn, D.; Mecham, R.; Barondes, S. *Science* 1988, 239, 1539–154
- [48]-Hinek A, Rabinovitch M. 67-kD elastin-binding protein is a protective “companion” of extracellular insoluble elastin and intracellular tropoelastin. *J Cell Biol* 1994;126:563–74
- [49]-Robert L. Interaction between cells and elastin, the elastin-receptor. *Connect Tissue Res* 1999;40:75–82.
- [50]-Mecham RP, Hinek A, Entwistle R, Wrenn DS, Griffin GL, Senior RM. Elastin binds to a multifunctional 67-kilodalton peripheral membrane protein. *Biochemistry* 1989;28:3716–22
- [51]-Mecham RP, Whitehouse L, Hay M, Hinek A, Sheetz MP. Ligand affinity of the 67-kD elastin/laminin binding protein is modulated by the protein’s lectin domain: visualization of elastin/laminin-receptor complexes with gold-tagged ligands. *J Cell Biol* 1991;113:187–94
- [52]-Bellingham CM, Lillie MA, Gosline JM, Wright GM, Starcher BC, Bailey AJ, et al. Recombinant human elastin polypeptides self-assemble into biomaterials with elastin-like properties. *Biopolymers* 2003;70:445–55
- [53]-Rosenbloom J, Abrams WR, Mecham RP. Extracellular matrix 4: The elastic fiber. *FASEB J* 1993;7:1208–18
- [54]-Jerome A Werkmeister and John A M Ramshaw. Recombinant Protein scaffolds for Tissue Engineering; *Biomed. Mater.* 7 (2012) 012002
- [55]-Broekelmann T J, Kozel B A, Ishibashi H, Werneck C C, Keeley F W, Zhang L and Mecham R P 2005
- [56]-Grosso L E and Scott M 1993 PGAI<sup>PG</sup>. A repeated hexapeptide of bovine tropoelastin, is a ligand for the 67-kDa bovine elastin receptor *Matrix* 13 157–64
- [57]-W.F. Daamena, J.H. Veerkampa, J.C.M. van Hestb, T.H. van Kuppevelt. Elastin as a biomaterial for tissue engineering; *Biomaterials* 28 (2007) 4378–4398
- [58]-Indik Z, Abrams W R, Kucich U, Gibson C W, Mecham R P and Rosenbloom J 1990 Production of recombinant human tropoelastin: characterization and demonstration of immunologic and chemotactic activity *Arch. Biochem. Biophys.* 280 80–6
- [59]-Martin S L, Vrhovski B and Weiss A S 1995 Total synthesis and expression in *Escherichia coli* of a gene encoding human tropoelastin *Gene* 154 159–66

- [60]-Urry D W, Pattanaik A, Xu J, Woods T C, McPherson D T and Parker T M 1998 Elastic protein-based polymers in soft tissue augmentation and generation *J. Biomater. Sci. Polym. Ed.* 9 1015–48;
- [61]-Meyer D E and Chilkoti A 2002 Genetically encoded synthesis of protein-based polymers with precisely specified molecular weight and sequence by recursive directional ligation: examples from the elastin-like polypeptide system *Biomacromolecules* 3 357–67
- [62]-Dana L. Nettles, Ashutosh Chilkoti, Lori A. Setton, Applications of elastin-like polypeptides in tissue engineering. *Advanced Drug Delivery Reviews* 62 (2010) 1479–1485
- [63]-Urry, D. W. “Free-energy transduction in polypeptides and proteins based on inverse temperature transitions”, *Progress in Biophysics & Molecular Biology* 1992, 57 (1), 23–57
- [64]-Megeed, Z.; Cappello, J.; Ghandehari, H. “Genetically engineered silk-elastinlike protein polymers for controlled drug delivery”, *Adv. Drug Deliv. Rev* 2002, 54 (8), 1075–1091
- [65]-Urry, D. W. “Elastic molecular machines in metabolism and soft-tissue restoration”, *Trends In Biotechnology* 1999, 17 (6), 249–257
- [66]-Van Hest, J.; Tirrell, D. A. “Protein-based materials, toward a new level of structural control”, *Chemical Communications* 2001, 19, 1897–1904
- [67]-Arias, F. J.; Reboto, V.; Martin, S.; Lopez, I.; Rodriguez-Cabello, J. C. “Tailored recombinant elastin-like polymers for advanced biomedical and nano(bio)technological applications”, *Biotechnology Letters* 2006, 28 (10), 687–695
- [68]-Diehl, M. R. M. R.; Zhang, K. K.; Lee, H. J. H. J.; Tirrell, D. A. D. A. “Engineering cooperativity in biomotor-protein assemblies”, *Science* 2006, 311 (5766), 1468–1471
- [69]-Heilshorn, S. C.; DiZio, K. A.; Welsh, E. R.; Tirrell, D. A. “Endothelial cell adhesion to the fibronectin CS5 domain in artificial extracellular matrix proteins”, *Biomaterials* 2003, 24, 4245–4252
- [70]-Urry DW. Elastic-contractile model proteins: Physical chemistry, protein function and drug design and delivery. *Advanced Drug Delivery Reviews* 62 (2010) 1404–1455
- [71]- Urry, D. W. *Physical Chemistry of Biological Free Energy Transduction As Demonstrated by Elastic Protein-Based Polymers* †*Journal of Physical Chemistry B*, 101, 11007,(1997)
- [72]-Reguera, J.; Urry, D. W.; Parker, T. M.; McPherson, D. T.; Rodriguez-Cabello, J.C. Differential scanning calorimetry study of the hydrophobic hydration of the elastin-based polypentapeptide, poly(VPGVG), from deficiency to excess of water *Biomacromolecules*, 8, 354,(2007)
- [73]-Urry, D. W.; Trapane, T. L.; Prasad, K. U. Phase-structure transitions of the elastin polypentapeptide–water system within the framework of composition–temperature studies *Biopolymers*, 24, 2345,(1985)
- [74]- Serrano, V.; Liu, W.; Franzen, S. An Infrared Spectroscopic Study of the Conformational Transition of Elastin-Like Polypeptides *Biophysical Journal*, 93, 2429,(2007)
- [75]-Yao, X. L.; Hong, M. Structure Distribution in an Elastin-Mimetic Peptide (VPGVG)<sub>3</sub> Investigated by Solid-State NMR *Journal of the American Chemical Society*, 126, 4199,(2004)
- [76]-Martino, M.; Coviello, A.; Tamburro. *International Journal of Biological Macromolecules*, 27, 59,(2000) *International Journal of Biological Macromolecules*, 27, 59,(2000)
- [77]-Ohgo, K.; Niemczura, W. P.; Ashida, J.; Okonogi, M.; Asakura, T.; Kumashiro, K.K. Heterogeneity in the Conformation of Valine in the Elastin Mimetic (LGGVG)<sub>6</sub> as Shown by Solid-State <sup>13</sup>C NMR Spectroscopy *Biomacromolecules*, 7, 3306,(2006)
- [78]-Bochicchio, B.; Pepe, A.; Tamburro. Investigating by CD the molecular mechanism of elasticity of elastomeric proteins. , *A. M. Chirality*, 20, 985,(2008)
- [79]-Ahmed, Z.; Scaffidi, J. P.; Asher, S. A. Circular dichroism and UV-resonance Raman investigation of the temperature dependence of the conformations of linear and cyclic elastin *Biopolymers*, 91, 52,(2009)

- [80]-Brovchenko, I.; Krukau, A.; Smolin, N.; Oleinikova, A.; Geiger, A.; Winter, R. Thermal breaking of spanning water networks in the hydration shell of proteins *Journal of Chemical Physics*, 123,(2005)
- [81]- Rodriguez-Cabello, J. C.; Alonso, M.; Perez, T.; Herguedas, M. M. Differential scanning calorimetry study of the hydrophobic hydration of the elastin-based polypeptide, poly(VPGVG), from deficiency to excess of water *Biopolymers*, 54, 282,(2000)
- [82]-Kunz, W.; Henle, J.; Ninham, B. W. 'Zur Lehre von der Wirkung der Salze' (about the science of the effect of salts): Franz Hofmeister's historical papers *Current Opinion in Colloid & Interface Science*, 9, 19,(2004)
- [83]-Jungwirth, P.; Winter, B. Ions at Aqueous Interfaces: From Water Surface to Hydrated Proteins *In Annual Review of Physical Chemistry* 2008; Vol. 59, p 343
- [84]-Ali Ghoorchian and Nolan B. Holland. Molecular Architecture Influences the Thermally Induced Aggregation Behavior of Elastin-like Polypeptides, *Biomacromolecules*, 2011, 12 (11), pp 4022–4029
- [85]-Urry, D. W. Entropic elastic processes in protein mechanisms. Elastic structure due to an inverse temperature transition and elasticity due to internal chain dynamics *Journal of Protein Chemistry*, 7, 1,(1988)
- [86]-Carpino, L. A.; Han, G. Y. 9-Fluorenylmethoxycarbonyl function, a new base-sensitive amino-protecting group *Journal of the American Chemical Society*, 92, 5748,(1970)
- [87]- Simnick, A. J.; Lim, D. W.; Chow, D.; Chilkoti, A. Biomedical and Biotechnological Applications of Elastin-Like Polypeptides *Polymer Reviews*, 47, 121,(2007)
- [88]-Cappello, J.; Crissman, J.; Dorman, M.; Mikolajczak, M.; Textor, G.; Marquet, M.; Ferrari, F. Genetic Engineering of Structural Protein Polymers *Biotechnology Progress*, 6, 198,(1990)
- [89]-Meyer, D. E.; Chilkoti, A. Quantification of the Effects of Chain Length and Concentration on the Thermal Behavior of Elastin-like Polypeptides *Biomacromolecules*, 3, 357,(2002)
- [90]-Daamen, W. F.; Veerkamp, J. H.; van Hest, J. C. M.; van Kuppevelt, T. H. Elastin as a biomaterial for tissue engineering *Biomaterials*, 28, 4378,(2007)
- [91]-Hafemann, B.; Ghofrani, K.; Gattner, H. G.; Stieve, H.; Pallua, N. Cross-linking by 1-ethyl-3-(3-dimethylaminopropyl)-carbodiimide (EDC) of a collagen/elastin membrane meant to be used as a dermal substitute: effects on physical, biochemical and biological features in vitro *Journal of Materials Science-Materials in Medicine*, 12, 437,(2001)
- [92]-Koria, P.; Yagi, H.; Kitagawa, Y.; Megeed, Z.; Nahmias, Y.; Sheridan, R.; Yarmush, M. L Self-assembling elastin-like peptides growth factor chimeric nanoparticles for the treatment of chronic wounds. *Proceedings of the National Academy of Sciences of the United States of America*, 108, 1034,(2011)
- [93]-Betre, H.; Setton, L. A.; Meyer, D. E.; Chilkoti, A. Characterization of a Genetically Engineered Elastin-like Polypeptide for Cartilaginous Tissue Repair *Biomacromolecules*, 3, 910,(2002)
- [94]-Woodhouse, K. A.; Klement, P.; Chen, V.; Gorbet, M. B.; Keeley, F. W.; Stahl, R.; Fromstein, J. D.; Bellingham, C. M. Investigation of recombinant human elastin polypeptides as non-thrombogenic coatings *Biomaterials*, 25, 4543,(2004)
- [95]-Megeed, Z.; Yarmush, M. L.; Rajagopalan, P. Cellular response to nanoscale elastin-like polypeptide polyelectrolyte multilayers *Acta Biomaterialia*, 4, 827,(2008)
- [96]-Liu, J. C.; Tirrell, D. A. Cell Response to RGD Density in Cross-Linked Artificial Extracellular Matrix Protein Films *Biomacromolecules*, 9, 2984,(2008)
- [97]-Swierczewska, M.; Hajicharalambous, C. S.; Janorkar, A. V.; Megeed, Z.; Yarmush, M. L.; Rajagopalan, P. Cellular response to nanoscale elastin-like polypeptide polyelectrolyte multilayers *Acta Biomaterialia*, 4, 827,(2008)
- [98]-Huang, L.; McMillan, R. A.; Apkarian, R. P.; Pourdeyhimi, B.; Conticello, V. P Generation of Synthetic Elastin-Mimetic Small Diameter Fibers and Fiber Networks. *Macromolecules*, 2000, 33 (8), pp 2989–2997

- [99]-Langer, R.; Vacanti, Preparation and characterization of poly(l-lactic acid) foams *Polymer* Volume 35, Issue 5, March 1994, Pages 1068–1077
- [100]-Nowatzki, P. J.; Tirrell, D. A. Physical properties of artificial extracellular matrix protein films prepared by isocyanate crosslinking *Biomaterials*, 25, 1261,(2004).
- [101]-Kannan, R. Y.; Salacinski, H. J.; Butler, P. E.; Hamilton, G.; Seifalian, A. M. Current status of prosthetic bypass grafts: A review *Journal of Biomedical Materials Research Part B-Applied Biomaterials*, 74B, 570,(2005)
- [102]-Swartz, D. D.; Russell, J. A.; Andreadis, S. T. Engineering of fibrin-based functional and implantable small-diameter blood vessels *American Journal of Physiology- Heart and Circulatory Physiology*, 288, H1451,(2005)
- [103]-Welsh, E. R.; Tirrell, D. A. Engineering the Extracellular Matrix: A Novel Approach to Polymeric Biomaterials. I. Control of the Physical Properties of Artificial Protein Matrices Designed to Support Adhesion of Vascular Endothelial Cells *Biomacromolecules*, 1, 23,2000
- [104]-Wise, S. G.; Byrom, M. J.; Waterhouse, A.; Bannon, P. G.; Ng, M. K. C.; Weiss, A. S. A multilayered synthetic human elastin/polycaprolactone hybrid vascular graft with tailored mechanical properties” *Acta Biomater.* 7 (2011) 295–303
- [105]-Carmen Garcia-Arevalo, Maria Pierna, Alessandra Girotti, Francisco Javier Arias and Jose Carlos Rodriguez-Cabello. A comparative study of cell behavior on different energetic and bioactive polymeric surfaces made from elastin-like recombinamers. *The Royal Society of Chemistry 2012- Soft Matter*
- [106]-Cao B., Hutt OE., Zhang Z., Li S., Heazelwood S.Y., Williams B., Smith J.A, Haylock D.N, Savage P, Nilsson S. Design, synthesis and binding properties of a fluorescent  $\alpha 9\beta 1/\alpha 4\beta 1$  integrin antagonist and its application as an in vivo probe for bone haematopoietic stem cells. *Royal society of Chemistry. Biomolecular Chemistry*, 2014,12,965-978
- [107]-S.C. Heilshorn, K.A. DiZio, E.R. Welsh, D.A. Tirrell, Endothelial cell adhesion to the fibronectin CS5 domain in artificial extracellular matrix proteins, *Biomaterials* 24 (2003) 4245–4252
- [108]-Kaplan DL, Mello SM, Arcidiacono S, Fossey S, Senecal KWM. In: McGrath KKD, editor. *Protein based materials*. Boston: Birkhauser; 1998. p. 103–31
- [109]-Wong Po Foo C, Kaplan DL. Genetic engineering of fibrous proteins: spider dragline silk and collagen. *Adv Drug Deliv Rev* 2002;54(8):1131–43
- [110]-Bini E, Knight DP, Kaplan DL. Mapping domain structures in silks from insects and spiders related to protein assembly. *J Mol Biol* 2004;335(1):27–40
- [111]-Moy RL, Lee A, Zalka A. Commonly used suture materials in skin surgery. *Am Fam Physician* 1991;44(6):2123–8
- [112]-Vollrath F, Knight DP. Liquid crystalline spinning of spider silk. *Nature* 2001;410(6828):541–8
- [113]-Charu Veparia, David L. Kaplan. Silk as a biomaterial, *Prog. Polym. Sci.* 32 (2007) 991–1007
- [114]-Guerette PA, Ginzinger DG, Weber BHF, Gosline JM. Silk properties determined by gland-specific expression of a spider fibroin gene family. *Science* 1996;272:112
- [115]-Zhou CZ, Confalonieri F, Medina N, Zivanovic Y, Esnault C, Yang T, Jacquet M, Janin J, Duguet M, Perasso R, Li ZG. Fine organization of *Bombyx mori* fibroin heavy chain gene. *Nucleic Acids Res* 2000;28:2413–9
- [116]-Gregory H. Altman, Frank Diaz, Caroline Jakuba, Tara Calabro, Rebecca L. Horan, Jingsong Chen, Helen Lu, John Richmond, David L. Kaplan. Silk-based biomaterials, *Biomaterials* 24 (2003) 401–416
- [117]- Ner Y, Stuart J A, Whited G and Sotzing G A 2009 Electrospinning nanoribbons of a bioengineered silk-elastin-like protein (SELP) from water *Polymer* 50 5828–36

## 4 CHAPTER: MATERIALS AND METHODS



## 4.1 MATERIALS

The elastin like bioactivated polymers (REDV and HRGD) and the Silk-ELP copolymer were produced by Bioforge-TPNTB in Valladolid, as reported by Girotti et.al and Colino et al. [1];[2];[3].

2,2,2-Trifluoroethanol, 1,6-Hexamethylene diisocyanate, Genipin, Kaiser test kits were purchased from Sigma-Aldrich (Italy). Dry Acetone was purchased from DelChimica-Scientific Glassware(Italy). All the balloons used for the realization of the ELP and Silk coating were produced by Conic Vascular Technology España, Spain.

In vivo implants of coated balloons were performed using Hematoxillin/ Eosin staining and Masson Tricrome staining purchased from Sigma (Sigma-Aldrich,Italy).

For in vitro experiments, Human Umbelical Endothelial Vein cells were used and purchased from (InvitroGen and Applied Biosystems, Italy). M200 medium were purchased from Gibco©. For histology carachterization, Hematoxillin and Eosin were purchased from Sigma ,.Masson Tricrome staining were purchased from...

## 4.2 ELASTIN LIKE POLYMERS

### 4.2.1 PREPARATION OF ELASTIN LIKE POLYMERS SAMPLES

HRGD (Mw:60 kDa) and REDV (Mw:84 kDa) were produced biotechnologically as described in previous work, from Bioforge- Technical Proteins NanoBiotechnology (TPNTB). Polymeric sequences represented in figure 3.5, are mainly composed by repeated alternating blocks -VPGIG, -VPGKG. These repeated blocks are derived from the base sequence of the elastin molecule, -VPGXG and are composed from hydrophobic aminoacids.

Inside the base sequence of elastin were inserted two amino acids: Isoleucine which imparts to the polymer the elastic characteristics typical of the endogenous protein and Lysine, which is a positively charged residue that serves as a crosslink site for the formation of intra-chain interactions. The two polymers were subsequently bioactivated through the insertion of specific sequences of cellular recognition, RGD and REDV.

First experiments were done in order to select the suitable solvent for both polymers, as well as the concentration of the solution. After some preliminary tests (made dissolving HRGD and REDV polymers in different organic solvents), the solvent selected was 2,2,2-Trifluoroethanol; for its

chemical properties (boiling point, conductivity, low toxicity, viscosity and permittivity) this solvent is ideal for the electrospinning process.

Solvent	RGD	REDV
Ethanol	Insoluble	Insoluble
Acetone	Insoluble	Insoluble
Dichloromethane	Soluble	Soluble
2,2,2-TrifluoroEthanol	Soluble	Soluble
Concentration	5%, 10%, 15%, 20%	5%, 10%, 15%, 20%

**Figure 4.1 Elastin like polymer solubility index in different solvents(top of the table); concentration settings(down of the table)**

#### 4.2.2 ELECTROSPINNING OF ELP SOLUTIONS

HRGD(Mw:60 kDa) and REDV(Mw:84 kDa) were suspended in 2,2,2-Trifluoroethanol at concentration of 15%(w/v). The solutions were maintained under stirring for one hour at room temperature and then were put at 4 °C for 24 hours, in order to obtain a clear solution. A stable Taylor cone is required for the formation of uniform fibres, so preliminary electrospinning experiments were conducted in order to evaluate the best conditions while maintaining its stability. A collecting distance of 150 mm, a flow rate ranging from 0.3 to 0.5 mL h<sup>-1</sup> and a needle of 27 gauge have shown the optimum conditions and therefore were kept constant in all the experiments while the influence of the applied electrical field and concentration on fiber diameter and its distribution were characterized.

All the Electrospinning experiments were conducted with Nanofiber NF-500 Electrospinning Machine (MECC-LTD, Japan). Polymer solutions were placed in plastic syringes of 6 ml (Norm-Ject Luer Lock) and fitted by a 27X15mm needle. Fibers were collected on a flat Aluminum collector using different process parameters for both the polymers. HRGD solution 15% (w/v) in TFE was electrospun at 20 Kv, 0.3 mL h<sup>-1</sup> and 150 mm of distance while REDV solution 15% (w/v) in TFE was electrospun at 15 Kv, 0.5 mL h<sup>-1</sup> and 150 mm of distance. All the process parameters are resume in table 4.2.

<i>PROCESS PARAMETERS</i>	<i>HRGD</i>	<i>REDV</i>
<i>Applied Voltage (Kv)</i>	<i>20</i>	<i>13</i>
<i>Flow Rate (ml/h)</i>	<i>0.3</i>	<i>0.3</i>
<i>Distance (mm)</i>	<i>150</i>	<i>150</i>

**Table 4.2 Resume table of electrospinning process parameters used for Elastin-like polypeptides**

In order to favour the completely drying of samples, all the flat matrices were left under hood for 24 hours, prior to Scanning Electron Microscopy analysis.

REDV and HRGD polymers solutions of elastin like polymers have been used to obtain two different types of scaffolds. During the first phase of the project, we focused on the realization of scaffold constituted by a coating of ELP realized around balloons, unflated and semi-inflated. This first type of scaffolds has been used for ex vivo studies with rabbits.

A second type of scaffold ELP has been obtained through the use of an appropriate collector with the diameter of 4 mm; this collector has allowed to obtain the composite devices ELP. Both types of scaffolds were characterized morphologically using ImageJ software.

#### 4.2.1 *THICKNESS OF FLAT MONOLAYER AND ELECTROSPUN ELP COATED BALLOON*

ELP monolayer and balloons electrospun was tested in order to assess the thickness. The samples flat were electrospun on glass in order to measure the thickness, using a profilometer (modello profilometro). Flat Samples were directly electrospun using process parameters previously setup, for about 4 hours in order to obtain a layer useful for the purposes of measurement.

Balloons of 2.5x20 mm, directly electrospun were used for the thickness measurement by image analysis. Samples obtained were cut in two parts and analyzed by Scanning Electron Microscopy (FESEM ULTRAPLUS-ZEISS). Images obtained were processed using ImageJ software.

#### 4.2.2 *ELP MECHANICAL CHARACTERIZATION*

Electrospun meshes I were immersed at 37°C in physiological solution.

Tensile tests were carried out on wet specimens with a thickness ( $t$ ) in the range of 0.02÷0.06 mm and a width of 5.0 mm. An initial grips separation ( $l_0$ ) (i.e. gauge length) of 20 mm was selected.. All the tests were performed on wet specimens at a rate of 10 mm/min using an INSTRON 5566 testing machine. The engineering stress ( $\sigma$ ) was calculated as follows:

$$\sigma = \frac{F}{A}$$

where  $F$  represents the force measured by the load cell and  $A$  the cross section ( $t \cdot w$ ).

The engineering strain ( $\epsilon$ ) was evaluated as the ratio between the elongation ( $\Delta l$ ) and the gauge length ( $l_0$ ):

$$\epsilon = \frac{\Delta l}{l_0}$$

Tensile modulus and maximum stress were reported as mean value  $\pm$  standard deviation.

#### 4.2.3 DEGRADATION PROFILES OF ELP ELECTROSPUN SCAFFOLDS

Dissolution profiles of the flat layer were obtained for two weeks.

Flat REDV/HRGD were cut 1cmx1cm and crosslinked with increasing mixtures (5%, 10%, 20% v/v) of Acetone/HMDI. The samples obtained were placed in Posphate Buffer Saline (pH 7.4) at 37 °C for two weeks. At time intervals of 1 day, 3 days, and two weeks samples were taken, dried and analyzed by Scanning Electron Microscopy (FESEM ULTRAPLUS-ZEISS).

#### 4.2.4 TUBULAR SCAFFOLD DEVELOPMENT

REDV and HRGD polymers were used to obtain a composite device with appropriate morphological and mechanical carachteristics.

HRGD(Mw:60 kDa) and REDV(Mw:84 kDa) were suspended in 2,2,2-Trifluoroethanol at concentration of 15%(w/v). The solutions were mantained under stirring for one hour at room temperature and then were put at 4 °C for 24 hours, in order to obtain a clear solution

The Electrospinning was conducted with Nanofiber NF-500 Electrospinning Machine (MECC-LTD, Japan). Polymer solutions were placed in plastic syringes of 6 ml (Norm-Ject Luer Lock) and fitted by a 27X15mm needle. The composite device was obtained through the use of a rotating mandrel and a conic rotating collector with an internal diameter of 4 mm. Velocity of the rotating mandrel was set at 60 rpm.

ELP polymers solutions were electrospun at 20 Kv, 0.3 ml/h and 15 cm of distance while REDV solution 15% (w/v) in 2,2,2 Trifluoroethanol (TFE) was electrospun at 15 Kv, 0.5 ml/h and 15 cm of distance. Morphological characterization were done by Scanning Electron Microscopy and all the obtained images were processed using ImageJ Software.

#### 4.2.5 *IN VITRO CELL PROLIFERATION ON SCAFFOLDS*

Humbelical endothelial cordon vein cells (Invitrogen, Life technologies-Italy) were seeded on ELP and SILK-ELP dried scaffold in order to assess adhesion and proliferation. The cells were seeded at a density of  $1 \times 10^6$  cells per scaffold and maintained in culture for 24 hours.

Cells were cultured with M200 Medium (Gibco®, Life Technologies-Italy) supplemented with low serum growth supplement kit (LSGS kit-Gibco®, Life Technologies-Italy) containing 2% FBS, Basic Fibroblast Growth factor (3 ng/ml), Human Epidermal growth factor (10ng/ml), Hydrocortisone (1 mg/ml), Heparin (10 mg/ml). For the ELP in vitro test, cells were seeded and cultured on top of the RGD layer, in order to verify the adhesion.

After 4, 8 and 24 hours, cells were counted and fixed with Paraformaldehyde 4% (Sigma-Aldrich, Italy). Sytox green (Invitrogen, Life technologies-Italy) was used to visualize cell nuclei while Phalloidin (Invitrogen, Life technologies-Italy) were used for the cell's cytoskeleton staining.

Fluorescent images of stained cells were collected using Confocal transmission microscopy (CLSM LEICA TCS SP5)

#### 4.2.6 *ELECTROSPINNING CATHETER COATING*

Catheters were produced by Conic-Vascular Technology (Spain) in three different measure: 2.5x20mm, 3.5x20mm and 3.0x20mm.

Scaffolds electrospun ELP balloons 2.5x20 mm were inflated into rabbits Iliac arteries in order to visualize the in situ delivery. Experiments has been performed by a three balloon catheter,

performed into cylinders; the cylinder would be mounted on a modified balloon catheter, with cylindrical head portion inflatable at low pressure and expanding in a semi compliant fashion in order not to dilate the vessel. For this purpose the cylindrical inflatable head is calibrated to the reference vessel diameter (3,5,7,9 and 11 mm). In this way the full apposition of the ELP cylindrical fibers mesh composite (CFMC) is equally distributed along the vessel and its adhesion assured avoiding barotraumas. Samples were then treated and fixed with Masson Tricrome staining.

For in vivo experiments, 5 kg rabbits were anesthetised according to approved protocols, abdomen prepared and opened to isolate the abdominal aorta. After proximal balloon inflation and distal clamping arterial incision was obtained in order to allow formerly inflated balloon to enter the vessel. We tested 5 different conditions according to:

1. passage through a 5 F introducer
2. presence/absence of flow
3. reflow in artery after deployment
4. direct or arterial tracking

After inflating, samples were treated with Masson Tricrome staining and Hematoxylin/Eosin in order to see the attachment of ELP scaffolds. In all cases, aortas were explanted, washed and immersed in formalin for histology.

### 4.3 *CROSSLINK OF ELASTIN LIKE POLYMERS MATRIX*

#### 4.3.1 *CHEMICAL CROSSLINK WITH HEXAMETHYLENEDIISOCYANATE(HMDI)*

In order to avoid degradation in an aqueous environment and improving the degradation kinetics, all fiber's matrices of elastin like polymers were subjected to crosslink reaction with 1,6-Hexamethylene diisocyanate (HMDI, Sigma-Aldrich, Italy) .

Matrices of elastin like polymers have been cut to size 1cmx1cm and were immersed in increasing solutions of Acetone/HDMI, from 5 to 20% (v/v) . The reaction was carried out under a hood for increasing time intervals, from 30 min until 2 hours, in order to assess the degree of crosslink reached. Samples were then washed several times with dry acetone (DelChimica-Scientific Glassware,Italy), rinsed ten times with distilled water and finally dried under a hood for 24 h.

The final products were characterized in terms of morphology and mechanical properties. The degree of crosslink was also calculated for all the obtained matrices using the colorimetric reaction with ninhydrin (Sigma-Aldrich, Italy). The assay was conducted in homogeneous phase by dissolving fiber matrices in the organic component of the kit and at the final stage of reaction developing the pigment in an organic solvent.. The free amino density present within the crosslinked samples was calculated by comparing the absorbance at 570 nm with a previously obtained calibration curve.

#### 4.3.2 *CHEMICAL CROSSLINK WITH GENIPIN*

A suitable three-dimensional porous bioresorbable scaffold is considered mandatory for the successful development of an engineered tissue as a biological substitute. To this end, the scaffold should display structural and chemical properties matching as far as possible those of the extracellular matrix.

In order to improve the crosslinking process and the properties of the scaffold, genipin reactions with ELP fiber mats were carried out.

Among the alternative crosslinking agents genipin has been reported to provide materials with higher biocompatibility and less cytotoxicity. This naturally occurring crosslinking agent(which can

be obtained from an iridoid glucoside geniposide) abundant in gardenia fruits, has been successfully applied to both collagenous tissues and gelatin materials. Recently genipin was investigated as crosslinking agent for electrospun gelatin.

Matrices of elastin like polymers have been cut to size 1cmx1cm and were immersed in increasing solutions of Acetone/Genipin, from 0.1 to 5% (w/v) . The reaction was carried out at 37 °C in oven for increasing time intervals, from 24 hours until 72 hours, in order to evaluate the crosslink degree. Samples were left under hood in order to allow the complete evaporation of Acetone. Then, the matrices were washed and rinsed ten times with distilled water and finally dried under hood for 24 hours.

## 4.4 SILK-ELP SCAFFOLDS

### 4.4.1 PREPARATION OF SILK-ELP SAMPLES

Silk–ELP polymer (Mw: 121012 Da) was produced biotechnologically by Technical Proteins NanoBiotechnology (TPNBT, Valladolid- Spain).

The structure of the polymer is shown in fig. These new classes of materials consisting of multiple blocks of a silk-like sequence (-GAGAGS) combined with an elastin-like portion in which the most commonly used elastin pentamer is –VPGVG. These Silk-elastin like proteins are inspired by nature and composed of multiple repeats of silk and- elastin like blocks founded on the conservative amino acid motifs present in the natural protein, silk fibroin and elastin. Combining the high tensile strength of silk fibroin with the elasticity and resiliency of elastin, it was possible to create copolymers that will combine the properties of both polymers.

The silk-like units spontaneously self-assemble into packed antiparallel  $\beta$ -sheet structures stabilized by hydrogen bonding [4], providing crystallinity and mechanical strength. The elastin-like unit, on the other hand, has been reported as displaying a highly flexible conformation [5], [6].

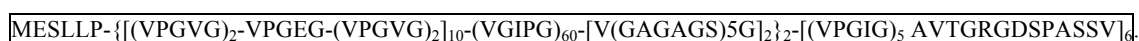


**Figure 4.4 SILK-ELP structure**

Several SELP combinations, with different size and silk to elastin block ratio have been reported in the literature [7] and, depending on their specific sequence and composition, are able to display an

irreversible sol-to-gel transition at body temperature or even at room temperature. This temperature-mediated gelation process allowed its exploitation for a variety of applications [8].

First experiments were done in order to set the concentration of the solutions. The concentration range used for the manufacturing of the fibers was set at 10% (w/v). The solvent used to dissolve the copolymer silk-elastin was 2,2,2- Trifluoroethanol.

#### 4.4.2 ELECTROSPINNING OF SILK-ELP SOLUTIONS

Silk-ELP polymer (Mw: 121012 Da) was dissolved in 2,2,2- Trifluoroethanol to obtain 10% (w/v)solutions. The polymer was dissolved and promptly electrospun in order to avoid the gelation. The Electrospinning was conducted with Nanofiber NF-500 Electrospinning Machine (MECC-LTD,Japan). Polymer solutions were placed in plastic syringes of 6 ml (Norm-Ject Luer Lock) and fitted by a 27X15mm needle.

All the flat matrices were obtained using a flat Aluminum collector. First experiments were conducted to find the conditions and process parameters suited to obtaining fibers, without beads and defects. The ultimate process parameters used are resume in table nr **4.4**

<i>PROCESS PARAMETERS</i>	<i>SILK-ELP</i>
<i>Applied Voltage (Kv)</i>	<i>13 Kv; 20 Kv</i>
<i>Flow Rate (ml/h)</i>	<i>0.3 ml/h</i>
<i>Distance (mm)</i>	<i>150 mm</i>

**Table 4.4** Resume table of process parameters for SILK-ELP

Flat matrices were carachterized morphologically by Scanning Electron Microscopy, using ImageJ software.

## 5 CHAPTER: RESULT AND DISCUSSION



## 5.1 ELASTIN LIKE POLYMERS ELECTROSPUN SCAFFOLDS

### 5.1.1 MORPHOLOGICAL ANALYSIS

Morphological analysis of the fibers was conducted by Scanning Electron Microscopy (FESEM ULTRAPLUS- ZEISS) . Samples were sputter coated with 10 nm Au (CRESSINGTON 208 HR, High Resolution Sputter Coater) and images were obtained at 10KV. Images were analyzed using ImageJ software. Measurements were conducted in order to calculate the average size of the fibers and the porosity of the matrices obtained.

HRGD polymer was electrospun at concentration of 15% (w/v). The resulting solutions show no signs of gelling or aggregation. Different process parameters were used for the electrospinning process. The value of the minimum voltage at which the fibers free from defects are obtained varies between 13 Kv and 20Kv, the flow rate between 0.2 and 0.3 ml/h and the distance set to 150 mm. At lower voltage values, the density of fibers deposited is poor (**fig 5.1 A**). In **fig 5.1 B** is shown the formation of beads. Beads are defects as a result of the break of jet caused by the high surface tension of the solution.

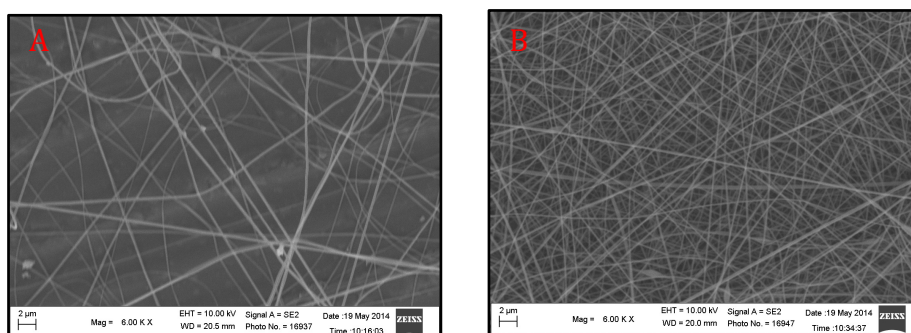


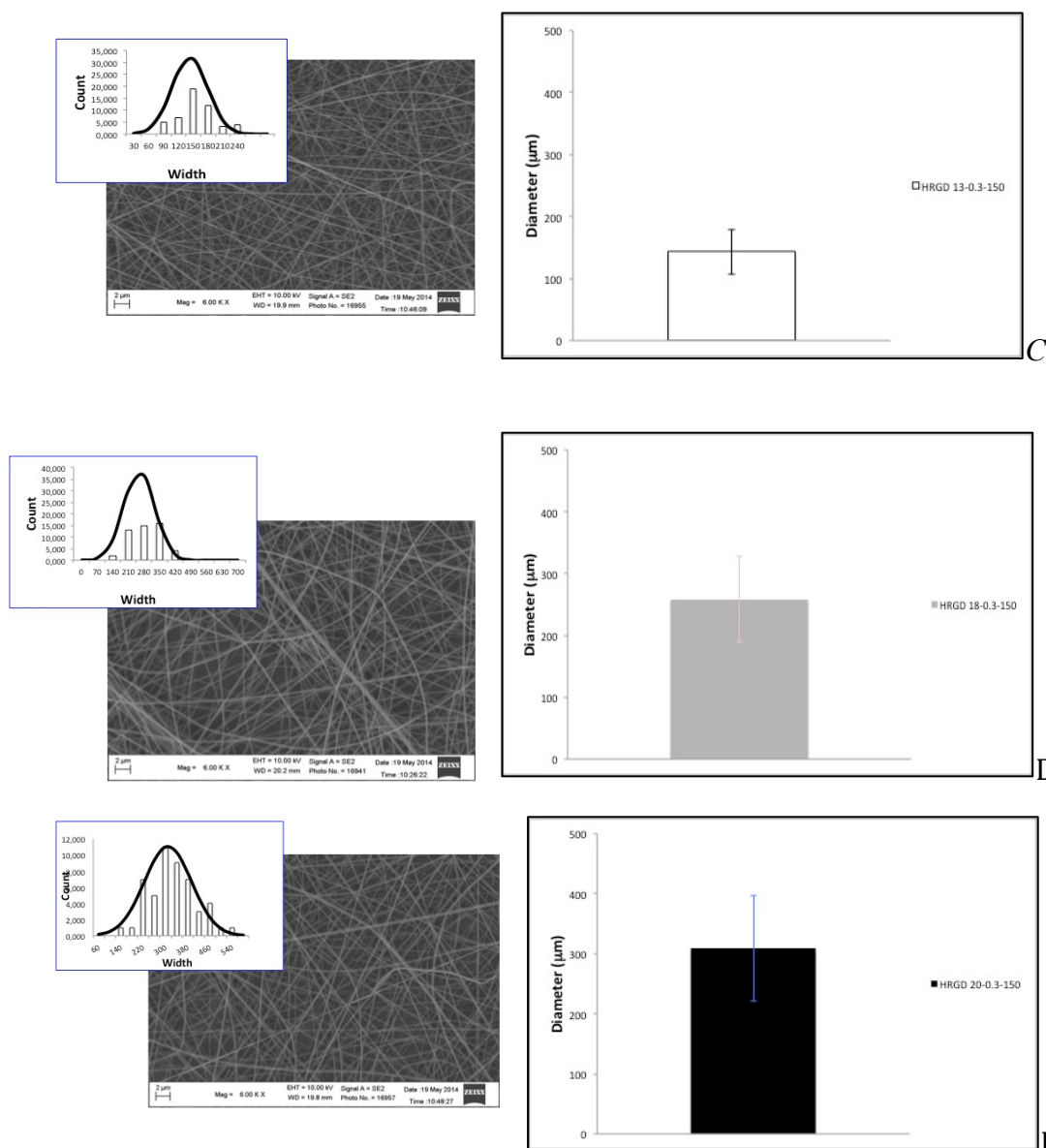
**Figure 5.1 HRGD electrospun fibers:(A) HRGD 13 Kv,0.2 ml/h,150 mm ;(B) HRGD 13 Kv,0.3 ml/h, 150 mm**

By changing process parameters values, an assortment of different electrospun fiber's diameter was obtained. Increasing feed rate and distance values, fibers with an average diameter of  $143\pm 36$  (fig 4.6 C) nm are obtained . This behavior is due to the greater amount of solution concentrated at the tip of the needle;the liquid is stretched with an higher intensity such as to form fibers, avoid of beads and defects but with a smaller diameter.

An increase of the voltage from 13Kv to 18 Kv, while maintaining the distance and the flow rate fixed, causes a corresponding increase in the size of the fibers, from 143 nm to  $258\pm 69$ . The diameter distribution in this case, is wider and favoring the formation of fibers with diameters up to 350 nm (fig 4.6 B).

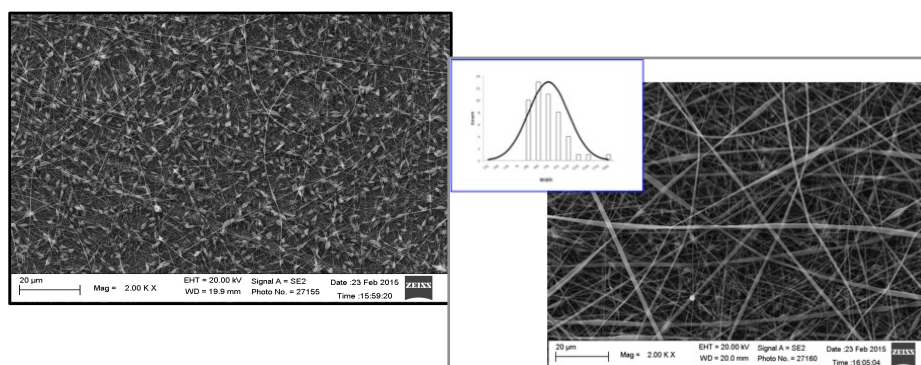
Maintaining unchanged the flow rate and the distance but still increasing the intensity from 18 Kv to 20 Kv, causes an increase in diameter. In this case, the distribution shows an average diameter equal to  $308 \pm 87$  nm. The effect of increasing the intensity acts in concomitation with the high concentration. The viscosity of the solution combined with an intensity equal to 20 Kv shows the fibers devoid of defects and a good density of deposition. A graphical comparison between diameter of the three fiber's types is show in **fig 5.2**. Porosity of flat HRGD matrices were calculated using the threshold ImgeJ function. HRGD flat matrices show a porosity between 20 and 37 %.

Fibrous matrices obtained with these parameters have been selected and used for the biological carachterization and for the obtaining of the mesh, formed by the two overlying polymeric layers.



**Figure 5.2 SEM images of the electrospun fibers obtained from HRGD polymer at concentration of 15%(w/v) with different process parameters: (C) HRGD 13 Kv,0.3 ml/h, 150 mm; (D) HRGD 18 Kv,0.3 ml/h,150 mm, (E) HRGD 20 Kv, 0.3 ml/h, 150 mm.**

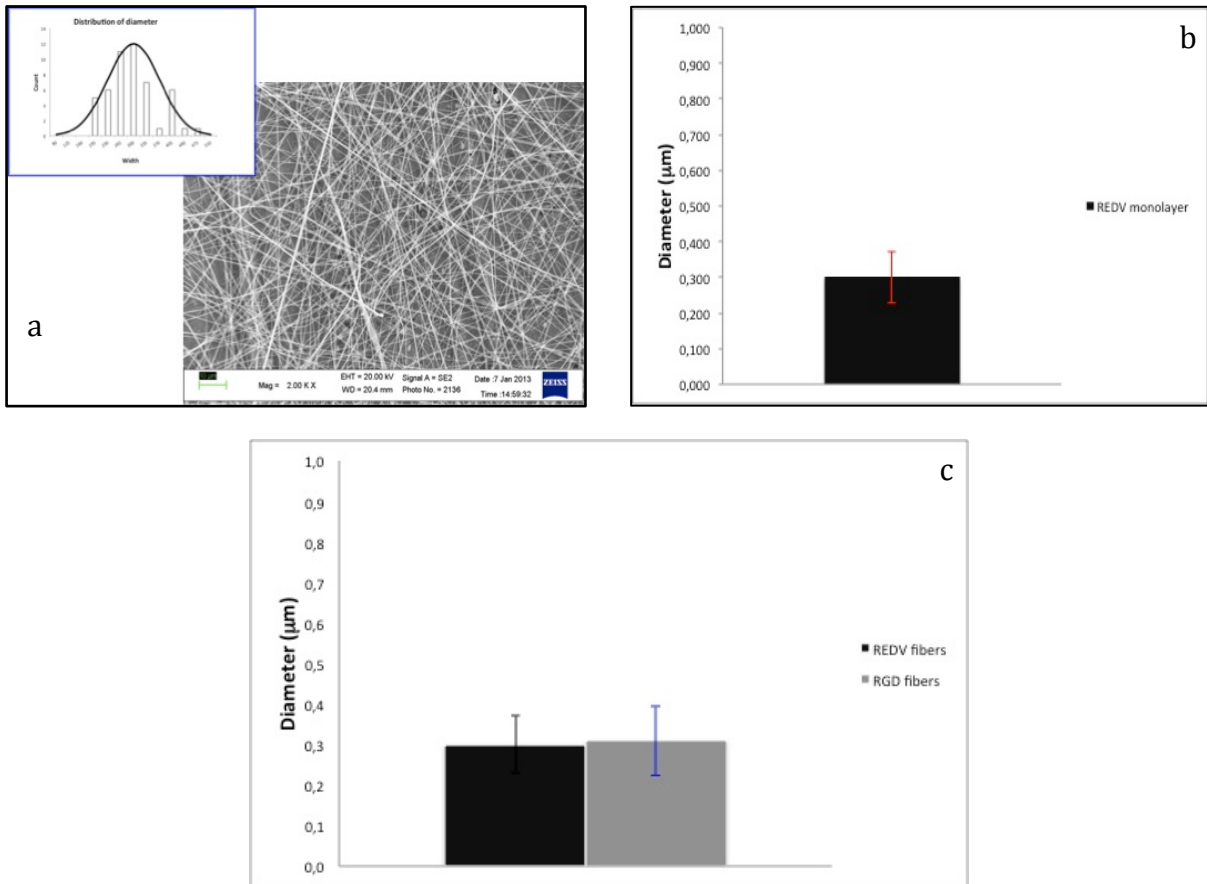
As what concerne the REDV polymer, clear 15% (w/v) solutions were used for the electrospinning process. Starting voltages of 13 kV up to 18 Kv, is known as both the size and the morphology of the fibers changes significantly. In particular, it is evident that, at high voltages, with a flow rate that varies between 0.2 and 0.3 ml/h, the fibers appear consistent but equally rich in beads and morphological defects. This phenomenon is due to a lower viscosity of the solution and its excessive concentration at the tip of the needle that affect in a negative way on the stretching of the solution (**fig 5.3**).



**Figure 5.3 SEM images of REDV electrospun fibers (15% w/v) electrospun at 15 Kv, 0.5 ml/h, 130 mm.**

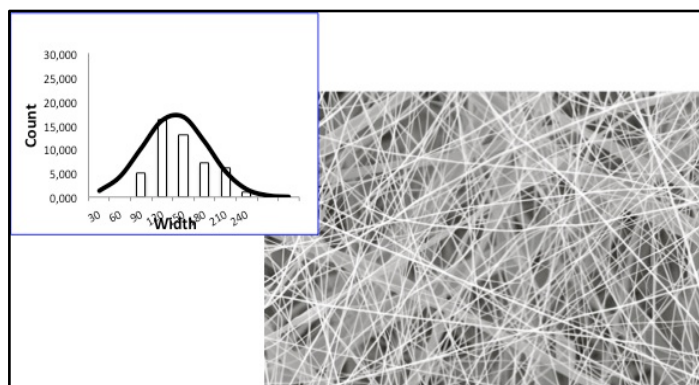
Lowering the voltage and leaving fixed the flow rate and the distance, the amount of liquid concentrate to the tip of the needle undergoes plan the effects of reduced intensity. This phenomenon is reflected in the formation of fibers of dimension considerably higher but not morphologically prived of beads and defects (fig 5.3). Regarding the REDV 15 Kv, 0.5 ml/h, 130 mm the formation of a mix population of fibres and ribbons, contributing to the wide dispersion of diameters around  $704 \pm 419$  nm observed in figure 5.3, in contrasts with the regular fibres obtained with REDV 13 Kv-0.3 ml/h-130 mm. In fact, morphological defects disappear lowering the voltage until 13 Kv, while mantaining the flow rate at 0.3 ml/h and distance at 130 mm. Distribution of diameter settles between 0,300 and 0,195 mm with an average around  $299 \pm 71$  nm (**fig 5.4 a**).

A graphical comparison is resume in fig nr 5.4 HRGD fibers are larger than REDV. This behaviour is attributed to a higher viscosity for HRGD solution. Even if the concentration is 15% (w/v) for both the polymers, a higher solution viscosity is observed only for the HRGD. The higher viscosity favors the establishment of a greater number of entanglement between the polymer chains that are reflected in the formation of larger fibers but morphologically free of defects.



**Figure 5.4 Scanning Electron Microscopy of REDV flat monolayer (a); Histogram of REDV flat monolayer fiber's diameter (b); Histogram of flat REDV and HRGD flat monolayer (c) Mean diameter measured as result from 50 different measures.**

Double layer ELP mesh made of REDV and HRGD were prepared using the same process parameters, while increasing the electrospinning time in order to obtain a thicker layer. Flat meshes of ELP polymers were electrospun starting from 15% (w/v) solution in 2,2,2-trifluoroethanol (TFE). Electrospinning was carried on for up to 2 hours, for both the polymers. Increasing electrospinning time allows the obtaining of a double layer thicker than 150 μm. Scanning Electron Microscopy shows a different shape of fibers referred to the different polymer, REDV and HRGD; in particular, REDV fibers are smaller than HRGD fibers but a good diameter distribution that is in good agreement with the flat electrospun monolayer obtained (fig 5.5).



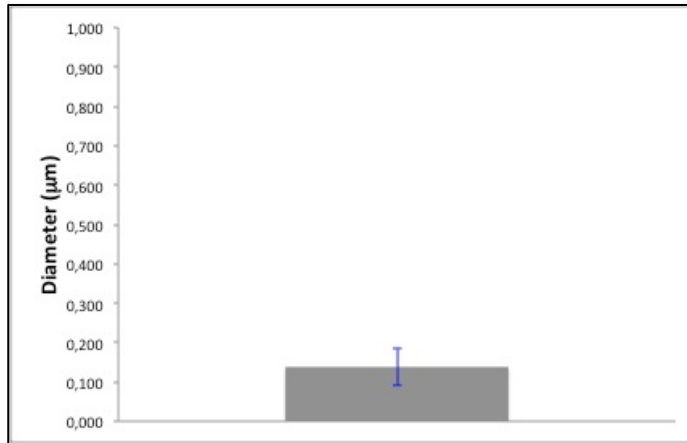


Figure 5.5 SEM images of REDV/HRGD flat bilayer (a); Histogram of flat double layer and monolayer fiber's diameter.(n=50)

#### 5.1.1 FLAT ELP MECHANICAL CHARACTERIZATION

Results from tensile tests on the different kinds of electrospun meshes displayed similar stress-strain curves, however evidencing different values of tensile modulus and maximum stress.

The stress-strain curve generally showed an initial linear region and then a decrease of the slope until a maximum stress value was reached. Successively, the first macroscopic signs of damage was evident as a consequence of fibers splitting.

Tensile modulus (E) and maximum stress ( $\sigma_{max}$ ) are reported as mean value  $\pm$  standard deviation in Table I.

Mesh	E (kPa)	$\sigma_{max}$ (kPa)
<b>HRGD 20 Kv-03ml/h-150 mm</b>	302.1 $\pm$ 43.2	29.2 $\pm$ 4.2
<b>REDV 15 Kv-0.5ml/h.150 mm</b>	242.2 $\pm$ 34.1	24.5 $\pm$ 3.5
<b>REDV/HRGD 18 Kv-0.3ml/h-150 mm</b>	234.4 $\pm$ 35.9	22.4 $\pm$ 3.3
<b>REDV/HRGD 20 Kv-0.3 ml/h-150 mm</b>	223.3 $\pm$ 33.0	21.3 $\pm$ 3.4

Table I. Results from tensile tests: modulus (E) and maximum stress ( $\sigma_{max}$ ) reported as mean value  $\pm$  standard deviation

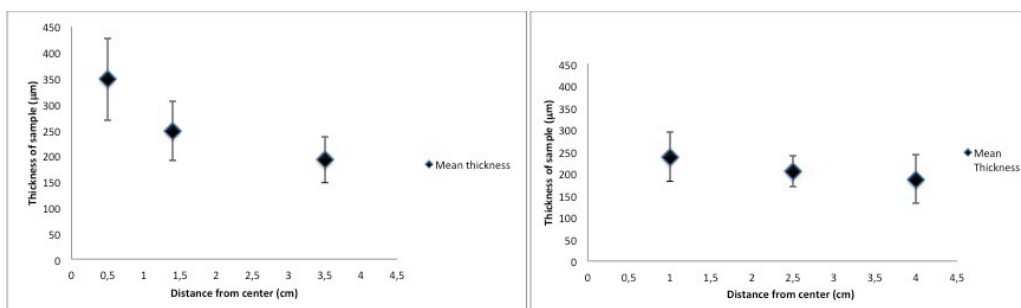
### 5.1.2 THICKNESS OF FLAT ELP SCAFFOLDS

Thickness profiles were measured on ELP scaffold flat. Monolayer REDV and HRGD with monolayer REDV/HRGD and bilayer REDV/HRGD were electrospun onto glass and measured with profilometer (VEECO Dektak 150). The thickness profiles were measured by making 12 cuts from the center of the sample to the outside.

A typical profilometer curve measures the difference between the thickness of the tip of the machinery on the glass and the thickness of the scaffold. From the images shown, it is possible distinguish a trend and a decreasing trend of the curves as a function of distance from the center. In all cases, there is a smaller thickness at points further away from the center. This appearance is due to the conical shape that the jet polymeric assumes during the process of electrospinning. however, lesser thickness of samples affects very little the mechanical properties of the scaffold.

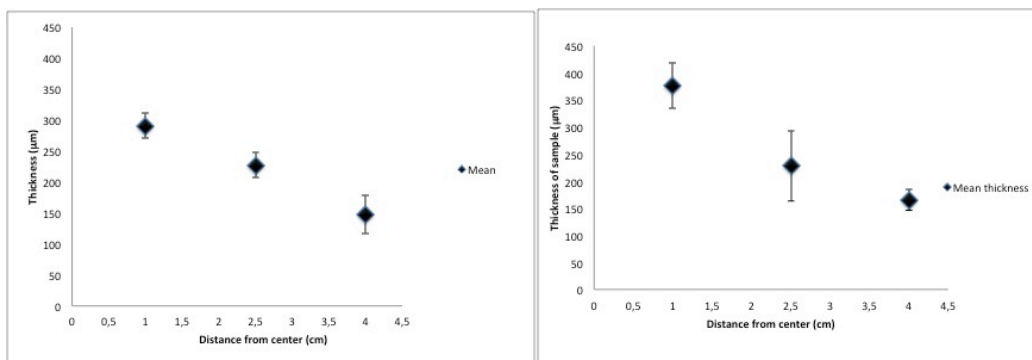
The decreasing thickness trend is more clear in the case of the HRGD monolayer (**fig 5.6, a1**); the greater amount of fibers is given by the high voltage applied during the electrospinning phase. On the contrary, for the REDV polymer, the decreasing thickness trend is less accentuated due to the lower voltage applied wich involves the formation of fibers with a greater diameter but a smaller amount of polymer in the center of the sample (**fig 5.6,b1**).

REDV/HRGD monolayer displayed a different thickness trend similar to the REDV monolayer and starts from 300  $\mu\text{m}$ . In this work, we used double layered scaffolds made by electrospinning REDV and HRGD one above the other for the higher thickness of the fiber's layer. Thickness of the double layered scaffolds (**fig 5.8 b2**) is higher due to the sovrapposition of the two different layers. The thickness starts to decrease from 400  $\mu\text{m}$ .



a 1

b 1



a 2

b 2

**Figure 5.6 Profilometer thickness trends of ELP scaffolds; HRGD monolayer(a1), REDV monolayer(b1), mono REDV/HRGD 50:50 (a2), REDV/HRGD double layer (b2). (n=3)**

### 5.1.3 DETERMINATION OF CROSSLINK DEGREE: HMDI

ELP fiber matrices were crosslinked in order to improve the degradation kinetics in aqueous environment. Samples of 1cmx1cm were cut and put in contact with increasing Acetone/HMDI, Genipin mixtures. Both the crosslinking agent (HMDI and Genipin) were dissolved in Acetone because of the higher solubility of fibers.

The isocyanates belong to a family of compounds commonly used in industry and not only. Synthesized for the first time in 1848, the use of these compounds is due to their properties and the ability that they have to lead to crosslinking reactions. This type of reactions are favorable for the mechanical stability of products such as paints, for the improvement of chemical resistance, and abrasion. Among the isocyanates used industrially there are compounds polyisocyanate, polyureas, polyaziridins, epoxides, aldehydes, carbodimidi, metal salts and ionic.

The high reactivity of these substances depends on their chemical nature (aliphatic isocyanates are less reactive than aromatic) and from the compounds with which they react. Reactions with hydroxyl functions give rise to the formation of urethane bonds to carry a carbamate as a final product. The reaction with the amine groups has a speed directly proportional to the chemical nature of the amine itself; the reaction with amines is 10-1000 times faster than the reaction with the hydroxyl groups and the water. In this case polyureas are obtained as final products. This type of reactions are widely used in the preparation of leathers.

The hexamethylenediisocyanate has a high concentration of -NCO groups and imparts to products containing it good adhesion and elasticity. Hexamethylenediisocyanate is a chemical crosslinking agent that reacts with nucleophilic functional groups such as amines, alcohols and protonated acids. HMDI, in particular, reacts with side chains of backbone-protected Lysine, Cysteine and Histidine and to a lesser extent of Tyrosine, in water (**fig 5.7**).

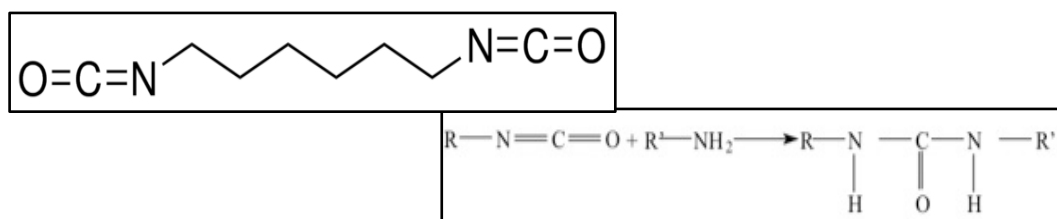


*Figure 5.7 Molecular structure of 1,6- Hexamethylenediisocyanate and its chemical reaction with amino groups forming a disubstituted Urea.*

Recently, Arevalo et al. crosslinked different ELP types of matrices obtained by Electrospinning using Hexamethylenediisocyanate. ELP samples (RGD and IKa24) were crosslinked using mixtures of HMDI/Acetone (10% v/v) in order to allow the slow degradation and the attachment of fibroblast upon matrices.

REDV/HRGD fiber mats were crosslinked in order to prevent dissolution of fibers in aqueous environment.

The crosslink of fibrous matrices at 5, 10 and 20% HMDI / acetone depicted in panel 5.8 (**image A, B and C**), showing in all three cases a good crosslink density but a low porosity, due mainly to the action of the solvent. In order to select an optimized sample, the degree of crosslink, and the kinetics of dissolution in an aqueous environment were evaluated,

The degree of crosslink was assessed by colorimetric reaction with Ninhydrin.

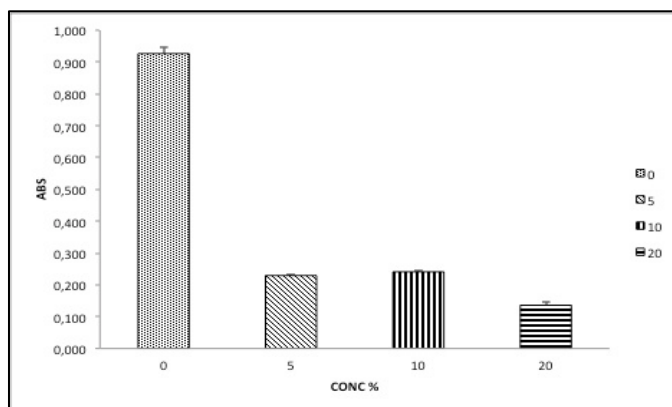
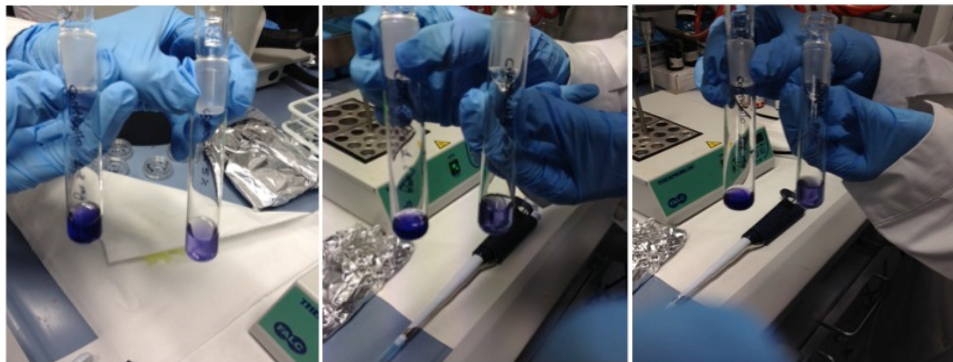
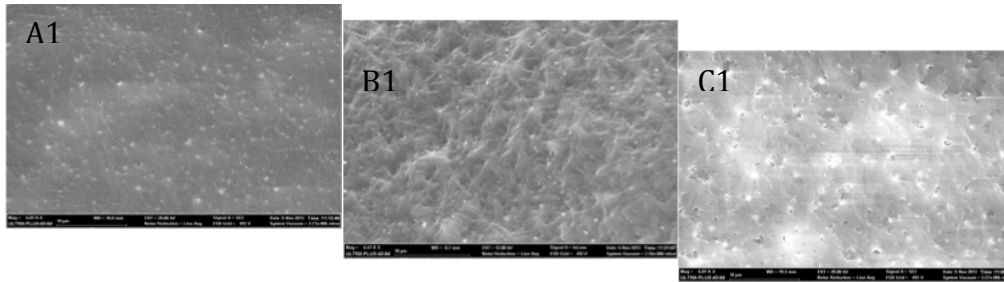
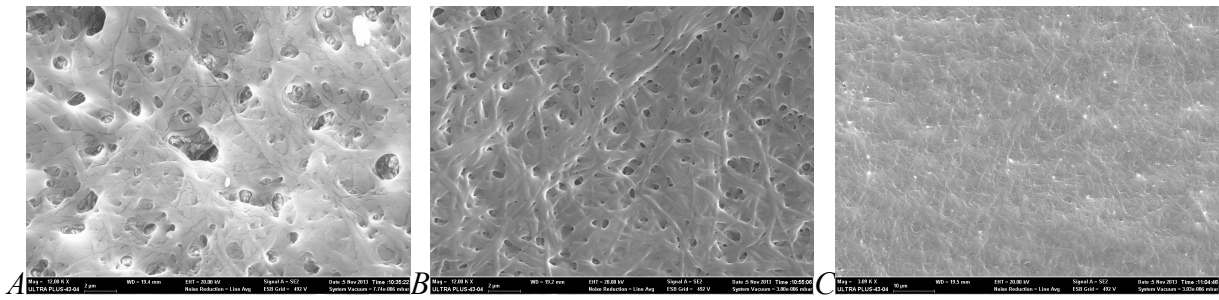


Figure 5.8 Scanning Electron Microscopy image of HMDI/Acetone crosslink double layer: and flat crosslinked double layer after 5 days in water (A, A1) HMDI/Acetone 5%;(B,B1) HMDI/Acetone 10%;(C,C1) HMDI/Acetone 20%.

The crosslink reaction leads to the formation of a complex between ninhydrin and the free amino groups still present in the solution ; the complex display a typycal pruple-blue color that is visible in 5.8 picture.

The degree of crosslink can be assessed both quantitatively and qualitatively. In particular, at 570 nm, is read the absorbance of samples crosslinked with various concentrations (**fig 5.8**).

The less value of absorbance for the 20% crosslinked HMDI/Acetone indicates the presence of a small amount of free amino groups in solution. Both 5 and 10% crosslinked HMDI/Acetone scaffolds dispalyed the same value of absorbance.

Even if the amount of amino groups is smallest for the 20% crosslinked scaffolds, for the in vitro test 10% crosslinked scaffolds have been used. This was mainly done for the because of the lowest concentration of crosslinking agent used for the reaction.

#### 5.1.4 *CROSSLINK SCAFFOLD'S DEGRADATION PROFILES*

To study the dissolution profiles of REDV/HRGD double layer dried scaffolds, in vitro test were carried out by immersing scaffolds in PBS (pH 7.4) for two weeks.

Images of scanning electron microscopy show the dissolution profiles of the ELP scaffolds immersed in increasing HMDI/Acetone mixtures.

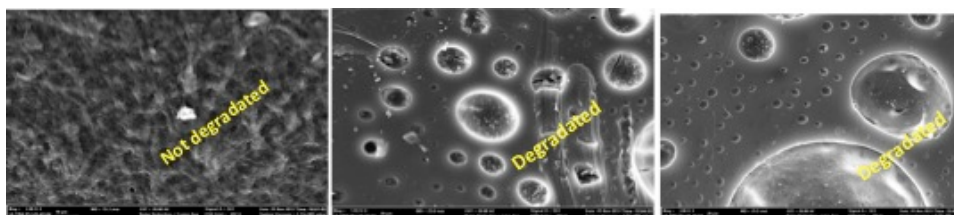


**Figure 5.9** Scanning Electron Microscopy of HMDI/Acetone 5%(v/v) crosslinked ELP scaffolds. After 3 days (a), 1 week(b), 2 weeks (c)

Starting from the mixture crosslinked at 5% (v/v), after 3 days the double layer REDV/HRGD is yet crosslinked but fibers are less porous and starting to lose their morphological characteristics. This behaviour is mainly favoured by the water that penetrates inside the scaffold's structure allowing the swelling of fibers; swelling of fibers increases the loss of porosity that is evident since the second day (**fig 5.9**). After 1 week, the dissolution of fibers is nearly complete; there are only few material residual that completely disappear after two weeks. For the 5%(v/v) HMDI/Acetone, the dissolution is complete after twelve days (**fig 5.9**).

REDV/HRGD scaffolds crosslinked at 10% (v/v) HMDI/Acetone are apparently more stable in aqueous environment since 10 days. The dissolution of fibers that starts from the swelling and losing of porosity became evident after ten days (**fig 5.10**). Fibers starts to lose their morphology and became more dense, flattened and less porous, after 5 days. The complete dissolution is evident at two weeks (**fig 5.10**).

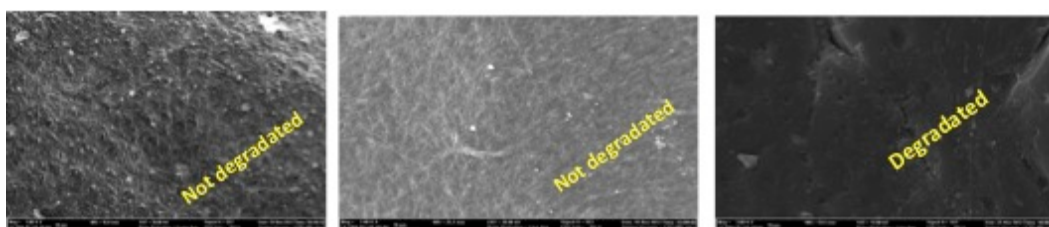


**Figure 5.10** Scanning Electron Microscopy of HMDI/Acetone 10%(v/v) crosslinked ELP scaffolds. After 3 days (d), 1 week(e), 2 weeks (f)

Crosslinking at 20% (v/v) seems to have the more durable dissolution profile. Dissolution of fibers does not affect scaffolds exceed two weeks. Fibers tends to lose their morphology since the first days: the porosity is is less extensive and highly concentrated crosslinking agent seem to affect negatively fiber morphology; this is evident since the third day (**fig 5.11**). Aniwany, dissolution profile of the 20% (v/v) crosslinked scaffolds have a good stability and seems to be the most suitable for the proposed application (**fig 5.11**).

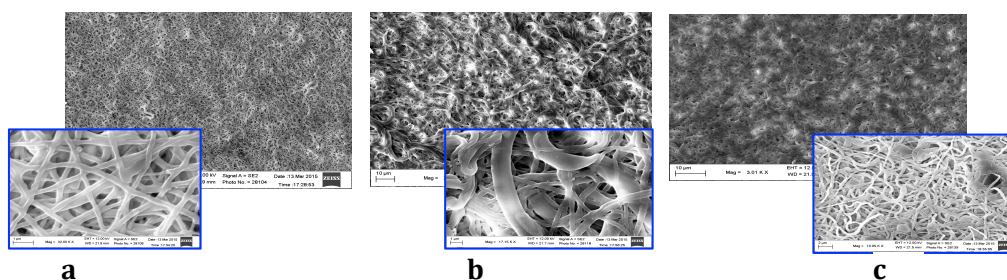


**Figure 5.11 Scanning Electron Microscopy of HMDI/Acetone 10%(v/v) crosslinked ELP scaffolds. After 3 days (g), 1 week(h), 2 weeks (i)**

The dissolution results showed that the morphology of scaffolds underwent a fiber-like structure to a sheet-like structure where fibers are more flattened and less porous, by increasing the HMDI concentration. HMDI crosslinkg remarkably changes the morphology of fibers and the pore size of scaffolds even when is less concentrated (10%). The highest concentration of HMDI for the 20%(v/v) scaffolds determines a higher stability but, at the same time, a possible increased toxicity to the cells. This is why, despite the greater stability of the samples crosslinked to 20%, in this study scaffolds crosslinked at 10% have been used for in vitro evaluation of cell adhesion.

In this work a comparison between two types of crosslinkg reaction was done in order to assess the biocompatibility of the crosslinked material for a future application. For this reason, genipin was used as an alternative crosslinking reaction for flat REDV/HRGD scaffolds. They were crosslinked for 72 hours, starting from 0.01% to 1% (w/v) solutions in Acetone.

In 5.12 picture Scanning Electron Microscopy of genipin crosslinked double layer ELP scaffolds are shown.



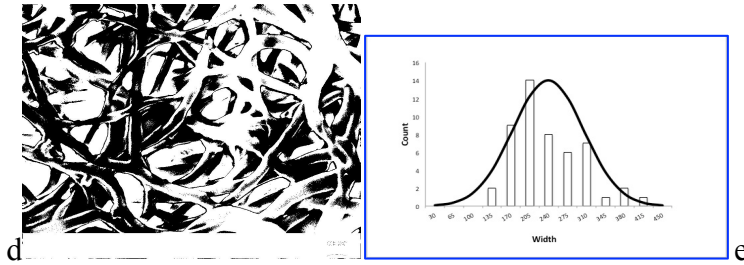


**Figure 5.12** Scanning Electron Microscopy Images of REDV/HRGD double layer ELP scaffolds crosslinked with increasing concentrations of Genipin/Acetone mixtures: (a) REDV/HRGD scaffold crosslinked in 0.1% Genipin/Acetone; (b) REDV/HRGD scaffold crosslinked in 0.5% Genipin/Acetone; (c) REDV/HRGD scaffold crosslinked in 1% Genipin/Acetone; (d) Scanning electron microscopy of REDV/HRGD double layer crosslinked 0.1% Genipin/Acetone threshold and correspondent distribution of diameter(e).

Genipin 0.1% crosslinked double layer show a good diameter distribution with a mean diameter of  $238 \pm 65$  nm (**fig 5.12,c**). The porosity of the crosslinked ELP scaffolds is 46% as depicted as threshold of the Scanning Electron Microscopy Image (**fig nr. 5.12 d**).

For their morphological characteristics, the crosslinked 0.1% Genipin/Acetone are the most suitable for the in vitro test.

## 5.1 SILK-ELP SCAFFOLDS

### 5.1.1 SCANNING ELECTRON MICROSCOPY(SEM)

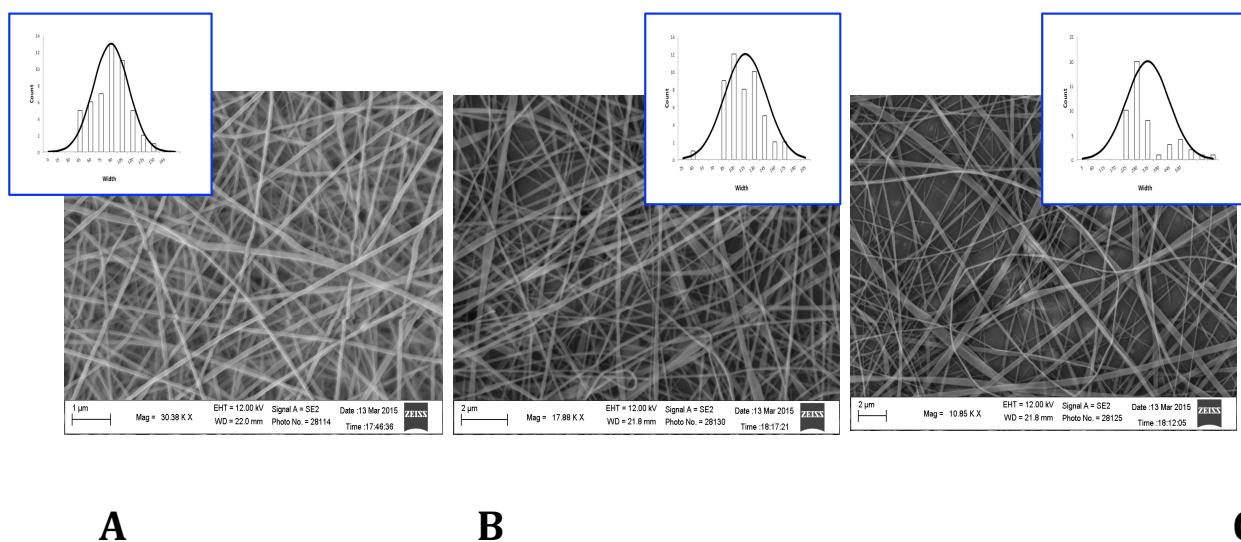
SILK-ELP was dissolved in 2,2,2 trifluoroethanol at a concentration of 10% (w/v) as reported in section 4.4.2. The solutions obtained are immediately electrospun in order to avoid gelation of the material. The process parameters used for the copolymer SILK-ELP are summarized in table 4.1.

Silk-elp was electrospun starting from low to higher voltages (13-20 Kv).

Fibers electrospun at 13 Kv, 0.3 ml/h and 150 mm have an average diameter of  $73\pm 25$  nm and a good distribution of the diameter, as depicted in **fig 5.13 (A)**

By increasing the voltage and maintaining unchanged the distance and the feed rate, contrary to what was seen for the polymers ELP, the fiber diameter increases until to get to  $169\pm 30$ . This behavior can be attributed to the high evaporation rate of the solvent and the low viscosity of the solution **fig 5.13 (B)**. Moreover, it can be seen the presence of some defects and beads within the sample.

Increasing voltage to 20 Kv, fiber's diameter proportionally increases until less than 200 nm. Distribution of diameter shows an average size of fiber's equal to  $169\pm 107$ . The higher dimensions are accompanied to the beads that are present in the sample. Presence of beads is mainly due to the breakage of the polymer jet because of the high surface tension **fig 5.13(C)**.



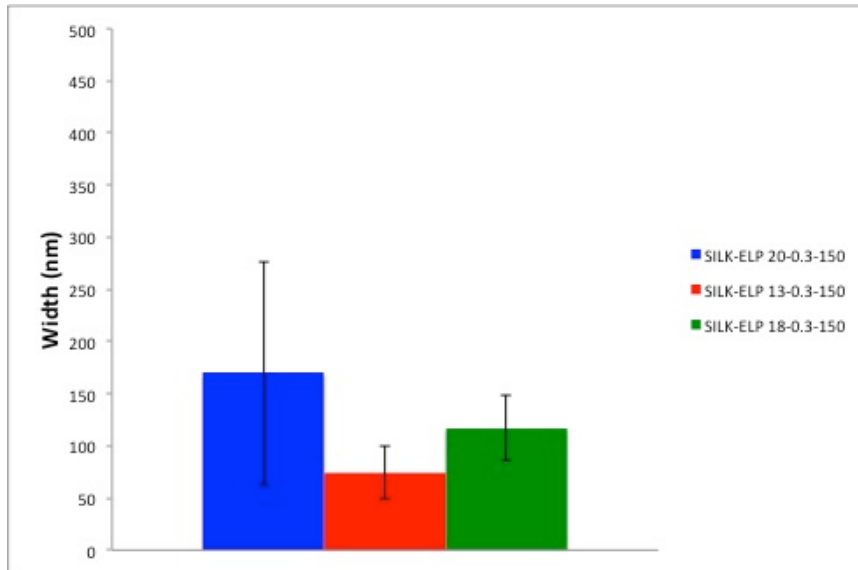


**Figure 5.13 Scanning Electron Microscopy Images of SILK-ELP scaffolds: (A) SILK-ELP electrospun at 13 Kv,0.3 ml/h and 150 mm; (B)SILK-ELP electrospun at 18 Kv,0.3 ml/h and 150 mm; (C)SILK-ELP electrospun at 20 Kv,0.3 ml/h and 150 mm. Histogram of SILK-ELP scaffold's diameter.**

## 5.2 SCAFFOLD'S INTERACTION WITH HUVEC

### 5.2.1 CELL PROLIFERATION ON ELP SCAFFOLDS

A biological validation with ELP flat double layer and flat monolayer 50:50 was performed in order to qualitatively identify the adhesion and spreading of HUVEC cells onto scaffold's surface. The effect of different type of surface differently affect cellular behaviour.

Fig nr.5.14 shows the number of cells at 4,8 and 24 hours after seeding.

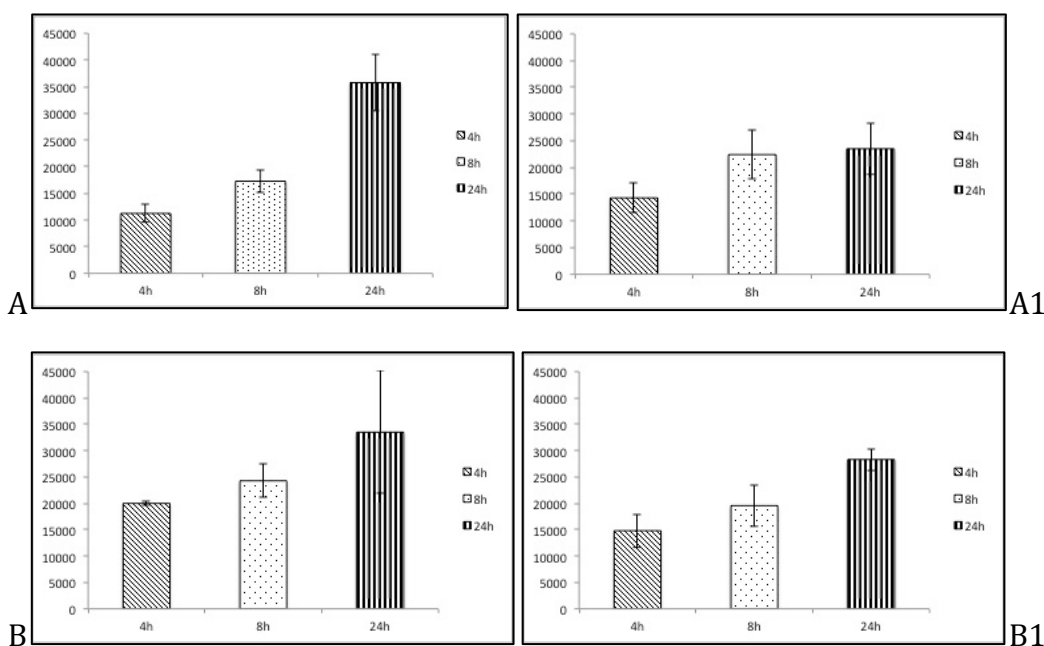


**Figure 5.14** Histogram bar of HUVEC number on top of ELP scaffolds; (A) Cell number on REDV/HRGD monolayered scaffolds; (B) Cell number on REDV/HRGD monolayered crosslinked scaffolds; (A1) Cell number on REDV/HRGD double layered scaffolds; (B1) Cell number on REDV/HRGD double layered crosslinked scaffolds

After 4 hours of culture, cells began to proliferate after the adhesion to the scaffold's surface. In particular, for all samples there is an exponential proliferation with the increasing time of culture. The higher proliferation rate is visible at 24 hour for the REDV/HRGD 50:50 monolayer (**fig 5.14, A,B**). Crosslink monolayer and double layer scaffolds shows a proliferation rate less than the sample not crosslinked. This Behaviour is probably due to the higher stiffness and less porosity of the crosslinked samples which does not allow the adhesion of cells.

After 8 hours in culture with M200-rich medium, Huvec cells showed a good spreading and attachment to the fibers, inducing elongation of cytoskeleton along the fiber's axis. In particular, the higher proliferation rate is visible for the non crosslinked scaffolds.

Confocal images of HUVEC cultured onto ELP scaffolds shows adhesion and proliferation of cells for all the treated samples. In particular, it's evident the adhesion, proliferation and spreading of cells that starts at 8 hours.

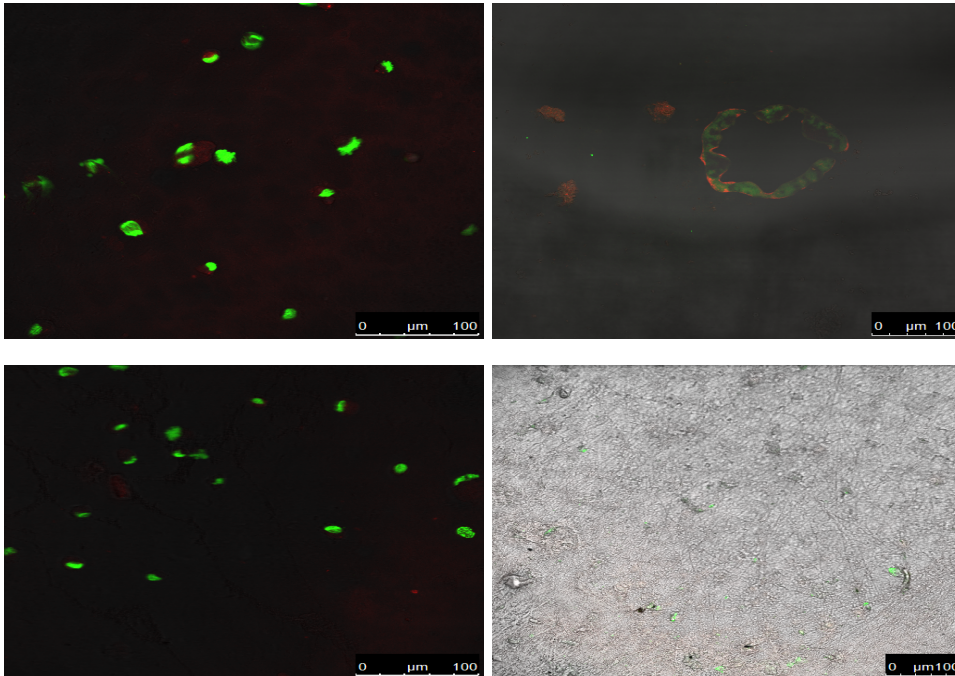
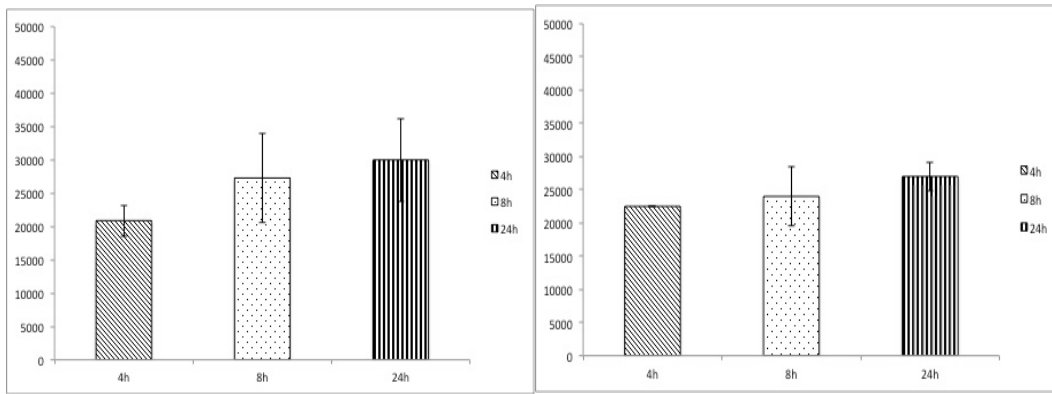


**Figure 5.15** Confocal Transmission images of ELP double layered scaffold stained with SYTOX green and Phalloidin

### 5.2.2 CELL PROLIFERATION ON SILK-ELP SCAFFOLDS

Humbelical Vein Endothelial cells were cultured onto SILK-ELP scaffolds in order to see the adhesion and spreading upon this type of fibrous matrix.

Cells were removed and counted at 4 hours, 8 hours and 24 hours. As you can see from figure nr 5.18, as in the case of the scaffolds ELP, also in this case the number of cells increases proportionally with time. In particular, it has a maximum growth of the cells at 24 hours.



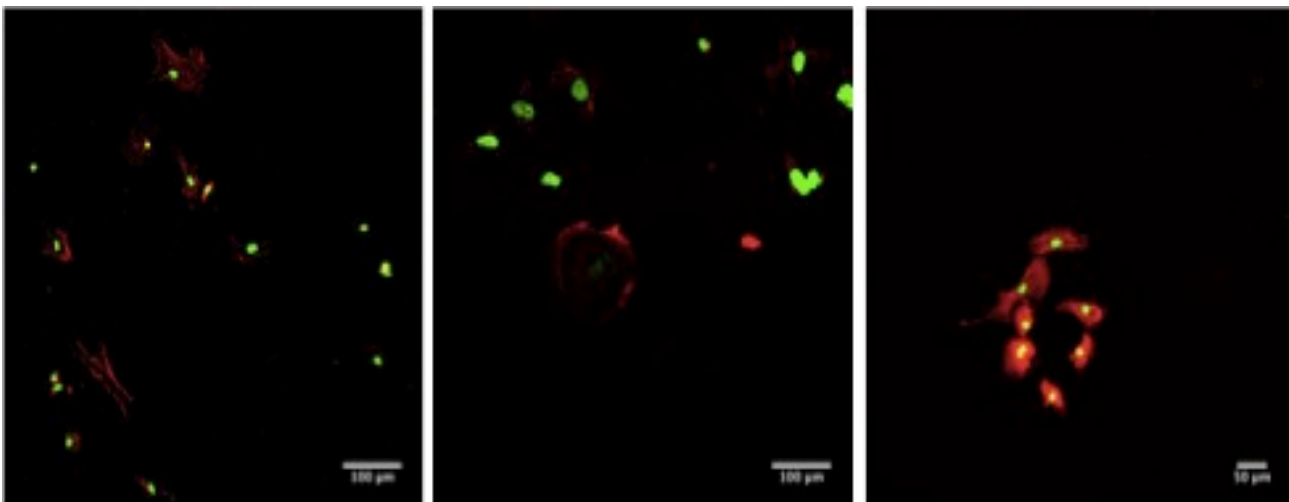
A

B

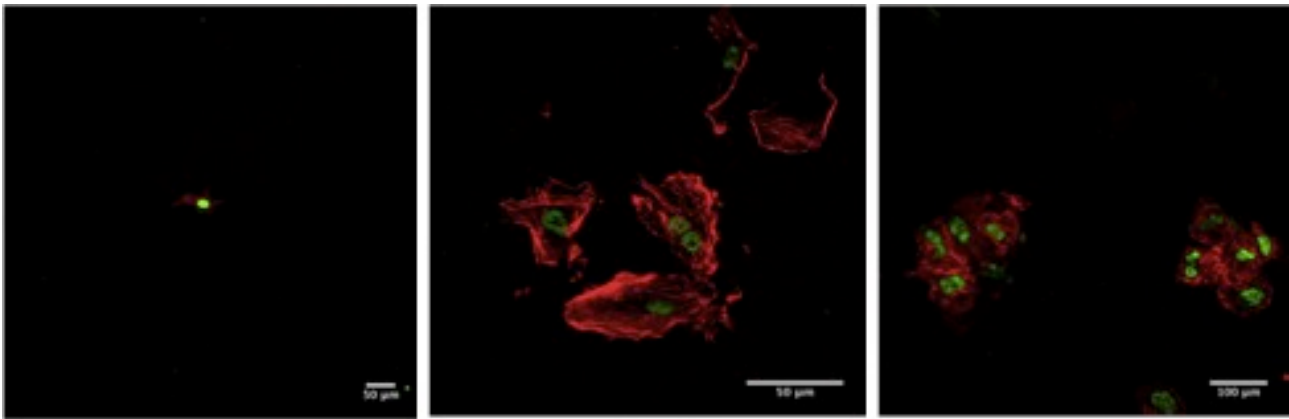
**Figure 5.16** Histogram bar of HUVEC number on top of SILK-ELP scaffolds (A) and on gelatin coated dishes(B) as a function of seeding time.

At each time point, the cells, fixed and stained, show viable and greater in number; in particular, number of cells increase in the same way, in gelatin coated dishes and in silk-elp scaffolds, for the first 4 hours (**fig 5.16**). In the next 8 hours, cells upon the gelatin coated dishes grows less than the silk-elp scaffolds. This is mainly due to the high infiltration rate of cells in the case of the silk-elp scaffolds. Finally, at 24 hours, increasing in cell's number of silk-elp scaffolds is corroborated by the higher spreading that is visible in the fluorescence images (**fig nr. 5.17**)

Fluorescent images were obtained by fixing with SYTOX green and Phalloidin.



A



B

**Figure 5.17** Optical microscopy fluorescent images of Gelatin coated controls stained with SYTOX green and Phalloidin(A); fluorescent microscopy images of HUVEC on top of SILK-ELP scaffolds stained with SYTOX green and Phalloidin (B).

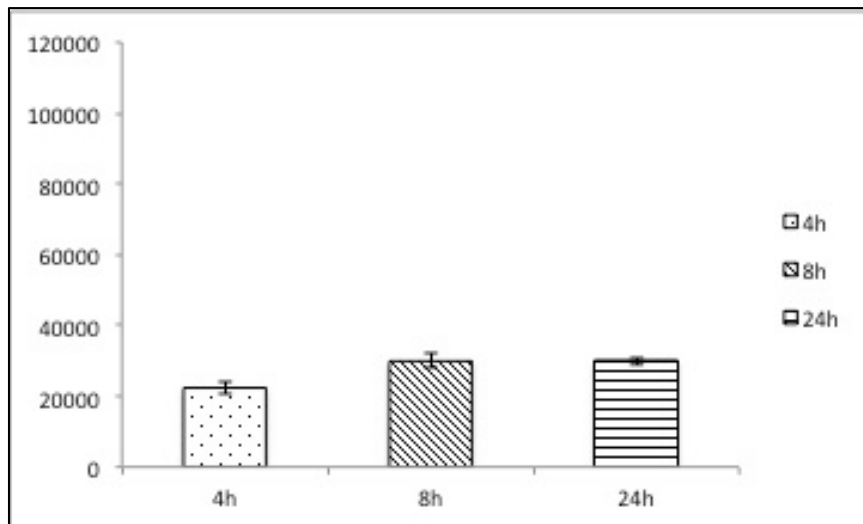
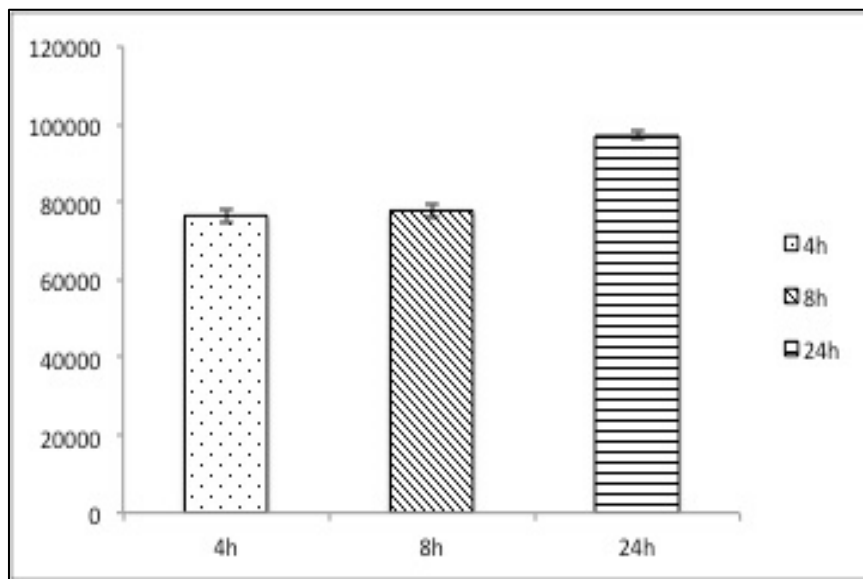
As you can see from picture, in the case of gelatin coated dishes, HUVEC cells attached and tend to spread after 8 hours. Number of cells is lower than the silk-elp scaffolds at 8 hours (**fig 5.17**).

Even more, at 24 hours, attaching and spreading of HUVEC cells is higher for the silk-ELP scaffolds than the gelatin coated control. This preliminary results show a greater number of cells in the case of the silk-elp scaffolds and the spreading more pronounced than in the case of the controls with gelatin (**fig 5.17 B**)

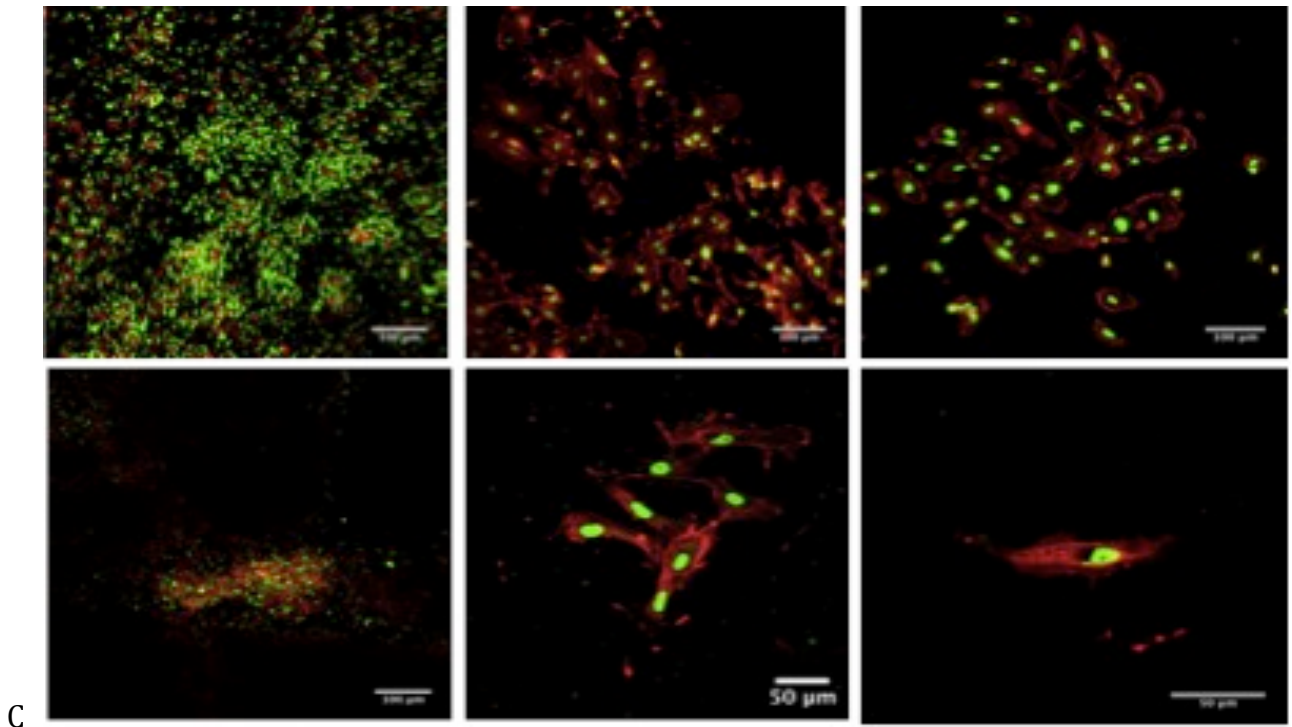
ELP crosslinked with Genipin/Acetone 0.1% were biologically tested with HUVEC in order to prove the adhesion and spreading of cells.

In fig 5.18 growth of HUVEC on top of ELP genipin/Acetone 0.1% crosslinked versus Gelatin coating controls are depicted, for 4, 8 and 24 hours of culture. For the crosslinked scaffolds, it's possible to evidence the increasing growth at 8 hours. The increasing number of cells is related to an increasing spreading, as shown in Confocal microscope Image nr. **5.19**

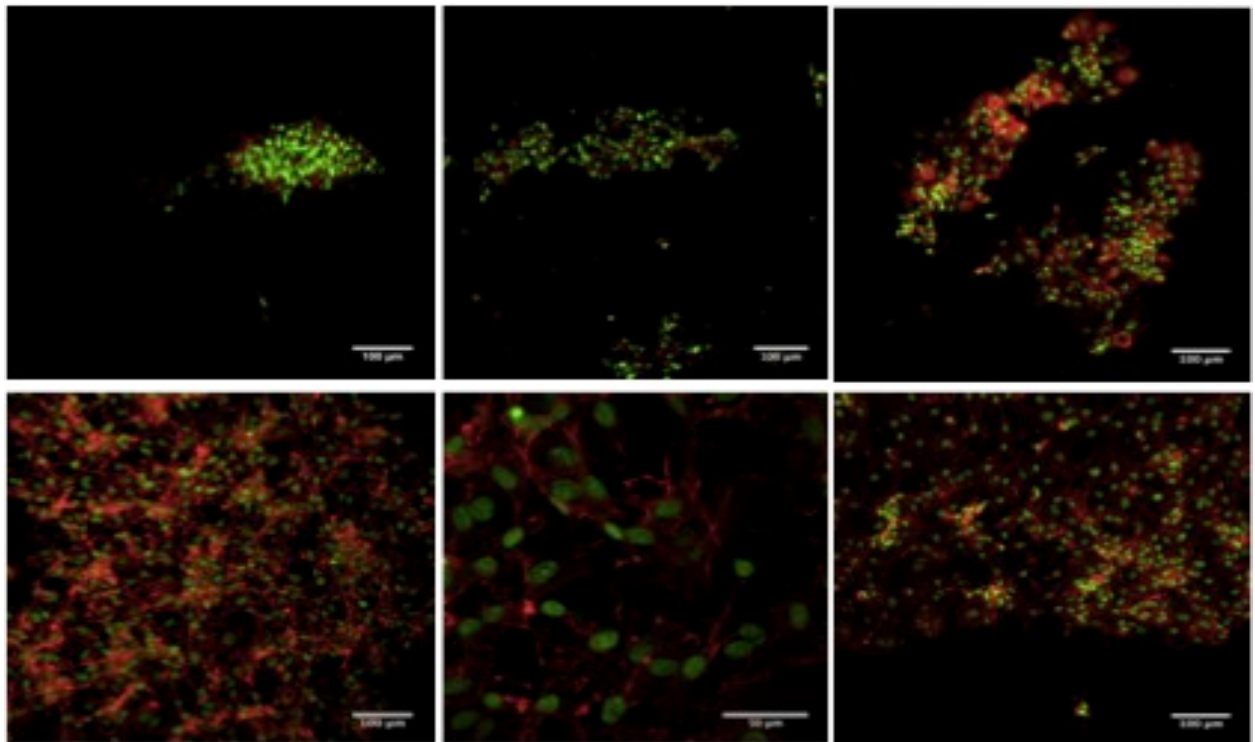
Cells are more stretched at 24 hours, as depicted in **fig 5.19, D** (down of the panel) The increasing growth of cells is mainly due by the higher porosity of this type of scaffolds, compared to the ELP HMDI/Acetone crosslinked one. This results suggest that the Genipin/Acetone crosslinked scaffolds are good substrates that promotes attachment, spreading and viability of cells.



**Figure 5.18** Histogram bar of HUVEC number on top of ELP Genipin/Acetone 0.1% crosslinked scaffolds (A) and on gelatin coated dishes(B) as a function of seeding time.



C



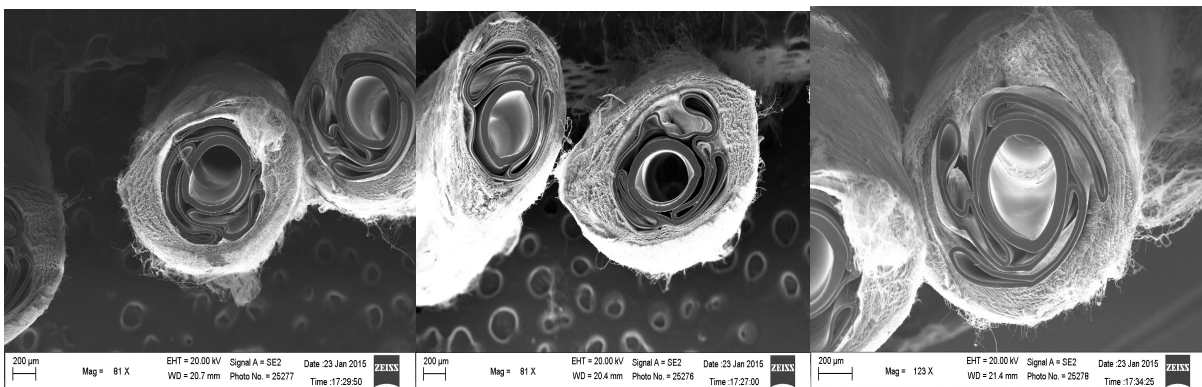
D

Figure 5.19 Confocal microscopy images of Gelatin coated controls stained with SYTOX green and Phalloidin (C); 25 Confocal microscopy images of HUVEC on top of ELP Genipin/Acetone 0.1% crosslinked scaffolds stained with SYTOX green are depicted in panel D.

### 5.2.3 THICKNESS OF DIRECTLY ELECTROSPUN CATETHERS

Directly electrospun balloons were processed using Scanning Electron Microscopy soon after electrospinning in order to see the texture of fibers around nylon balloons. (**fig 5.20**).

In this work samples thickness and fiber's diameter were measured using ImageJ software. SEM micrographs of directly electrospun balloons shows texture of fibers around balloons that are strictly attached to the central part of the catheter. The spatial distribution of fibers for the directly electrospun samples allow to the delivery of the material, once in contact with the artery.



**Figure 5.20** SEM images of directly electrospun balloons obtained from the REDV and HRGD (n=20).

Thickness of ELP directly electrospun balloons is assessed around 300 µm (**fig 5.21**). Angioplasty catheters of 2.5x20mm coated with elastin like polymers were characterized morphologically by Scanning Electron Microscopy. An important component of the cell response onto a biomaterial is related to the cell attachment which may determine cell fate, including viability, proliferation and function. Cell fate can be manipulated in vitro by modifying substrates. In particular, for the electrospun scaffolds, cell fate can be modulated with a proper topographic design of fiber scaffolds. Anisotropy of ELP scaffolds was measured using FFT function in order to quantify the alignment as function of the rotation rate. In general, randomly oriented fibers usually generate an output image in which pixel intensities seems to be uniformly distributed in a circular pattern. On the contrary, aligned fibers generate an output FFT image where a group of pixel intensities are oriented in a preferential direction (**fig 5.21**).

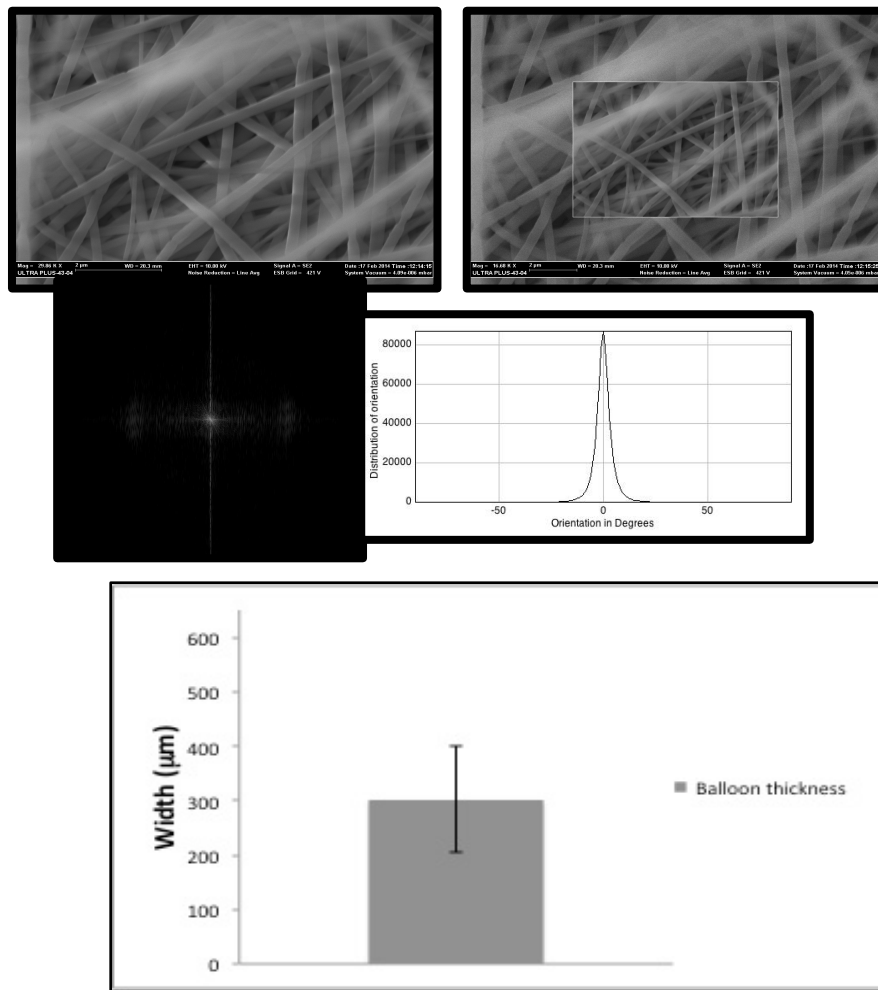


**Figure 5.21 SEM images of directly electrospun REDV/HRGD bilayer Angioplasty balloons. FFT image and distribution of orientation plot of the REDV/HRGD aligned fibers upon Angioplasty balloon. Histogram of REDV/HRGD double layered thickness balloon (n=20).**

### 5.3 IN SITU DEPLOYMENT OF ELP SCAFFOLD

3.5x20mm, 2.5x20mm and 2.0x20mm produced by Conic vascular Technology were used for preliminary ex vivo experiments. In order to obtain a feasible ELP coating, both polymers were electrospun onto the 2.5x20 mm catheters.

Electrospinning of polymers REDV and HRGD was carried on using the same concentrations ( section 4.2.5). All the ELP coatings were realized in unflated and semi-inflated balloons in order to set up the complete delivery of the material. All the balloons were fixed within the rotating mandrel in order to obtain a direct coating.

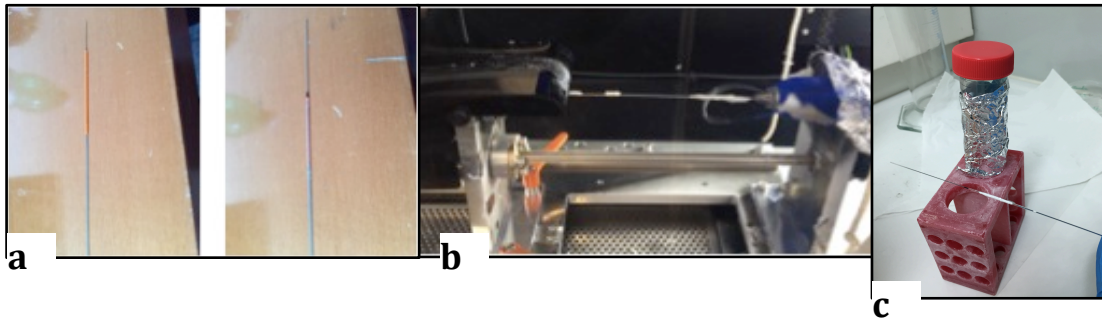
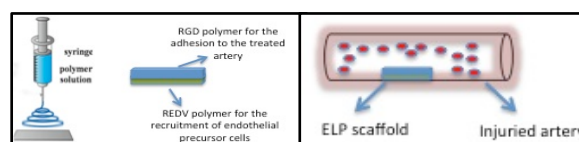


**Figure 5.22** Electrospinning of balloons: A) 2.5x20 mm balloons without ELP coating; B) image of balloons into the rotating mandrel; C) resulting coated ELP balloon

The rotation speed of mandrel was set at 60 rpm (**fig 5.22 B.**). The obtained electrospun balloon is depicted in **fig 5.22,C.**

In order to obtain a suitable coating for the subsequent application within a blood vessel, the polymers were electrospun in the following order: REDV to promote the recruitment of circulating endothelial cells and RGD to obtain the recognition and subsequent attachment of the endothelial cells of the blood vessel (**Scheme nr. 5**). Electrospun ELP scaffolds were used onto rabbits arteries. Cylinder plastic balloons coated with ELP scaffolds were applied facing half of their circumference onto opened and flattened rabbits aorta arteries.



**Scheme nr.5** ELP scaffold fabrication for Atherosclerotic diseased arteries

The deployment of ELP scaffold has been done in Aortas arteries of rabbits, as reported in section 4.2.2. All samples were fixed in formalin and treated with Masson Tricrome and Hematoxylin/Eosin for histology.

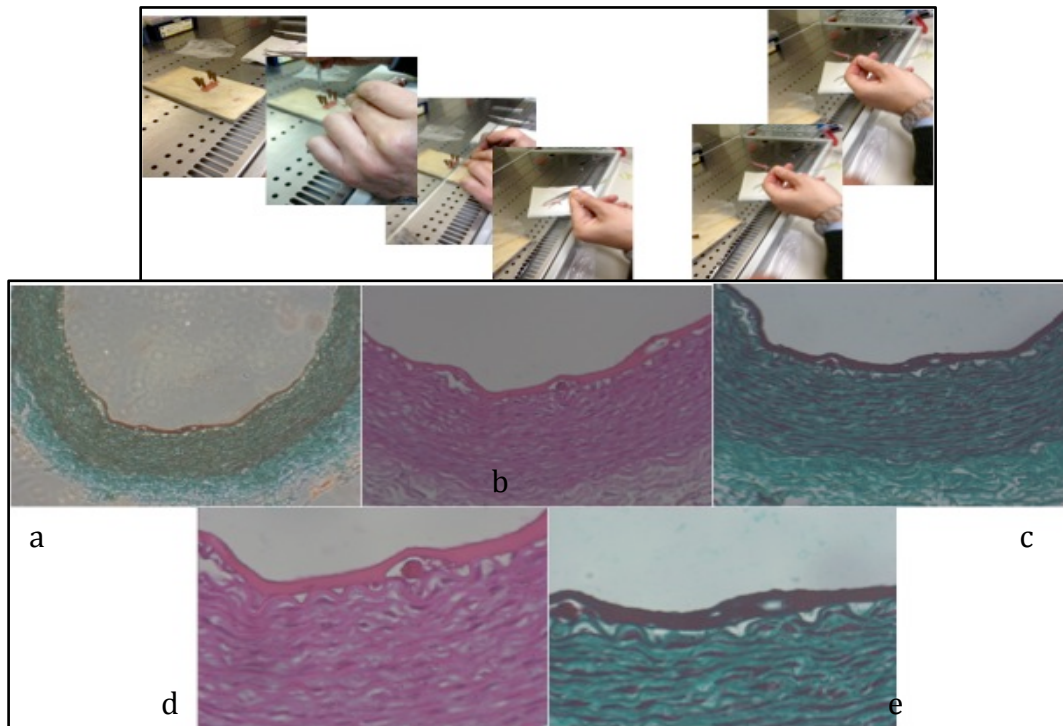


**Figure 5.23** Optical Microscopy characterization of ELP coated balloon inflated on flattened aorta (top of the picture). Masson Tricrome staining of ELP treated arteries (a,c,e). Scale bar were respectively 10X,20X and 40X; Hematoxyllin/Eosin staining ELP trated arterie (b,d). Scale bar were 20X and 40X

Histology results shows in all cases the presence within the treated arterie of the ELP mesh (**fig 5.23**).

In particular, Masson tricrome staining shows that the fiber mesh is deposited on top of the intima as a thin layer. (**fig 5.23 a,c and e**). These thin layer is adherent to the arterie, as it shows with Ematoxyllin/Eosin staining and seems to have a different texture when in contact with the intima layer of the vessel.

ELP directly electrospun balloons were used to perform in vivo test. Deployment of ELP mesh is direct and easy to do. Histology of sacrificed animals shows the delivery of the fiber mesh and the resident material that is present within the arterie after the catheter removal (fig 5.23). There is no material interference and scaffolds could be delivered easily by inflating catether in the artery. Texture of the mesh seems to be different, even in this case; it is evident the presence of fiber mesh as a thin layer of gel. The behaviour of the material can be explained by the structural change that the ELP polymers undergoes once in contact with acqueous environment. This change allows the formation of a gel-like structure that seems to be more stable and evident within the vessel (**fig 5.24**). Taking together these results shows that in situ delivery of fiber mesh is feasible and efficient in vitro and in vivo preliminary experiments.

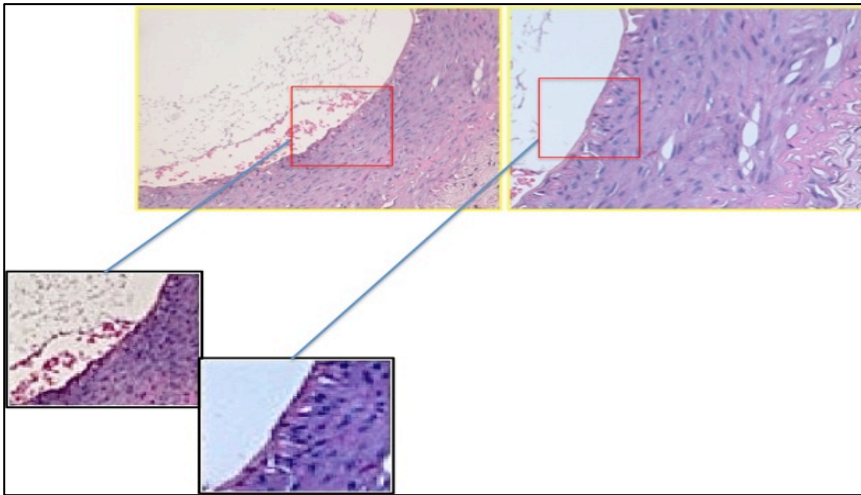


**Figure 5.24** Optical Microscopy Image of ELP treated artery with Hematoxylin/Eosin. Scale bar was 20X and 40X.

Confocal transmission was used to assess the presence of the mesh inside the artery.

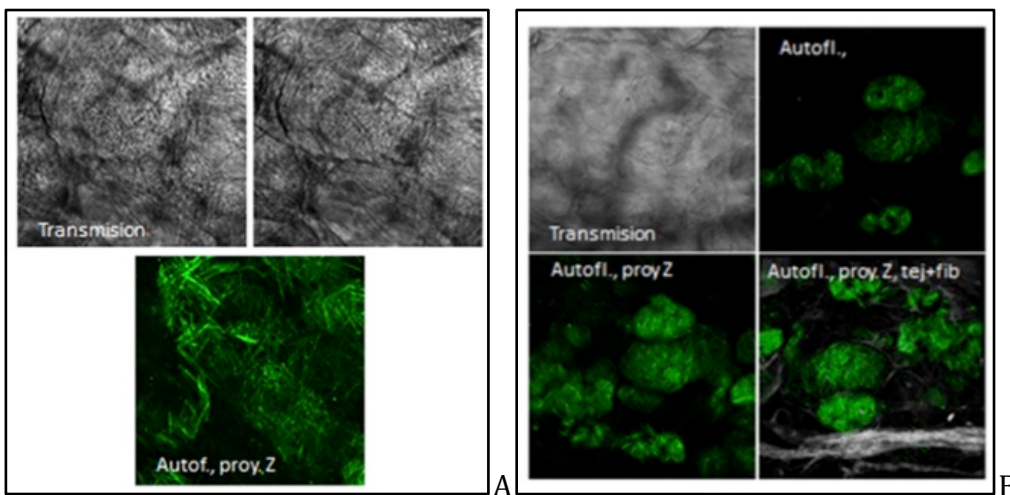


**Figure 5.25** Confocal Transmission image of ELP treated artery (A) and control artery(B).

Confocal images show the structure and the texture of the scaffold, once placed in contact with the artery (**fig 5.25,A**). You can still see the fibers composing the elp scaffolds that seem to be closely adherent to the intima vessel, unlike artery image control. These results also show that the scaffold not crosslinked, once placed in contact with the artery maintains the morphology and the fibers are well distinguishable and adherent to the intima vessel surface.

## **6 CHAPTER: CONCLUSION AND FUTURE PROSPECTS**



In this work we have realized a fully characterized fibrous scaffolds using two types of materials. ELP coated balloons shows a great and feasible adhesion to endothelial inner lamina, both in vivo and in vitro.

The mechanical properties and the porosity of this type of scaffold were appropriate to the use of balloons, inflated inside the arteries. Necessary additional characterizations, as well as a slower degradation of the material is indispensable for their clinical use.

Silk-elp scaffolds were obtained by electrospinning and characterized in terms of morphology and mechanical properties. In this case, the results obtained show a good porosity and morphology.

The in vitro tests conducted maintaining cultured HUVEC on this type of scaffold show good proliferation and cell viability, as well as the ability of cells to make spreading that appears to be better than for the gelatin coated controls.

## 7 BIBLIOGRAPHY

- [1]-Fernández-Colino A1, Arias FJ, Alonso M, Rodríguez-Cabello JC., Spain. Self-organized ECM-mimetic model based on an amphiphilic multiblock silk-elastin-like corecombinamer with a concomitant dual physical gelation process. *Biomacromolecules*. 2014 Oct 13;15(10):3781-93
- [2]-Rodríguez-Cabello JC1, Girotti A, Ribeiro A, Arias FJ. Synthesis of genetically engineered protein polymers (recombinamers) as an example of advanced self-assembled smart materials. *Methods Mol Biol*. 2012;811:17-38
- [3]-Girotti A1, Reguera J, Rodríguez-Cabello JC, Arias FJ, Alonso M, Matestera A. Design and bioproduction of a recombinant multi(bio)functional elastin-like protein polymer containing cell adhesion sequences for tissue engineering purposes. *J Mater Sci Mater Med*. 2004 Apr;15(4):479-84.)
- [4]-Fossey S A, N'emethy G, Gibson K D and Scheraga H A 1991 Conformational energy studies of  $\beta$ -sheets of model silk fibroin peptides: I. Sheets of poly(Ala-Gly) chains *Biopolymers* 31 1529-41
- [5]-Rodríguez-Cabello J C, Alonso M, Díez M I, Caballero M I and Herguedas M M 1999 Structural investigation of the poly(pentapeptide) of elastin, poly(GVGVP), in the solid state *Macromol. Chem. Phys.* 200 1831-8.
- [6]-Urry D W 2006 *What Sustains Life? Consilient Mechanisms for Protein-Based Machines and Materials*, New York: Springer
- [7]-Gustafson J A and Ghandehari H 2010 Silk-elastinlike protein polymers for matrix-mediated cancer gene therapy *Adv. Drug Deliv. Rev.* 62 1509-23
- [8]-Raul Machado<sup>1,6</sup>, Andre da Costa, Vitor Sencadas, Carmen Garcia-Arevalo, Carlos M Costa, Jorge Padrao, Andreia Gomes, Senentxu Lanceros-Mendez, Jose Carlos Rodríguez-Cabello and Margarida Casal. Electrospun silk-elastin-like fibre mats for tissue engineering applications *Biomed. Mater.* 8-2013

## **RINGRAZIAMENTI**

*Anzitutto ringrazio la mia famiglia; la ringrazio per avermi permesso di raggiungere quest'altro traguardo, per aver creduto in me, sempre, per avermi sostenuto economicamente e amorevolmente.*

*Ringrazio il mio fidanzato, Davide per il suo amore, il suo appoggio amorevole (a volte anche economico) costante e paziente. Ringrazio la famiglia del mio fidanzato: Pia, Antonio e Riccardo per il loro appoggio e per la loro presenza costante e affettuosa.*

*Ringrazio i miei amici di una vita che mi hanno supportato e aiutato anche da lontano.*

*Ringrazio tutti i miei colleghi per questi faticosi ma meravigliosi tre anni; li ringrazio per la loro amicizia, per il loro aiuto e per le risate anche nelle giornate faticose, dove tutto sembra ti remi contro. Ringrazio in particolar modo il Dott. Vincenzo Lettera, la Dott.ssa Virginia Brancato e la Dott.ssa Claudia Mazio, per il loro prezioso aiuto in quest'ultimo anno.*

*Ringrazio la mia scialuppa di salvataggio, il dott. Maurizio Cao il quale anche da lontano non ha mai smesso di aiutarmi e insegnarmi a essere sempre più "Ingegnere".*

*Ringrazio i miei colleghi ma soprattutto amici, la Dott.ssa Valeria Panzetta, il dott. Giuseppe Amalfitano, il dott. Gianluigi Manzo, il dott. Vincenzo Lettera per il loro affetto, la loro amicizia e per avermi fatto sentire meno la mancanza di casa, nel corso di questi tre anni.*

*Ringrazio la mia AMICA e compagna di scrivania, di pranzi, di risate, di chiacchiere, di uscite e soprattutto di vita, la dott.ssa Chiara Cosenza, senza la quale le giornate a lavoro non sarebbero state così allegre, anche nei periodi peggiori.*

*Ringrazio la “Federico II” di Napoli nella persona del Prof. Paolo Antonio Netti per la splendida opportunità concessami ma soprattutto ringrazio il mio tutor, il Prof. Filippo Causa che mi ha sostenuto, aiutato e permesso di fare esperienze che mai avrei pensato di poter affrontare.*

*Ringrazio te, che mi segui ogni giorno e vegli su di me: ogni traguardo della mia vita e ogni esperienza che vivo l’ho dedicata e la dedicherò a te.*